

BIVARIATE SPLINES FOR OZONE CONCENTRATION PREDICTIONS

by

BREE ETTINGER

(Under the direction of Ming-Jun Lai)

ABSTRACT

For ground level ozone prediction, we consider a functional linear regression model where the explanatory variable is a real random surface and the response is a real random variable. We use bivariate splines over triangulations to represent the random surfaces. Then we use this representation to construct two solutions, a least squares estimate of the regression function based on a brute force approach, and an autoregressive estimator based on a principal component analysis. We apply these two functional linear models to ground level ozone forecasting over the United States to illustrate the predictive skills of these two methods. We also extend the brute force approach to a model where both the explanatory variable and the response are both real random surfaces.

INDEX WORDS: Functional Linear Models, Functional Data, Regression, Splines, Principle Component Analysis

BIVARIATE SPLINES FOR OZONE CONCENTRATION PREDICTIONS

by

BREE ETTINGER

B.S., The University of Georgia, 2002

M.A., The University of Georgia, 2004

M.S., The University of Georgia, 2009

A Dissertation Submitted to the Graduate Faculty
of The University of Georgia in Partial Fulfillment

of the

Requirements for the Degree

DOCTOR OF PHILOSOPHY

ATHENS, GEORGIA

2009

© 2009

Bree Ettinger

All Rights Reserved

BIVARIATE SPLINES FOR OZONE CONCENTRATION PREDICTIONS

by

BREE ETTINGER

Approved:

Major Professor: Ming-Jun Lai

Committee: E. Azoff
R. Varley
M. Adams
C. Kazanci

Electronic Version Approved:

Maureen Grasso
Dean of the Graduate School
The University of Georgia
August 2009

DEDICATION

Dedicated to my grandfathers Bernard Ettinger and Frank Leighton.

ACKNOWLEDGMENTS

I would like to acknowledge and extend my heartfelt gratitude to the following persons who have made the completion this dissertation possible. First, I would like to thank my Advisor, Dr. Ming-Jun Lai, for his vital encouragement, patience and support. He has always had my best interest in mind and sought out good opportunities for me. I would also like to thank the rest of my committee, Dr. Malcolm R. Adams, Dr. Edward A. Azoff, Dr. Caner Kazanci and Dr. Robert Varley for their guidance and support. I have always enjoyed my time at the University of Georgia knowing their office doors are open. A special thanks goes to Dr. Azoff. He was my first math teacher at the University of Georgia and I cannot thank him enough for all of the clear explanations he has given and for always encouraging me to ride my bike to school. I would also like to thank Dr. Sybilla Beckmann, my teaching mentor, for her insight and guidance. The staff of the mathematics department, for their constant reminders, support, and much needed motivation. I would also like to thank my officemates and fellow graduate students for their help and inspiration. Finally, I would like to thank my family and friends. To my brother, for always explaining things to me, to my dad for teaching me how to read and to my mother for being a great role model. Of course to my husband, Jamie, for always encouraging me to do my best and always letting me be me.

TABLE OF CONTENTS

	Page
ACKNOWLEDGMENTS	v
LIST OF FIGURES	vii
CHAPTER	
1 INTRODUCTION	1
2 PRELIMINARIES	4
2.1 BIVARIATE SPLINES	4
2.2 UNIVARIATE FUNCTIONAL LINEAR MODELS	31
3 AUTOREGRESSIVE APPROACH FOR FUNCTIONAL LINEAR MODELS	34
4 BRUTE FORCE APPROACH TO FUNCTIONAL LINEAR MODELS	40
5 BRUTE FORCE EXTENSION	55
6 NUMERICAL EXPERIMENTS	68
6.1 ATLANTA	70
6.2 BOSTON	88
6.3 CINCINNATI	105
7 CONCLUSION	122
7.1 SIMILARITIES AND DIFFERENCES BETWEEN THE TWO APPROACHES	122
7.2 SUMMARY OF NUMERICAL EXPERIMENTS	124
BIBLIOGRAPHY	127

LIST OF FIGURES

2.1	For the triangle above, $T = \langle v_1, v_2, v_3 \rangle$, the barycentric coordinates b_1 , b_2 and b_3 for the point v have the geometric interpretation of being the areas of the sub-triangles formed by v	7
2.2	For the triangle above defined by v_1 , v_2 and v_3 the barycentric coordinates are shown at each of the vertices and at the center of the edge opposite v_3	8
2.3	Set of domain points for a polynomial of degree 2	10
6.1	Locations of EPA stations and a Triangulation	69
6.2	Three different sizes of triangulation of the southeast part of U.S.	71
6.3	Brute force predictions (blue \cdot , red $+$, and black \times) and exact measurement(green line) on Sept. 1, 2005 in Atlanta	72
6.4	Brute force predictions (blue \cdot , red $+$, and black \times) and exact measurement(green line) on Sept. 2, 2005 in Atlanta	72
6.5	Brute force predictions (blue \cdot , red $+$, and black \times) and exact measurement(green line) on Sept. 3, 2005 in Atlanta	73
6.6	Brute force predictions (blue \cdot , red $+$, and black \times) and exact measurement(green line) on Sept. 4, 2005 in Atlanta	73
6.7	Brute force predictions (blue \cdot , red $+$, and black \times) and exact measurement(green line) on Sept. 5, 2005 in Atlanta	74
6.8	Brute force predictions (blue \cdot , red $+$, and black \times) and exact measurement(green line) on Sept. 6, 2005 in Atlanta	74
6.9	Brute force predictions (blue \cdot , red $+$, and black \times) and exact measurement(green line) on Sept. 7, 2005 in Atlanta	75

6.10	Brute force predictions (blue \cdot , red $+$, and black \times) and exact measurement(green line) on Sept. 8, 2005 in Atlanta	75
6.11	Brute force predictions (blue \cdot , red $+$, and black \times) and exact measurement(green line) on Sept. 9, 2005 in Atlanta	76
6.12	Brute force predictions (blue \cdot , red $+$, and black \times) and exact measurement(green line) on Sept. 10, 2005 in Atlanta	76
6.13	Brute force predictions (blue \cdot , red $+$, and black \times) and exact measurement(green line) on Sept. 11, 2005 in Atlanta	77
6.14	Brute force predictions (blue \cdot , red $+$, and black \times) and exact measurement(green line) on Sept. 12, 2005 in Atlanta	77
6.15	Brute force predictions (blue \cdot , red $+$, and black \times) and exact measurement(green line) on Sept. 13, 2005 in Atlanta	78
6.16	Brute force predictions (blue \cdot , red $+$, and black \times) and exact measurement(green line) on Sept. 14, 2005 in Atlanta	78
6.17	Brute force predictions (blue \cdot , red $+$, and black \times) and exact measurement(green line) on Sept. 15, 2005 in Atlanta	79
6.18	Autoregressive predictions (blue \cdot , red $+$, and black \times) and exact measurement(green line) on Sept. 1, 2005 in Atlanta	80
6.19	Autoregressive predictions (blue \cdot , red $+$, and black \times) and exact measurement(green line) on Sept. 2, 2005 in Atlanta	81
6.20	Autoregressive predictions (blue \cdot , red $+$, and black \times) and exact measurement(green line) on Sept. 3, 2005 in Atlanta	81
6.21	Autoregressive predictions (blue \cdot , red $+$, and black \times) and exact measurement(green line) on Sept. 4, 2005 in Atlanta	82
6.22	Autoregressive predictions (blue \cdot , red $+$, and black \times) and exact measurement(green line) on Sept. 5, 2005 in Atlanta	82

6.23	Autoregressive predictions (blue \cdot , red $+$, and black \times) and exact measurement(green line) on Sept. 6, 2005 in Atlanta	83
6.24	Autoregressive predictions (blue \cdot , red $+$, and black \times) and exact measurement(green line) on Sept. 7, 2005 in Atlanta	83
6.25	Autoregressive predictions (blue \cdot , red $+$, and black \times) and exact measurement(green line) on Sept. 8, 2005 in Atlanta	84
6.26	Autoregressive predictions (blue \cdot , red $+$, and black \times) and exact measurement(green line) on Sept. 9, 2005 in Atlanta	84
6.27	Autoregressive predictions (blue \cdot , red $+$, and black \times) and exact measurement(green line) on Sept. 10, 2005 in Atlanta	85
6.28	Autoregressive predictions (blue \cdot , red $+$, and black \times) and exact measurement(green line) on Sept. 11, 2005 in Atlanta	85
6.29	Autoregressive predictions (blue \cdot , red $+$, and black \times) and exact measurement(green line) on Sept. 12, 2005 in Atlanta	86
6.30	Autoregressive predictions (blue \cdot , red $+$, and black \times) and exact measurement(green line) on Sept. 13, 2005 in Atlanta	86
6.31	Autoregressive predictions (blue \cdot , red $+$, and black \times) and exact measurement(green line) on Sept. 14, 2005 in Atlanta	87
6.32	Autoregressive predictions (blue \cdot , red $+$, and black \times) and exact measurement(green line) on Sept. 15, 2005 in Atlanta	87
6.33	Three different sizes of triangulation of the northeast part of U.S.	88
6.34	Brute force predictions (blue \cdot , red $+$, and black \times) and exact measurement(green line) on Sept. 1, 2005 in Boston	89
6.35	Brute force predictions (blue \cdot , red $+$, and black \times) and exact measurement(green line) on Sept. 2, 2005 in Boston	90
6.36	Brute force predictions (blue \cdot , red $+$, and black \times) and exact measurement(green line) on Sept. 3, 2005 in Boston	90

6.37	Brute force predictions (blue \cdot , red $+$, and black \times) and exact measurement(green line) on Sept. 4, 2005 in Boston	91
6.38	Brute force predictions (blue \cdot , red $+$, and black \times) and exact measurement(green line) on Sept. 5, 2005 in Boston	91
6.39	Brute force predictions (blue \cdot , red $+$, and black \times) and exact measurement(green line) on Sept. 6, 2005 in Boston	92
6.40	Brute force predictions (blue \cdot , red $+$, and black \times) and exact measurement(green line) on Sept. 7, 2005 in Boston	92
6.41	Brute force predictions (blue \cdot , red $+$, and black \times) and exact measurement(green line) on Sept. 8, 2005 in Boston	93
6.42	Brute force predictions (blue \cdot , red $+$, and black \times) and exact measurement(green line) on Sept. 9, 2005 in Boston	93
6.43	Brute force predictions (blue \cdot , red $+$, and black \times) and exact measurement(green line) on Sept. 10, 2005 in Boston	94
6.44	Brute force predictions (blue \cdot , red $+$, and black \times) and exact measurement(green line) on Sept. 11, 2005 in Boston	94
6.45	Brute force predictions (blue \cdot , red $+$, and black \times) and exact measurement(green line) on Sept. 12, 2005 in Boston	95
6.46	Brute force predictions (blue \cdot , red $+$, and black \times) and exact measurement(green line) on Sept. 13, 2005 in Boston	95
6.47	Brute force predictions (blue \cdot , red $+$, and black \times) and exact measurement(green line) on Sept. 14, 2005 in Boston	96
6.48	Brute force predictions (blue \cdot , red $+$, and black \times) and exact measurement(green line) on Sept. 15, 2005 in Boston	96
6.49	Autoregressive predictions (blue \cdot , red $+$, and black \times) and exact measurement(green line) on Sept. 1, 2005 in Boston	97

6.50	Autoregressive predictions (blue \cdot , red $+$, and black \times) and exact measurement(green line) on Sept. 2, 2005 in Boston	98
6.51	Autoregressive predictions (blue \cdot , red $+$, and black \times) and exact measurement(green line) on Sept. 3, 2005 in Boston	98
6.52	Autoregressive predictions (blue \cdot , red $+$, and black \times) and exact measurement(green line) on Sept. 4, 2005 in Boston	99
6.53	Autoregressive predictions (blue \cdot , red $+$, and black \times) and exact measurement(green line) on Sept. 5, 2005 in Boston	99
6.54	Autoregressive predictions (blue \cdot , red $+$, and black \times) and exact measurement(green line) on Sept. 6, 2005 in Boston	100
6.55	Autoregressive predictions (blue \cdot , red $+$, and black \times) and exact measurement(green line) on Sept. 7, 2005 in Boston	100
6.56	Autoregressive predictions (blue \cdot , red $+$, and black \times) and exact measurement(green line) on Sept. 8, 2005 in Boston	101
6.57	Autoregressive predictions (blue \cdot , red $+$, and black \times) and exact measurement(green line) on Sept. 9, 2005 in Boston	101
6.58	Autoregressive predictions (blue \cdot , red $+$, and black \times) and exact measurement(green line) on Sept. 10, 2005 in Boston	102
6.59	Autoregressive predictions (blue \cdot , red $+$, and black \times) and exact measurement(green line) on Sept. 11, 2005 in Boston	102
6.60	Autoregressive predictions (blue \cdot , red $+$, and black \times) and exact measurement(green line) on Sept. 12, 2005 in Boston	103
6.61	Autoregressive predictions (blue \cdot , red $+$, and black \times) and exact measurement(green line) on Sept. 13, 2005 in Boston	103
6.62	Autoregressive predictions (blue \cdot , red $+$, and black \times) and exact measurement(green line) on Sept. 14, 2005 in Boston	104

6.63	Autoregressive predictions (blue \cdot , red $+$, and black \times) and exact measurement(green line) on Sept. 15, 2005 in Boston	104
6.64	Three different sizes of triangulation of the northeast part of U.S.	105
6.65	Brute force predictions (blue \cdot , red $+$, and black \times) and exact measurement(green line) on Sept. 1, 2005 in Cincinnati	106
6.66	Brute force predictions (blue \cdot , red $+$, and black \times) and exact measurement(green line) on Sept. 2, 2005 in Cincinnati	107
6.67	Brute force predictions (blue \cdot , red $+$, and black \times) and exact measurement(green line) on Sept. 3, 2005 in Cincinnati	107
6.68	Brute force predictions (blue \cdot , red $+$, and black \times) and exact measurement(green line) on Sept. 4, 2005 in Cincinnati	108
6.69	Brute force predictions (blue \cdot , red $+$, and black \times) and exact measurement(green line) on Sept. 5, 2005 in Cincinnati	108
6.70	Brute force predictions (blue \cdot , red $+$, and black \times) and exact measurement(green line) on Sept. 6, 2005 in Cincinnati	109
6.71	Brute force predictions (blue \cdot , red $+$, and black \times) and exact measurement(green line) on Sept. 7, 2005 in Cincinnati	109
6.72	Brute force predictions (blue \cdot , red $+$, and black \times) and exact measurement(green line) on Sept. 8, 2005 in Cincinnati	110
6.73	Brute force predictions (blue \cdot , red $+$, and black \times) and exact measurement(green line) on Sept. 9, 2005 in Cincinnati	110
6.74	Brute force predictions (blue \cdot , red $+$, and black \times) and exact measurement(green line) on Sept. 10, 2005 in Cincinnati	111
6.75	Brute force predictions (blue \cdot , red $+$, and black \times) and exact measurement(green line) on Sept. 11, 2005 in Cincinnati	111
6.76	Brute force predictions (blue \cdot , red $+$, and black \times) and exact measurement(green line) on Sept. 12, 2005 in Cincinnati	112

6.77	Brute force predictions (blue \cdot , red $+$, and black \times) and exact measurement (green line) on Sept. 13, 2005 in Cincinnati	112
6.78	Brute force predictions (blue \cdot , red $+$, and black \times) and exact measurement (green line) on Sept. 14, 2005 in Cincinnati	113
6.79	Brute force predictions (blue \cdot , red $+$, and black \times) and exact measurement (green line) on Sept. 15, 2005 in Cincinnati	113
6.80	Autoregressive predictions (blue \cdot , red $+$, and black \times) and exact measurement (green line) on Sept. 1, 2005 in Cincinnati	114
6.81	Autoregressive predictions (blue \cdot , red $+$, and black \times) and exact measurement (green line) on Sept. 2, 2005 in Cincinnati	115
6.82	Autoregressive predictions (blue \cdot , red $+$, and black \times) and exact measurement (green line) on Sept. 3, 2005 in Cincinnati	115
6.83	Autoregressive predictions (blue \cdot , red $+$, and black \times) and exact measurement (green line) on Sept. 4, 2005 in Cincinnati	116
6.84	Autoregressive predictions (blue \cdot , red $+$, and black \times) and exact measurement (green line) on Sept. 5, 2005 in Cincinnati	116
6.85	Autoregressive predictions (blue \cdot , red $+$, and black \times) and exact measurement (green line) on Sept. 6, 2005 in Cincinnati	117
6.86	Autoregressive predictions (blue \cdot , red $+$, and black \times) and exact measurement (green line) on Sept. 7, 2005 in Cincinnati	117
6.87	Autoregressive predictions (blue \cdot , red $+$, and black \times) and exact measurement (green line) on Sept. 8, 2005 in Cincinnati	118
6.88	Autoregressive predictions (blue \cdot , red $+$, and black \times) and exact measurement (green line) on Sept. 9, 2005 in Cincinnati	118
6.89	Autoregressive predictions (blue \cdot , red $+$, and black \times) and exact measurement (green line) on Sept. 10, 2005 in Cincinnati	119

6.90	Autoregressive predictions (blue \cdot , red $+$, and black \times) and exact measurement(green line) on Sept. 11, 2005 in Cincinnati	119
6.91	Autoregressive predictions (blue \cdot , red $+$, and black \times) and exact measurement(green line) on Sept. 12, 2005 in Cincinnati	120
6.92	Autoregressive predictions (blue \cdot , red $+$, and black \times) and exact measurement(green line) on Sept. 13, 2005 in Cincinnati	120
6.93	Autoregressive predictions (blue \cdot , red $+$, and black \times) and exact measurement(green line) on Sept. 14, 2005 in Cincinnati	121
6.94	Autoregressive predictions (blue \cdot , red $+$, and black \times) and exact measurement(green line) on Sept. 15, 2005 in Cincinnati	121

CHAPTER 1

INTRODUCTION

When we think about ozone, we often think about ozone in the upper atmosphere and the depletion of the ozone layer. However, when ozone is present in the lower atmosphere it can be toxic. Many human activities such as driving, daytime fueling of automobiles, and the normal practices of industrial facilities and electric utilities contribute to ground level ozone. We do not emit ozone directly into the air but these activities produce nitrogen oxides (NO_x) and volatile organic compounds (VOC). When exposed to heat and sunlight the NO_x and VOC produce ozone. High quantities of ground level ozone produce adverse reactions in humans. Headaches, coughing, eye irritation and chest discomfort can all be caused by an overexposure to ozone. For these reasons, we want to predict future ozone values so we can protect “at risk” groups of people from overexposure to ozone. Since there are many contributing factors it is hard to derive a model from first principles of chemistry and physics. Hence we look to statistics to create a predictive model.

In statistics, there are many approaches for prediction. See [Crambes, Kneip, and Sarda, 2009 (9)] and [Damon and Guillas’02, (10)] and its references. For problems with large data sets, like ozone prediction, we can use Functional Data Analysis (FDA). The statistical objects in FDA are curves, surfaces and manifolds, as well as traditional numbers or vectors (22; 13). FDA aggregates consecutive discrete recordings and views them as sample values of a random curve or random surface, keeping track of order or smoothness. A popular approach to ozone prediction is to use an the autoregressive functional linear model. A functional linear model is defined as a regression model with a random function as the explanatory variable and a real random variable as the response, (see Ramsay and Silverman, 2005 (22)). In a series of

papers [Cardot, Ferraty, and Sarda'99 (5)], [Cardot, Ferraty, and Sarda'03(6)], and [Cardot and Sarda'05 (7)], Cardot and his collaborators study the autoregressive approach for random curves and a functional associated with the random curves. Their research uses univariate splines to approximate the empirical estimator for the function associated with the random functional. In particular, they introduce consistent estimates based on functional principal components, and decompositions in univariate splines spaces. We use bivariate splines to extend the autoregressive approach to random surfaces and a functional associated with the random surfaces. We want to deal with random surfaces and a functional associated with those random surfaces over a domain of irregular shape and hence bivariate splines are an excellent tool to approximate the surfaces. In practice, random surfaces are only observed at scattered locations and bivariate splines offer a natural way to approximate the surfaces in these models, (see [Lai'08, (19)]). Hence we use bivariate splines as the explanatory variable in the autoregressive functional linear model. Then we investigate how the autoregressive process based on bivariate splines can be used for the ozone concentration forecasting. The univariate autoregressive model can be extended to the bivariate setting as follows. Let Y be a real valued random variable. Let \mathcal{D} be a polygonal domain in \mathbb{R}^2 . The regression model is:

$$Y = \int_{\mathcal{D}} g(s)X(s)ds + \varepsilon, \quad (1.1)$$

where X is a random surface over the domain \mathcal{D} , $g \in H$ where H is usually $L^2(\mathcal{D})$, and ε is a real random variable that satisfies $E\varepsilon = 0$ and $EX(s)\varepsilon = 0$ for all $s \in \mathcal{D}$. The objective is to approximate the function g defined on the two dimensional spatial domain \mathcal{D} from a given set of design points in \mathcal{D} . For the ozone prediction problem, we take the ozone concentration for a particular location at a specific time to the the real random variable Y . The random surfaces are created by fitting ozone concentrations at previous times over a region that contains the location of interest.

The organization of this dissertation is as follows. In Chapter 2 we introduce some of the basics of bivariate splines and some useful theorems for approximation as well as several

scattered data fitting schemes. The univariate autoregressive functional linear models are also presented in Chapter 2. In Chapter 3, we extend the autoregressive functional linear models to the bivariate setting. We closely follow the ideas in [Cardot, Ferraty, and Sarda'03, (6)] and use bivariate splines instead of univariate splines. In Chapter 4 we consider an alternative approach to solving (1.1) by using the optimal approximation property of splines. We call this method the “brute force” approach. It is a new approach to ozone prediction using bivariate splines introduced in [Guillas and Lai'08,(17)]. In Chapter 5, we extend the ideas of the brute force method to a model with a random function as the explanatory variable and a random function as the response. Chapter 6 implements the the methods in Chapters 3 and 4 on real data. For our numerical experiments, we use a data set of ozone concentrations from various Environmental Protection Agency (EPA) stations over the continental United States. The data was collected over a span of three months in 2005. We demonstrate how the two methods predict tomorrow's ozone concentrations for a particular city based on the previous ozone concentrations. In Chapter 7, we explain the similarities and differences between these two methods, make some conclusions about each approach, and discuss future research directions.

CHAPTER 2

PRELIMINARIES

2.1 BIVARIATE SPLINES

In this section, we review some basics of bivariate splines and the necessary spline theory we need for our application to functional linear models. Most of the spline results presented in this section can be found in [Lai and Schumaker'07, (21)]. Let \mathcal{D} be a polygonal domain in \mathbb{R}^2 and Δ a triangulation of \mathcal{D} . That is, Δ is a finite collection of triangles $T \subset \mathcal{D}$ such that $\cup_{T \in \Delta} T = \mathcal{D}$ and the intersection of any two triangles is either the empty set, a common edge, or a common vertex. For each $T \in \Delta$, let $|T|$ denote the length of the longest edge of T , and let ρ_T be the radius of the inscribed circle of T . The longest edge length in the triangulation Δ is denoted by $|\Delta|$ and is referred to as the size of the triangulation. For any triangulation Δ we define its shape parameter by

$$\kappa_\Delta := \frac{|\Delta|}{\rho_\Delta}, \quad (2.1)$$

where ρ_Δ is the minimum of the radii of the incircles of the triangles of Δ . The shape parameter for a single triangle, κ_T , satisfies

$$\kappa_T := \frac{|T|}{\rho_T} \leq \frac{2}{\tan(\theta_T/2)} \leq \frac{2}{\sin(\theta_T/2)}, \quad (2.2)$$

where θ_T is the smallest angle in the triangle T . The shape of a given triangulation affects how well we can approximate a function over the triangulation. Hence we have the following definition of a β -quasi-uniform triangulation.

Definition 2.1.1 (β -Quasi-Uniform Triangulation). *Let $0 < \beta < \infty$. A triangulation Δ is a β -quasi-uniform triangulation provided that*

$$\frac{|\Delta|}{\rho_\Delta} \leq \beta.$$

Once we have a triangulation, we define the spline space of degree d and smoothness r over that triangulation as follows:

Definition 2.1.2 (Spline Space). *Let Δ be a given triangulation of a domain \mathcal{D} . Then we define the spline space of smoothness r and degree d over Δ by,*

$$S_d^r(\Delta) = \{s \in C^r(\mathcal{D}) \mid s|_T \in \mathcal{P}_d, \forall T \in \Delta\},$$

where \mathcal{P}_d is the space of polynomials of degree at most d .

When working with polynomials on triangulations, it is more useful to work with barycentric coordinates instead of Cartesian coordinates. We define them in the following lemma.

Lemma 2.1.1 (Barycentric Coordinates). *Let $T = \langle (x_1, y_1), (x_2, y_2), (x_3, y_3) \rangle = \langle v_1, v_2, v_3 \rangle$ be a non-degenerate triangle. Then any point $v := (x, y) \in \mathbb{R}^2$ has a unique representation of the form*

$$v = b_1 v_1 + b_2 v_2 + b_3 v_3 \tag{2.3}$$

with

$$1 = b_1 + b_2 + b_3. \tag{2.4}$$

The numbers b_1, b_2, b_3 are called barycentric coordinates of the point v relative to the triangle T .

Proof. Writing (2.3) and (2.4) in matrix form yields

$$\begin{bmatrix} 1 & 1 & 1 \\ x_1 & x_2 & x_3 \\ y_1 & y_2 & y_3 \end{bmatrix} \begin{bmatrix} b_1 \\ b_2 \\ b_3 \end{bmatrix} = \begin{bmatrix} 1 \\ x \\ y \end{bmatrix} \tag{2.5}$$

The area of T is given by

$$A_T = \frac{1}{2} \det \begin{bmatrix} 1 & 1 & 1 \\ x_1 & x_2 & x_3 \\ y_1 & y_2 & y_3 \end{bmatrix}. \quad (2.6)$$

We know A_T is positive when T is a non-degenerate triangle and its vertices are numbered in a counter-clockwise order. Hence (2.5) is a non singular system and by Cramer's rule we have the following formulas for the barycentric coordinates:

$$b_1 = \frac{1}{2A_T} \det \begin{bmatrix} 1 & 1 & 1 \\ x & x_2 & x_3 \\ y & y_2 & y_3 \end{bmatrix}, \quad b_2 = \frac{1}{2A_T} \det \begin{bmatrix} 1 & 1 & 1 \\ x_1 & x & x_3 \\ y_1 & y & y_3 \end{bmatrix}, \quad b_3 = \frac{1}{2A_T} \det \begin{bmatrix} 1 & 1 & 1 \\ x_1 & x_2 & x \\ y_1 & y_2 & y \end{bmatrix}. \quad (2.7)$$

□

Lemma 2.1.2 presents a useful algebraic characterization of the barycentric coordinates, b_1 , b_2 and b_3 that also have the nice geometric interpretation as areas of the sub-triangles formed by the given point v (see Figure 2.1).

Lemma 2.1.2. *For each $i = 1, 2, 3$ the function b_i is a linear polynomial in x and y which assumes the value 1 at the vertex v_i and vanishes at all points on the edge of T opposite v_i .*

Proof. When we expand (2.7) for b_1 by the first column, we obtain

$$b_1 = \frac{(x_2y_3 - y_2x_3) - x(y_3 - y_2) + y(x_3 - x_2)}{2A_T}.$$

Hence we see that b_1 is in fact a linear polynomial. When we evaluate b_1 at v_1 we obtain

$$b_1|_{v_1} = \frac{1}{2A_T} \det \begin{bmatrix} 1 & 1 & 1 \\ x_1 & x_2 & x_3 \\ y_1 & y_2 & y_3 \end{bmatrix} = \frac{1}{A_T} A_T = 1.$$

by (2.6). Finally, any point on the edge opposite of v_1 lies on the line between v_2 and v_3 and hence can be written as a linear combination of v_2 and v_3 . Therefore the determinate of the matrix in (2.7) is zero and so b_1 is zero. The proofs for b_2 and b_3 are similar. □

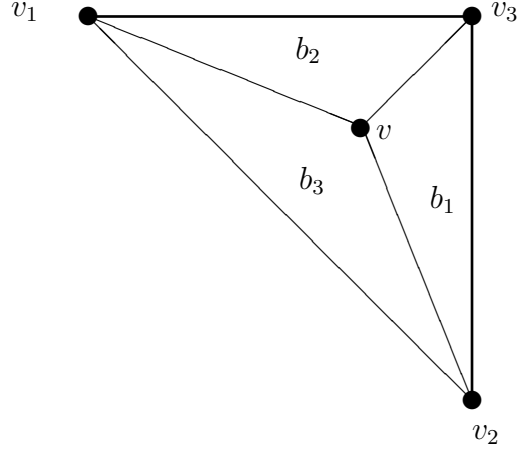


Figure 2.1: For the triangle above, $T = \langle v_1, v_2, v_3 \rangle$, the barycentric coordinates b_1 , b_2 and b_3 for the point v have the geometric interpretation of being the areas of the sub-triangles formed by v .

We use barycentric coordinates to define Bernstein-Bézier polynomials over a given triangle.

Definition 2.1.3 (Bernstein-Bézier Polynomials). *For a fixed degree $d > 0$ and non-negative integers i, j, k such that $i + j + k = d$, we define the Bernstein-Bézier polynomials to be*

$$B_{ijk}^d(x, y) = \frac{d!}{i!j!k!} b_1^i b_2^j b_3^k.$$

The Bernstein-Bézier polynomials are useful because they form a basis for the polynomials of degree d over a given triangle, T .

Theorem 2.1.1. *The set*

$$\mathcal{B}^d := \{B_{ijk}^d\}_{i+j+k=d} \tag{2.8}$$

of Bernstein-Bézier polynomials is a basis for the space of polynomials \mathcal{P}_d .

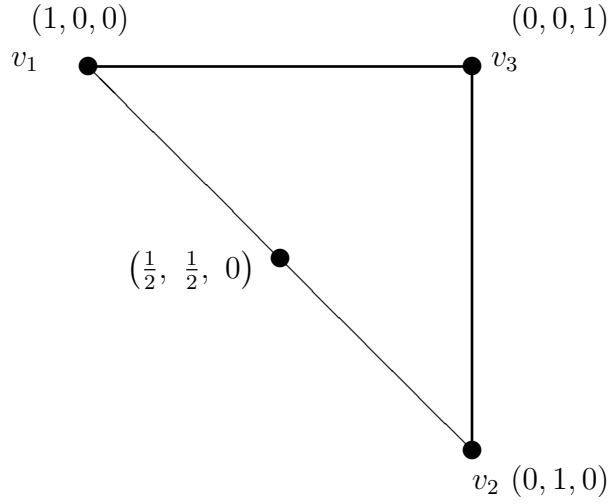


Figure 2.2: For the triangle above defined by v_1 , v_2 and v_3 the barycentric coordinates are shown at each of the vertices and at the center of the edge opposite v_3 .

Proof. The size of \mathcal{B}^d is $\binom{d+2}{2}$ which is the same dimension as \mathcal{P}_d . Hence we only need to show that all the polynomials of the form $x^\nu y^\mu$ for $\nu + \mu \leq d$ are in the span of \mathcal{B}^d . First, we show that $1 \in \mathcal{B}^d$. From the trinomial expansion we have

$$1 = (b_1 + b_2 + b_3)^d = \sum_{i+j+k=d} \frac{d!}{i!j!k!} b_1^i b_2^j b_3^k, \quad (2.9)$$

and hence

$$\sum_{i+j+k=d} B_{ijk}^d(v) \equiv 1 \quad \text{for all } v \in \mathbb{R}^2. \quad (2.10)$$

Hence $1 \in \mathcal{B}^d$ and we say the Bernstein-Bézier polynomials form a partition of unity. Now we show that $x, y \in \mathcal{B}^d$. By (2.3), we have

$$\begin{bmatrix} x \\ y \end{bmatrix} = b_1 \begin{bmatrix} x_1 \\ y_1 \end{bmatrix} + b_2 \begin{bmatrix} x_2 \\ y_2 \end{bmatrix} + b_3 \begin{bmatrix} x_3 \\ y_3 \end{bmatrix}. \quad (2.11)$$

Using the partition of unity (2.10) with $d - 1$, we have

$$\begin{aligned}
x &= b_1x_1 + b_2x_2 + b_3x_3 \\
&= (b_1x_1 + b_2x_2 + b_3x_3) \left(\sum_{i+j+k=d-1} B_{ijk}^{d-1}(x, y) \right) \\
&= \sum_{i+j+k=d} \frac{1}{d} (ix_1 + jx_2 + kx_3) B_{ijk}^d(x, y).
\end{aligned} \tag{2.12}$$

Similarly for y we have

$$y = \sum_{i+j+k=d} \frac{1}{d} (iy_1 + jy_2 + ky_3) B_{ijk}^d(x, y). \tag{2.13}$$

Now, we proceed by induction. Assume that the theorem holds for polynomials of degree $d - 1$. Then we have

$$x^{\nu-1}y^\mu = \sum_{i+j+k=d-1} c_{ijk} B_{ijk}^{d-1}(x, y)$$

for some coefficients c_{ijk} . To get a polynomial of degree d , we multiply by x using (2.12),

$$x^\nu y^\mu = (b_1x_1 + b_2x_2 + b_3x_3) \sum_{i+j+k=d-1} c_{ijk} B_{ijk}^{d-1}(x, y) \tag{2.14}$$

$$= \sum_{i+j+k=d} d_{ijk} B_{ijk}^d(x, y) \tag{2.15}$$

for some constants d_{ijk} . □

Since the Bernstein-Bézier polynomials form a basis for \mathcal{P}_d , we can write any polynomial of degree d over T uniquely in terms of Bernstein-Bézier polynomials. We call this the B-form of a polynomial.

Definition 2.1.4 (B-Form). *Let $s \in \mathcal{P}^d$ satisfy*

$$s|_T = \sum_{i+j+k=d} c_{ijk} B_{ijk}^d(x, y).$$

We use the coefficient vector $\mathbf{s} = (c_{ijk}, i + j + k = d, T \in \Delta)$ to denote a spline function in $S_d^{-1}(\Delta)$ [Lai and Schumaker'07, (21)].

The coefficients c_{ijk} are displayed using locations called domain points.

Definition 2.1.5 (Domain Points). For a given triangle $T = \langle (x_1, y_1), (x_2, y_2), (x_3, y_3) \rangle$ the domain points are defined as

$$\xi_{ijk} = \frac{i}{d}(x_1, y_1) + \frac{j}{d}(x_2, y_2) + \frac{k}{d}(x_3, y_3)$$

for $i + j + k = d$.

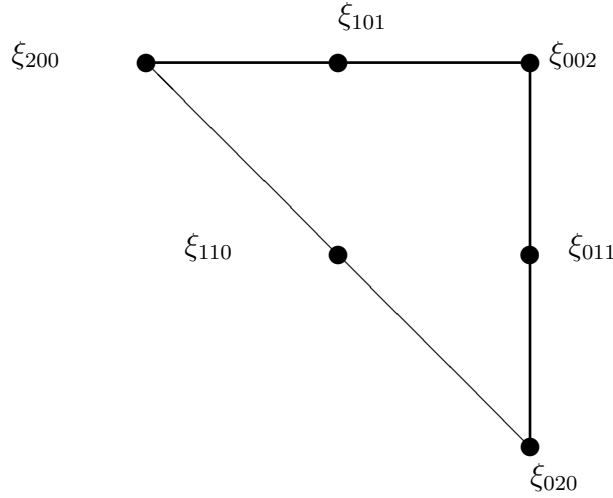


Figure 2.3: Set of domain points for a polynomial of degree 2

To store polynomials in B-form, we only need to store the coefficients. Fortunately, there is an efficient and stable algorithm to evaluate polynomials in B-form by using only the coefficients. This algorithm is known as the de Casteljau Algorithm and is based on the following recurrence relation

$$B_{ijk}^d = b_1 B_{i-1,j,k}^{d-1} + b_2 B_{i,j-1,k}^{d-1} + b_3 B_{i,j,k-1}^{d-1}. \quad (2.16)$$

The above recurrence relation follows directly from the definition of B_{ijk}^d and we use the convention that expressions with negative subscripts are considered to be zero.

Theorem 2.1.2 (de Casteljau Algorithm). Let p be a polynomial with coefficients $c_{ijk}^{(0)} := c_{ijk}$, $i + j + k = d$. Suppose v has barycentric coordinates $b := (b_1, b_2, b_3)$. Let

$$c_{ijk}^{(\ell)}(b) := b_1 c_{i+1,j,k}^{(\ell-1)}(b) + b_2 c_{i,j+1,k}^{(\ell-1)}(b) + b_3 c_{i,j,k+1}^{(\ell-1)}(b), \quad (2.17)$$

for $i + j + k = d - \ell$. Then

$$p(v) = \sum_{i+j+k=d-\ell} c_{ijk}^{(\ell)}(b) B_{ijk}^{d-\ell}(v), \quad (2.18)$$

for $0 \leq \ell \leq d$. In particular,

$$p(v) = c_{000}^{(d)}(b). \quad (2.19)$$

Proof. The de Casteljau algorithm is proved by induction. We note that (2.18) is true for $\ell = 0$. Now, we assume it holds for $\ell - 1$ and use (2.16) for degree $d - \ell + 1$

$$\begin{aligned} p(v) &= \sum_{i+j+k=d-\ell+1} c_{ijk}^{(\ell-1)} B_{ijk}^{d-\ell+1}(v) \\ &= \sum_{i+j+k=d-\ell+1} c_{ijk}^{(\ell-1)} (b_1 B_{i-1,j,k}^{d-\ell}(v) + b_2 B_{i,j-1,k}^{d-\ell}(v) + b_3 B_{i,j,k-1}^{d-\ell}(v)). \end{aligned}$$

Now, we split the above into three sums:

$$\begin{aligned} \sum_{i+j+k=d-\ell+1, i \geq 1} b_1 c_{ijk}^{(\ell-1)} B_{i-1,j,k}^{d-\ell}(v) &= \sum_{i+j+k=d-\ell} b_1 c_{i+1,j,k}^{(\ell-1)} B_{ijk}^{d-\ell}(v) \\ \sum_{i+j+k=d-\ell+1, j \geq 1} b_2 c_{ijk}^{(\ell-1)} B_{i,j-1,k}^{d-\ell}(v) &= \sum_{i+j+k=d-\ell} b_2 c_{i,j+1,k}^{(\ell-1)} B_{ijk}^{d-\ell}(v) \\ \sum_{i+j+k=d-\ell+1, k \geq 1} b_3 c_{ijk}^{(\ell-1)} B_{i,j,k-1}^{d-\ell}(v) &= \sum_{i+j+k=d-\ell} b_3 c_{i,j,k+1}^{(\ell-1)} B_{ijk}^{d-\ell}(v). \end{aligned}$$

Combining, the above sums yields (2.18). For $\ell = d$, (2.18) reduces to (2.19) because the only Bernstein-Bézier polynomial of degree zero is $B_{000}^0 \equiv 1$. \square

One important result of the de Casteljau algorithm is that the intermediate coefficients $c_{ijk}^{(\ell)}$ produced in the algorithm are polynomials of degree ℓ in v . Hence we have the following result.

Theorem 2.1.3. *The coefficients in the de Casteljau algorithm in equation (2.18) are given by*

$$c_{ijk}^{(\ell)} = \sum_{\nu+\mu+\kappa=\ell} c_{i+\nu,j+\mu,k+\kappa} B_{\nu\mu\kappa}^{\ell}(v), \quad i + j + k = d - \ell. \quad (2.20)$$

Proof. We start by noting that

$$c_{ijk}^{(1)} = c_{i+1,j,k}b_1 + c_{i,j+1,k}b_2 + c_{i,j,k+1}b_3, \quad i + j + k = d - 1 \quad (2.21)$$

are linear polynomials since b_1 , b_2 and b_3 are linear polynomials in v . Now, we rewrite the equation above as

$$c_{ijk}^{(1)} = (b_1E_1 + b_2E_2 + b_3E_3)c_{ijk},$$

where we define $E_1c_{ijk} = c_{i+1,j,k}$, $E_2c_{ijk} = c_{i,j+1,k}$ and $E_3c_{ijk} = c_{i,j,k+1}$. Similarly, we can express (2.17) in the de Casteljau algorithm as

$$c_{ijk}^{(\ell)} = (b_1E_1 + b_2E_2 + b_3E_3)c_{ijk}^{(\ell-1)}.$$

Now, we repeatedly use the formula for $c_{ijk}^{(\ell)}$, $\ell - 1$ times and apply the trinomial expansion to obtain:

$$\begin{aligned} c_{ijk}^{(\ell)} &= (b_1E_1 + b_2E_2 + b_3E_3)^\ell c_{ijk} \\ &= \sum_{\nu+\mu+\kappa=\ell} B_{\nu\mu\kappa}^\ell(v) E_1^\nu E_2^\mu E_3^\kappa c_{ijk} \\ &= \sum_{\nu+\mu+\kappa=\ell} c_{i+\nu,j+\mu,k+\kappa} B_{\nu\mu\kappa}^\ell. \end{aligned}$$

□

The de Casteljau Algorithm is also helpful in computing the directional derivative at a given point. Before we discuss the derivative we need the notion of directional coordinates of a vector u .

Definition 2.1.6 (Directional Coordinates). *The directional coordinates of a vector u are the triple (a_1, a_2, a_3) , defined by*

$$a_i := \alpha_i - \beta_i, \quad i = 1, 2, 3 \quad (2.22)$$

where $(\alpha_1, \alpha_2, \alpha_3)$ and $(\beta_1, \beta_2, \beta_3)$ are the barycentric coordinates of the two points w and \hat{w} such that $u := w - \hat{w}$.

Note that while the barycentric coordinates (b_1, b_2, b_3) of a point v sum to one, the directional coordinates (a_1, a_2, a_3) of a vector u sum to zero.

Theorem 2.1.4 (Differentiation). *Let $u := w - v$ be a vector with directional coordinates (a_1, a_2, a_3) with $a_i = \alpha_i - \beta_i, i = 1, 2, 3$. Then for any $i + j + k = d$, the derivative in the direction u is given by*

$$D_u B_{ijk}^d(v) = d [a_1 B_{i-1,j,k}^{d-1}(v) + a_2 B_{i,j-1,k}^{d-1}(v) + a_3 B_{i,j,k-1}^{d-1}(v)] \quad (2.23)$$

and

$$D_u p(v) = d \sum_{i+j+k=d-1} c_{ijk}^{(1)}(a) B_{ijk}(v), \quad (2.24)$$

where $c_{ijk}^{(1)}(a)$ are the quantities arising in the first step of the de Casteljau Algorithm (2.1.2) based on the triple a .

Proof. Let (b_1, b_2, b_3) be the barycentric coordinates for the point v . Then the barycentric coordinates of the point $v + tu$ are $(b_1 + ta_1, b_2 + ta_2, b_3 + ta_3)$ and

$$B_{ijk}^d(v + tu) = \frac{d!}{i!j!k!} [(b_1 + ta_1)^i (b_2 + ta_2)^j (b_3 + ta_3)^k].$$

Now, we differentiate with respect to t and evaluate the result at $t = 0$, yielding

$$\begin{aligned} D_u B_{ijk}^d(v) &= \frac{d!}{i!j!k!} [i b_i^{i-1} a_1 b_2^j b_3^k + b_1^i j b_2^{j-1} a_2 b_3^k + b_1^i b_2^j k b_3^{k-1} a_3] \\ &= d [a_1 B_{i-1,j,k}^{d-1}(v) + a_2 B_{i,j-1,k}^{d-1}(v) + a_3 B_{i,j,k-1}^{d-1}(v)]. \end{aligned}$$

To obtain (2.24), we differentiate the B-form of the polynomial and apply (2.23),

$$\begin{aligned} D_u p(v) &= \sum_{i+j+k=d} c_{ijk} D_u B_{ijk}^d(v) \\ &= \sum_{i+j+k=d} c_{ijk} (d [a_1 B_{i-1,j,k}^{d-1}(v) + a_2 B_{i,j-1,k}^{d-1}(v) + a_3 B_{i,j,k-1}^{d-1}(v)]) \\ &= d \sum_{i+j+k=d-1} c_{i+1,j,k} a_1 B_{ijk}^{d-1}(v) + c_{i,j+1,k} a_2 B_{ijk}^{d-1}(v) + c_{i,j,k+1} a_3 B_{ijk}^{d-1}(v) \\ &= d \sum_{i+j+k=d-1} c_{ijk}^{(1)}(a) B_{ijk}(v). \end{aligned}$$

□

By applying Theorem 2.1.4 repeatedly we obtain the following theorem for multiple derivatives.

Theorem 2.1.5. *Let p be a polynomial written in B-form, and suppose u is a vector with directional coordinates $a := (a_1, a_2, a_3)$. Then for any $1 \leq m \leq d$,*

$$D_u^m p(v) = \frac{d!}{(d-m)!} \sum_{i+j+k+d-m} c_{ijk}^{(m)}(a) B_{ijk}^{d-m}(v), \quad (2.25)$$

where $c_{ijk}^{(m)}(a)$ are the quantities obtained after m steps of the de Casteljau algorithm applied to the coefficients of p using the triple a .

Polynomials in B-form also have nice integration and inner product formulas.

Theorem 2.1.6 (Integration). *Let p be a polynomial written in B-form over a triangle T with coefficients $c_{ijk}, i + j + k = d$. Then*

$$\int_T p(x, y) \, dx dy = \frac{A_T}{\binom{d+2}{2}} \sum_{i+j+k=d} c_{ijk}, \quad (2.26)$$

where A_T is the area of T .

Proof. Using barycentric coordinates as defined by (2.5), we can write

$$\begin{bmatrix} x \\ y \end{bmatrix} = \begin{bmatrix} x_1 - x_3 & x_2 - x_3 \\ y_1 - y_3 & y_2 - y_3 \end{bmatrix} + \begin{bmatrix} x_3 \\ y_3 \end{bmatrix}, \quad (2.27)$$

and it follows the corresponding determinate is $2A_T$ as in (2.6). Now using the fact

$$\int_0^1 x^i (1-x)^j dx = \frac{i!j!}{(i+j+1)!}, \quad (2.28)$$

we have

$$\begin{aligned} \frac{i!j!k!}{d!} \int_T B_{ijk}^d(x, y) dx dy &= \int_T b_1^i b_2^j (1-b_1-b_2)^k db_1 db_2 \\ &= 2A_T \int_0^1 \int_0^{1-b_1} b_1^i b_2^j (1-b_1-b_2)^k db_1 db_2 \\ &= 2A_T \int_0^1 b_1^i (1-b_1)^{j+k+1} \int_0^{1-b_1} \left(\frac{b_2}{1-b_1}\right)^j \left(1 - \frac{b_2}{1-b_1}\right)^k \frac{db_2}{(1-b_1)} db_1 \\ &= 2A_T \int_0^1 u^i (1-u)^{j+k+1} du \int_0^1 t^j (1-t)^k dt \\ &= 2A_T \frac{i!(j+k+1)!}{(i+j+k+2)!} \frac{j!k!}{(j+k+1)!}. \end{aligned}$$

Hence we have

$$\int_T B_{ijk}^d(x, y) dx dy = \frac{2A_T}{(d+2)(d+1)} = \frac{A_T}{\binom{d+2}{2}}, \quad (2.29)$$

for all $i + j + k = d$. Then (2.26) follows by integrating the B-form of a polynomial term by term. \square

The inner product for is given in the following theorem [Chui and Lai'90, (8)].

Theorem 2.1.7 (Inner Product).

$$\int_T B_{ijk}(x, y) B_{\nu\mu\kappa}(x, y) dx dy = \frac{\binom{i+\nu}{i} \binom{j+\mu}{j} \binom{k+\kappa}{k} A_T}{\binom{2d}{d} \binom{2d+2}{2}}. \quad (2.30)$$

Proof. Consider the product of two Bernstein-Bézier polynomials

$$B_{ijk}^d B_{\nu\mu\kappa}^d = \frac{\binom{i+\nu}{i} \binom{j+\mu}{j} \binom{k+\kappa}{k}}{\binom{2d}{d}} B_{i+\nu, j+\mu, k+\kappa}^{2d}, \quad (2.31)$$

then applying (2.29) yields (2.30). \square

Now, that we have defined polynomials over a single triangle we want to connect the triangles in such a way that they connect smoothly to form our splines. Hence we introduce the following conditions for smoothness.

Theorem 2.1.8 (Smoothness). *Let $T = \langle v_1, v_2, v_3 \rangle$ and*

$\tilde{T} = \langle v_4, v_3, v_2 \rangle$ be triangles sharing the edge $e := \langle v_2, v_3 \rangle$. Let

$$p(v) = \sum_{i+j+k=d} c_{ijk} B_{ijk}^d(v) \quad (2.32)$$

and

$$\tilde{p}(v) = \sum_{i+j+k=d} \tilde{c}_{ijk} \tilde{B}_{ijk}^d(v), \quad (2.33)$$

where $\{B_{ijk}^d\}$ and $\{\tilde{B}_{ijk}^d\}$ are the Bernstein-Bézier basis polynomials associated with T and \tilde{T} respectively. Suppose u is any direction not parallel to e . Then

$$D_u^n p(v) = D_u^n \tilde{p}(v), \quad (2.34)$$

$v \in e$ and $n = 0, \dots, r$ if and only if

$$\tilde{c}_{nj k} = \sum_{\nu+\mu+\kappa=n} c_{\nu,k+\mu,j+\kappa} B_{\nu\mu\kappa}^n(v_4) \quad (2.35)$$

for $j + k = d - n$ and $n = 0, \dots, r$.

Proof. Along the edge, e both p and \tilde{p} reduce to a univariate splines hence for them to join continuously we need

$$\tilde{c}_{0jk} = c_{0jk}, \quad \text{for } j + k = d, \quad (2.36)$$

which is the case when $r = 0$. Now, for $r > 0$ we start by noting that all of the derivatives of p and \tilde{p} corresponding to the direction of $v_3 - v_2$ agree at every point along e , and all other derivatives will be linear combinations of $D_{v_4-v_2}$ and $D_{v_3-v_2}$. Hence (2.34) holds if and only if it holds for direction $u = v_4 - v_2$. Let $b = (b_1, b_2, b_3)$ be the barycentric coordinates of v_4 relative to T . Then the directional coordinates of u with respect to T and \tilde{T} are $a := (b_1, b_2 - 1, b_3)$ and $\tilde{a} := (1, 0, -1)$, respectively. Now, by Theorem 2.1.5 for each $0 \leq n \leq r$,

$$D_u^n p|_e = \frac{d!}{(d-n)!} \sum_{j+k=d-n} c_{0jk}^{(n)}(a) B_{0jk}^{d-n},$$

and

$$D_u^n \tilde{p}|_e = \frac{d!}{(d-n)!} \sum_{j+k=d-n} \tilde{c}_{0jk}^{(n)}(\tilde{a}) \tilde{B}_{0jk}^{d-n},$$

where $c_{ijk}^{(n)}(a)$ and $\tilde{c}_{ijk}^{(n)}(\tilde{a})$ are the coefficients obtained by applying n steps of the de Casteljau algorithm to $\{c_{ijk}\}$ and $\{\tilde{c}_{ijk}\}$ using a and \tilde{a} respectively. For any point v on the edge e , we have $B_{0kj}^{d-n}(v) = \tilde{B}_{0kj}(v)$, hence (2.34) holds if and only if

$$\tilde{c}_{0jk}^{(n)}(\tilde{a}) = c_{0kj}^{(n)}(a), \quad j + k = d - n, \quad n = 0, \dots, r. \quad (2.37)$$

Recall that $\tilde{a} := (1, 0, -1)$ then applying (2.20) yields

$$\tilde{c}_{ijk}^{(n)}(\tilde{a}) = \sum_{m=0}^n (-1)^{n-m} \binom{n}{m} \tilde{c}_{m,j,d-j-m}, \quad j + k = d - n. \quad (2.38)$$

Although, if we follow the proof of Theorem 2.1.3 we have

$$\begin{aligned}
c_{0jk}^{(n)} &= (b_1 E_1 + (b_2 - 1)E_2 + b_3 E_3)^n c_{ijk} \\
&= (b_1 E_1 + b_2 E_2 + b_3 E_3 - E_2)^n c_{ijk} \\
&= \sum_{m=0}^n (-1)^{n-m} \binom{n}{m} (b_1 E_1 + b_2 E_2 + b_3 E_3)^m c_{0,k+n-m,j} \\
&= \sum_{m=0}^n (-1)^{n-m} \binom{n}{m} c_{0,d-j-m,j}^{(m)}(b)
\end{aligned}$$

for $j + k = d - n$. Therefore (2.37) holds if and only if

$$\tilde{c}_{n,j,d-j-n} = c_{0,d-j-n,j}^{(n)}(b), \quad j = 0, \dots, n, \quad n = 0, \dots, r,$$

which is equivalent to (2.35). □

One of the main reasons we want to use splines is for their optimal approximation order. We need to show several results before we can get to the main theorem. We start with a result that connects the q -norms and ∞ -norms of polynomials on a given triangle. The following results can be found in [Lai and Schumaker'07, (21)].

Theorem 2.1.9. *Let T be a triangle, and let A_T be its area. Then for all $p \in \mathcal{P}_d$ and all $1 \leq q < \infty$,*

$$A_T^{-1/q} \|p\|_{q,T} \leq \|p\|_T \leq K A_T^{-1/q} \|p\|_{q,T}, \quad (2.39)$$

where K is a constant depending only on d and $\|p\|_T := \text{ess sup}_{u \in T} |p(u)|$.

Proof. By the definition of norm, we have

$$A_T^{-1/q} \|p\|_{q,T} \leq \|p\|_T.$$

For the second inequality, we consider the standard triangle $\tilde{T} = \{(x, y) : x \leq 0, y \leq 1, x + y \leq 1\}$ and use the fact that all norms on the finite dimensional space of polynomials are equivalent. Then

$$\|g\|_{\tilde{T}} \leq K \|g\|_{q,\tilde{T}},$$

for all polynomials $g \in \mathcal{P}_d$, where K is a constant depending only on d . Now, we can apply a change of variables to map any polynomial $p \in \mathcal{P}_d$ into a polynomial $g \in \mathcal{P}_d$ with $\|g\|_{\tilde{T}} = \|p\|_T$ and $\|g\|_{q,\tilde{T}} = A_T^{-1/q} \|p\|_{q,T}$ and hence

$$\|p\|_T = \|g\|_{\tilde{T}} \leq K \|g\|_{q,\tilde{T}} = K A_T^{-1/q} \|p\|_{q,T}.$$

□

The next theorem links the ∞ -norms of polynomials to the coefficients of their B-form representation. First need the following result which can be found in [Lai and Schumaker'07, (21)].

Lemma 2.1.3. *Let $\{g_1, \dots, g_n\}$ be the the Bernstein-Bézier basis polynomials of degree d and let $\{t_1, \dots, t_n\}$ be the associated domain points arranged in the same order. Define*

$$M := [g_j(t_i)]_{i,j=1}^n, \tag{2.40}$$

then the matrix M is nonsingular.

Theorem 2.1.10. *Let p be a polynomial written in B-form with coefficient vector c . Then*

$$\frac{\|c\|_\infty}{K} \leq \|p\|_T \leq \|c\|_\infty, \tag{2.41}$$

where K is a constant that depends only on d .

Proof. By Lemma 2.1.3, the coefficient vector c of a spline in B-form can be computed from the system of equations

$$Mc = r$$

where $r := (p(t_1), \dots, p(t_n))^T$. Then we have

$$\|c\|_\infty = \|M^{-1}r\|_\infty \leq \|M^{-1}\| \|r\|.$$

We obtain the first inequality by observing that $\|r\|_\infty \leq \|p\|_T$. The second inequality follows from geometric interpretation of barycentric coordinates which implies

$$0 \leq B_{ijk}^d(v) \leq 1 \text{ for all } v \in T, \tag{2.42}$$

and the partition of unity property of Bernstein-Bézier polynomials (2.10). □

Now, we can extend Theorem 2.1.10 to the q -norms of polynomials.

Theorem 2.1.11. *Given $1 \leq q < \infty$ there exists a constant $K > 0$ depending only on d such that if p is a polynomial written in B -form, then*

$$\frac{A_T^{1/q}}{K} \|c\|_q \leq \|p\|_{q,T} \leq A_T^{1/q} \|c\|_q. \quad (2.43)$$

Proof. First we note that

$$\|p\|_T \leq \|c\|_\infty \leq K_1 \|p\|_T \quad (2.44)$$

by Theorem 2.1.10. When we combine (2.44) with (2.39) and

$$\|c\|_q^q \leq \binom{d+2}{2} \|c\|_\infty^q$$

we obtain the first inequality. Combining (2.44) with (2.39) and $\|c\|_\infty \leq \|c\|_q$ yields the second inequality. \square

To develop error bounds we will apply the Markov inequality to compare the size of the derivative of a polynomial to the size of the polynomial itself on a given triangle T .

Theorem 2.1.12. *Let $T := \langle v_1, v_2, v_3 \rangle$ be a triangle, and fix $1 \leq q \leq \infty$. Then there exists a constant K depending only on d such that for every polynomial $p \in \mathcal{P}_d$, and any nonnegative integers α and β with $0 \leq \alpha + \beta \leq d$,*

$$\|D_x^\alpha D_y^\beta p\|_{q,T} \leq \frac{K}{\rho_T^{\alpha+\beta}} \|p\|_{q,T}, \quad 0 \leq \alpha + \beta \leq d, \quad (2.45)$$

where ρ_T denotes the radius of the largest circle inscribed in T .

Proof. The unit vector u pointing in the direction of the x -axis has the barycentric coordinates $(y_2 - y_3, y_3 - y_1, y_1 - y_2)/2A_T$, where A_T is the area of the triangle T . Thus for

$$p = \sum_{i+j+k=d} c_{ijk} B_{ijk}^d$$

we have

$$D_x p = \frac{d}{2A_T} \sum_{i+j+k=d-1} [(y_2 - y_3)c_{i+1,j,k} + (y_3 - y_1)c_{i,j+1,k} + (y_1 - y_2)c_{i,j,k+1}] B_{ijk}^{d-1}.$$

By the partition of unity property of B_{ijk}^{d-1} , we have

$$\|D_x p\|_{\infty, T} \leq \frac{d\|c\|_{\infty}(|y_2 - y_3| + |y_3 - y_1| + |y_1 - y_2|)}{2A_T}.$$

Since the area of a triangle is equal to its perimeter times $\rho_T/2$ it follows that

$$\frac{\rho_T}{2}(|y_2 - y_3| + |y_3 - y_1| + |y_1 - y_2|) \leq A_T.$$

Hence

$$\|D_x p\|_{\infty, T} \leq \frac{d\|c\|}{\rho_T}.$$

Now, we combine $\|c\|_{\infty} \leq \|c\|_q$ with Theorem 2.1.9 and Theorem 2.1.11 to obtain

$$\|D_x p\|_{q, T} \leq A_T^{1/q} \|D_x p\|_{\infty, T} \leq \frac{dA_T^{1/q}}{\rho_T} \|c\|_{\infty} \leq \frac{dA_T^{1/q}}{\rho_T} \|c\|_q \leq \frac{dK}{\rho_T} \|c\|_{q, T}$$

where K is the constant in (2.43). The proof for $\|D_y\|_{q, T}$ is similar and the general result follows from induction. \square

Now we can approximate any function in \mathcal{C}^{d+1} on a triangle T with approximation order $\mathcal{O}(|T|^{d+1})$ by the polynomial of degree d which interpolates f at the set of domain points. Before we can prove the main result on approximation order we need to introduce Lagrange polynomials, quasi-interpolants and some important inequalities we need to estimate our error bounds. We start by using the Lagrange polynomials, we can express the polynomial that interpolates the domain points by

$$p_{ijk}(v) := \prod_{\mu=0}^{i-1} \frac{a_{\mu}(v)}{a_{\mu}(\xi_{ijk})} \prod_{\nu=0}^{j-1} \frac{b_{\nu}(v)}{b_{\nu}(\xi_{ijk})} \prod_{\kappa=0}^{k-1} \frac{c_{\kappa}(v)}{c_{\kappa}(\xi_{ijk})} \quad (2.46)$$

where $a_{\mu}(v)$ is the line passing through the points $\xi_{\mu j k}$ with $\mu + j + k = d$, $b_{\nu}(v)$ is the line passing through the points $\xi_{i \nu k}$ with $i + \nu + k = d$, and $c_{\kappa}(v)$ is the line passing through the points $\xi_{i j \kappa}$ with $i + j + \kappa = d$. We also use the convention that a product is defined to be one when the upper limit is negative.

Theorem 2.1.13. *Let $\{\xi_{ijk}\}_{i+j+k=d}$ be the domain points defined in (2.1.5) and let $\{p_{ijk}\}_{i+j+k=d}$ be the corresponding Lagrange polynomials defined in (2.46). Then there*

exists a constant K depending only on d and θ_T such that for every $f \in \mathcal{C}^{m+1}(T)$ with $0 \leq m \leq d$, the interpolating polynomial

$$p_f = \sum_{i+j+k=d} f(\xi_{ijk}) p_{ijk}$$

satisfies

$$\|D_x^\alpha D_y^\beta (f - p_f)\|_T \leq K |T|^{m+1-\alpha-\beta} |f|_{m+1,T} \quad (2.47)$$

for all $0 \leq \alpha + \beta \leq m$ and $|f|_{m+1,T}$ denotes the L_∞ norm of the $m+1$ st derivative of f over T .

Proof. For each domain point, we let $\xi_{ijk} = (\xi_{ijk}^x, \xi_{ijk}^y)$ for $i+j+k=d$. Applying the Taylor expansion to f about a fixed point $(x, y) \in T$ yields

$$\begin{aligned} f(\xi_{ijk}) &= \sum_{0 \leq \mu + \nu \leq m} \frac{1}{\mu! \nu!} D_x^\mu D_y^\nu f(x, y) (\xi_{ijk}^x - x)^\mu (\xi_{ijk}^y - y)^\nu \\ &\quad + \sum_{\mu + \nu = m+1} \frac{1}{\mu! \nu!} D_x^\mu D_y^\nu f(\eta) (\xi_{ijk}^x - x)^\mu (\xi_{ijk}^y - y)^\nu \end{aligned}$$

where η is some point on the line from ξ_{ijk} to (x, y) . For any non-negative integers α and β with $\alpha + \beta \leq m+1$ differentiation of p_f yields

$$D_x^\alpha D_y^\beta p_f(x, y) = \sum_{i+j+k=d} f(\xi_{ijk}) D_x^\alpha D_y^\beta p_{ijk}(x, y).$$

Now, by the Taylor expansion given above we have

$$\begin{aligned} D_x^\alpha D_y^\beta p_f(x, y) &= \sum_{0 \leq \mu + \nu \leq m} \frac{1}{\mu! \nu!} \sum_{i+j+k=d} D_x^\mu D_y^\nu f(x, y) (\xi_{ijk}^x - x)^\mu (\xi_{ijk}^y - y)^\nu D_x^\alpha D_y^\beta p_{ijk}(x, y) \\ &\quad + \sum_{\mu + \nu = m+1} \frac{1}{\mu! \nu!} \sum_{i+j+k=d} D_x^\mu D_y^\nu f(\eta) (\xi_{ijk}^x - x)^\mu (\xi_{ijk}^y - y)^\nu D_x^\alpha D_y^\beta p_{ijk}(x, y). \end{aligned}$$

To simplify the above equation, we note that interpolation reproduces polynomials up to degree d hence

$$\begin{aligned}
& \sum_{i+j+k=d} (\xi_{ijk}^x - x)^\mu (\xi_{ijk}^y - y)^\nu D_x^\alpha D_y^\beta p_{ijk}(x, y) \\
&= D_x^\alpha D_y^\beta \sum_{i+j+k=d} (\xi_{ijk}^x - x)^\mu (\xi_{ijk}^y - y)^\nu p_{ijk}(u, v)|_{(u,v)=(x,y)} \\
&= D_x^\alpha D_y^\beta (u - x)^\mu (v - y)^\nu |_{(u,v)=(x,y)} \\
&= \begin{cases} \alpha! \beta! & \text{if } (\mu, \nu) = (\alpha, \beta) \\ 0 & \text{otherwise.} \end{cases}
\end{aligned}$$

Thus we can simplify the Taylor series expansion above to

$$\begin{aligned}
D_x^\alpha D_y^\beta p_f(x, y) &= D_x^\alpha D_y^\beta f(x, y) \\
&+ \sum_{\mu+\nu=m+1} \frac{1}{\mu! \nu!} \sum_{i+j+k=d} D_x^\mu D_y^\nu f(\eta) (\xi_{ijk}^x - x)^\mu (\xi_{ijk}^y - y)^\nu D_x^\alpha D_y^\beta p_{ijk}(x, y).
\end{aligned}$$

Then we have

$$\begin{aligned}
& |D_x^\alpha D_y^\beta (p_f(x, y) - f(x, y))| \\
&= \left| \sum_{\mu+\nu=m+1} \frac{1}{\mu! \nu!} \sum_{i+j+k=d} D_x^\mu D_y^\nu f(\eta) (\xi_{ijk}^x - x)^\mu (\xi_{ijk}^y - y)^\nu D_x^\alpha D_y^\beta p_{ijk}(x, y) \right| \\
&\leq K_1 |T|^{m+1} \sum_{i+j+k=d} \|D_x^\alpha D_y^\beta p_{ijk}\|_T |f|_{m+1, T}.
\end{aligned}$$

Applying the Markov inequality, Theorem 2.1.12, yields

$$\|D_x^\alpha D_y^\beta p_{ijk}\|_T \leq \frac{K_2}{\rho_T^{\alpha+\beta}} \|p_{ijk}\|_T. \quad (2.48)$$

From our definition of the Lagrange polynomials in (2.46) it is easy to see that

$$\|p_{ijk}\|_T \leq d^d. \quad (2.49)$$

Now by combining (2.1.12) and (2.49) we obtain

$$\|D_x^\alpha D_y^\beta (p_f(x, y) - f(x, y))\| \leq K_3 \frac{|T|^{m+1}}{\rho_T^{\alpha+\beta}} |f|_{m+1, T}. \quad (2.50)$$

The result in (2.47) follows from (2.50) and (2.2). \square

When $d \geq 3r + 2$ the spline space $S_d^r(\Delta)$ possesses an optimal approximation order which is achieved by the use of a quasi-interpolation operator. To define the quasi-interpolation operator we need linear functionals $\{\lambda_{ijk,T}\}_{i+j+k=d}$, $T \in \Delta$ which are based on values of f at the set of domain points over triangles in Δ , that is

$$\lambda_{ijk,T}(f) = \sum_{|\nu|=d} a_\nu^{ijk} f(\xi_\nu^T). \quad (2.51)$$

The quasi-interpolation operator of f is defined by

$$Qf := \sum_{T \in \Delta} \sum_{i+j+k=d} \lambda_{ijk,T}(f) B_{ijk}^T. \quad (2.52)$$

Now, we are ready for the crucial theorem on optimal approximation order [Lai and Schumaker'98, (20)].

Theorem 2.1.14 (Optimal Approximation Order). *Assume $d \geq 3r + 2$ and let Δ be a triangulation of \mathcal{D} . Then there exists a quasi-interpolatory operator $Qf \in S_d^r(\Delta)$ mapping $f \in L_1(\mathcal{D})$ into $S_d^r(\Delta)$ such that Qf achieves the optimal approximation order: if $f \in W_p^{m+1}(\mathcal{D})$,*

$$\|D_1^\alpha D_2^\beta(Qf - f)\|_{L_p(\mathcal{D})} \leq C |\Delta|^{m+1-\alpha-\beta} |f|_{m+1,p,\mathcal{D}} \quad (2.53)$$

for all $\alpha + \beta \leq m + 1$ with $0 \leq m \leq d$, where D_1 and D_2 denote the derivatives with respect to the first and second variables, $\|f\|_{L_p(\mathcal{D})}$ denotes the usual L_p norm of f over \mathcal{D} , $|f|_{m,p,\mathcal{D}}$ denotes the L_p norm of the m^{th} derivatives of f over \mathcal{D} , and $W_p^{m+1}(\mathcal{D})$ stands for the usual Sobolev space over \mathcal{D} . The constant C depends only on the degree d and the smallest angle θ_Δ and may be dependent on the Lipschitz condition on the boundary of \mathcal{D} .

We will also need the following lemma that relates the norm of the spline with the norm of the splines coefficients [Lai and Schumaker'98, (20)].

Lemma 2.1.4. *Suppose that Δ is a β -quasi-uniform triangulation. There exist two positive constants C_1 and C_2 independent of Δ such that for any spline function $S \in S_d^r(\Delta)$ with coefficient vector $\mathbf{s} = (s_1, \dots, s_m)^T$ with $S = \sum_{i=1}^m s_i \phi_j$,*

$$C_1 |\Delta|^2 \|\mathbf{s}\|^2 \leq \|S\|^2 \leq C_2 |\Delta|^2 \|\mathbf{s}\|^2. \quad (2.54)$$

Now we discuss the some useful results from [Awanou, Lai and Wenston'06, (1)]: the Lagrange Multiplier Method and the scattered data fitting schemes we implement in our functional linear models. The Lagrange Multiplier Method is a useful method for using splines to solve ill-posed problems. Let $\mathcal{S} := S_d^r(\Delta)$ be the spline space of degree d and smoothness r over a given triangulation Δ . Define a functional on \mathcal{S} by

$$J(u) = \frac{1}{2}a(u, u) - b(u)$$

where a is a continuous bilinear form and b is a continuous linear functional. Consider the constrained minimization problem:

$$J(s_G) = \min\{J(s), s \in \mathcal{S}, B(u) = G\} \quad (2.55)$$

where $B(u) = G$ is a set of side conditions such as smoothness and interpolation conditions.

Let

$$A = \left(a(B_{ijk}^{d,T}, B_{pqr}^{d,T'}) \right)_{\substack{i+j+k=d, T \in \Delta \\ p+q+r=d, T' \in \Delta}}$$

be the matrix associated with the bilinear form a . Let $F = (b(B_{ijk}^d))$ be the vector associated with the linear form b . The side conditions in matrix form are $B\mathbf{u} = \mathbf{g}$. Using the B-form of spline functions we can rewrite the above abstract problem as

$$\begin{aligned} \min J(\mathbf{c}) &= \frac{1}{2}\mathbf{c}^T A \mathbf{c} - \mathbf{c}^T F \\ \text{subject to } H\mathbf{c} &= 0, I\mathbf{c} = \mathbf{f}, \end{aligned}$$

where $H\mathbf{c} = 0$ is the linear system imposed by the smoothness conditions in Theorem 2.1.8 and $I\mathbf{c} = \mathbf{f}$ is an interpolation condition. The theory of Lagrange Multipliers yields

$$\mathcal{L}(\mathbf{c}, \lambda_1, \lambda_2) = \frac{1}{2}\mathbf{c}^T A \mathbf{c} - \mathbf{c}^T F + \lambda_1^T H\mathbf{c} + \lambda_2^T (I\mathbf{c} - \mathbf{f}) \quad (2.56)$$

for λ_1 and λ_2 such that

$$A\mathbf{c} + H^T \lambda_1 + I\lambda_2 = F$$

$$H\mathbf{c} = 0, I\mathbf{c} = \mathbf{f},$$

or in matrix form,

$$\begin{bmatrix} B^T & A \\ 0 & B \end{bmatrix} \begin{bmatrix} \lambda \\ \mathbf{c} \end{bmatrix} = \begin{bmatrix} F \\ G \end{bmatrix}. \quad (2.57)$$

We solve the system above using the following matrix iterative method [Awanou, Lai and Wenston'06, (1)].

Algorithm 2.1.1 (Matrix Iterative Method). *Let I be the identity matrix of \mathbb{R}^m . Fix $\epsilon > 0$, given an initial guess $\lambda_{(0)} \in \text{Im}(B)$. Compute*

$$\mathbf{c}^{(1)} = \left(A + \frac{1}{\epsilon} B^T B \right)^{-1} \left(F + \frac{1}{\epsilon} B^T G - B^T \lambda_0 \right).$$

Then iteratively compute

$$\mathbf{c}^{(k+1)} = \left(A + \frac{1}{\epsilon} B^T B \right)^{-1} \left(A \mathbf{c}^{(k)} + \frac{1}{\epsilon} B^T G \right)$$

for $k = 1, 2, \dots$

Below is the convergence theorem for the above matrix iterative method [Awanou and Lai'05, (2)].

Theorem 2.1.15. *Assume the linear system (2.57) has a solution (λ, \mathbf{c}) where \mathbf{c} is unique. Also assume that A is positive definite with respect to B . That is, $\mathbf{x}^T A \mathbf{x} \geq 0$ and $\mathbf{x}^T A \mathbf{x} = 0$ with $B \mathbf{x} = 0$ implies that $\mathbf{x} = 0$. Then there exists a constant $C_1(\epsilon)$ depending on ϵ but independent of k such that*

$$\|\mathbf{c} - \mathbf{c}^{k+1}\| \leq C_1(\epsilon) \left(\frac{C_2 \epsilon}{1 + C_2 \epsilon} \right)^{k+1}$$

for $k \geq 1$ where $C_2 = \|B^+\|^2 \|A\|$ and B^+ denotes the pseudo inverse of B .

We use the matrix iterative method in our discussion of several different methods for fitting scattered sets of data. For each scattered data fitting method we are given unstructured data $\{(x_i, y_i, f(x_i, y_i)), i = 1, \dots, N\}$. We want to find a smooth surface s_f that fits the data. We start by discussing the minimal energy method that interpolates the given data. Let

$\{(x_i, y_i, f(x_i, y_i)), i = 1, \dots, N\}$ be a scattered data set where all of the points are distinct and take Δ to be a triangulation of the given data locations with vertices at the given data locations. Let $\mathcal{S} := S_d^r(\Delta)$ be the spline space of degree d and smoothness r over Δ . Then we consider the set of interpolating splines,

$$\Lambda(f) := \{s \in \mathcal{S} : s(x_i, y_i) = f(x_i, y_i), i = 1, \dots, N\}, \quad (2.58)$$

and choose $s_f \in \Lambda(f)$ such that

$$E(s_f) := \min_{s \in \Lambda(f)} E(s)$$

where

$$E(s) := \sum_{T \in \Delta} \int_T (s_{xx}^2 + 2s_{xy}^2 + s_{yy}^2) dx dy. \quad (2.59)$$

The following existence and uniqueness theorem is given in [Awanou, Lai and Wenston'06, (1)].

Theorem 2.1.16. *Suppose that $\Lambda(f)$ is non-empty. Then there exists a unique $s_f \in \Lambda(f)$ minimizing (2.59).*

The convergence theorem for the minimal energy method is below [von Golitschek, Lai and Shumaker'02,(14)].

Theorem 2.1.17. *Suppose $\mathcal{S} \subseteq S_d^r(\Delta)$ where $d \geq 3r + 2$ and Δ is β -quasi-uniform triangulation. Then there exists a constant C depending only on d and β such that*

$$\|f - s_f\|_{L^\infty(\Omega)} \leq C|\Delta|^2|f|_{2,\infty,\Omega}.$$

To solve the minimal energy method we note that for $s \in \mathcal{S}$, the spline s satisfies the smoothness conditions in Theorem 2.1.8 which can be expressed as the linear system

$$H\mathbf{c} = 0.$$

The energy functional $E(s)$ can be expressed in terms of c as

$$E(s) = \mathbf{c}^T K \mathbf{c}$$

where $K = \text{diag}(K_T, T \in \Delta)$ is a block diagonal matrix with

$$K_T = \left[\int_T \left(D_x^2 B_{ijk}^{d,T} D_x^2 B_{pqr}^{d,T} + 2D_x D_y B_{ijk}^{d,T} D_x D_y B_{pqr}^{d,T} + D_y^2 B_{ijk}^{d,T} D_y^2 B_{pqr}^{d,T} \right) dx dy \right]_{\substack{i+j+k=d \\ p+q+r=d}} \quad (2.60)$$

where $B_{ijk}^{d,T}$ is the Bernstein basis polynomial of degree d with respect to the triangle T . Hence the minimal energy interpolation problem is equivalent to the following constrained minimization problem:

$$\begin{aligned} & \min \mathbf{c}^T K \mathbf{c} \\ & \text{subject to} \\ & H \mathbf{c} = 0, \quad I \mathbf{c} = f \end{aligned}$$

where $I \mathbf{c} = f$ is the linear system associated with the interpolation conditions. Finally we solve the above constrained minimization problem by the previously described matrix iterative method in Algorithm 2.1.1 since K is positive definite.

Next we discuss the discrete least squares method. Let $\{(x_i, y_i, f(x_i, y_i)), i = 1, \dots, N\}$ be a scattered data set where N is a relatively large integer. Let Ω be the convex hull of the given data locations and Δ a triangulation of Ω . For the discrete least squares method, we do not require the vertices of Δ to be data points. We also want the data locations to be evenly distributed over Δ with respect to d .

Definition 2.1.7. *For a given spline space $S_d^r(\Delta)$, let $d = \max\{d_T, T \in \Delta\}$. We say that the given data locations $v_\ell, \ell = 1, \dots, N$ are evenly distributed over Δ with respect to d if for each triangle $T \in \Delta$, the matrix*

$$[B_{ijk}^d(v_\ell)|_T, v_\ell \in T]$$

is of full rank.

The discrete least squares method finds $s_f \in \mathcal{S}$ such that

$$\sum_{i=1}^N |s_f(x_i, y_i) - f(x_i, y_i)|^2 = \min_{s \in \mathcal{S}} \sum_{i=1}^N |s(x_i, y_i) - f(x_i, y_i)|^2.$$

The existence and uniqueness of a solution is given in the theorem below [Awanou, Lai and Wenston'06, (1)].

Theorem 2.1.18. *Suppose that the data locations (x_i, y_i) for $i = 1, \dots, N$ are evenly distributed over Δ with respect to d . Then there exists a unique discrete least squares solution satisfying (2.61).*

The following is the convergence theorem for the discrete least squares method [von Golitschek and Shumaker'02, (15)].

Theorem 2.1.19. *Let $\mathcal{S} = S_d^r(\Delta)$ where $d \geq 3r+2$. Let Δ be a β -quasi-uniform triangulation of \mathcal{D} and s_0 denote the discrete least squares solution in (2.61). Then for all $f \in W_\infty^{m+1}(\mathcal{D})$,*

$$\|f - s_0\|_{L_\infty(\mathcal{D})} \leq C|\Delta|^{m+1}|f|_{m+1,\infty,\mathcal{D}}$$

where C is a constant depending only on the degree d and β if \mathcal{D} is convex and also on the Lipschitz constant $L_{\partial\mathcal{D}}$ of the boundary of \mathcal{D} if \mathcal{D} is not convex.

To compute the discrete least squares solution we let

$$L(\mathbf{c}) := \sum_{i=1}^N |s(x_i, y_i) - f(x_i, y_i)|^2.$$

We only need to find a local minimizer since $L(\mathbf{c})$ is convex. Hence by the Lagrange Multiplier Method, we let

$$\mathcal{F}(\mathbf{c}, \alpha) = L(\mathbf{c}) + \alpha^T H \mathbf{c}$$

and set

$$\begin{aligned} \frac{\partial}{\partial \mathbf{c}} \mathcal{F}(\mathbf{c}, \alpha) &= 0 \\ \frac{\partial}{\partial \alpha} \mathcal{F}(\mathbf{c}, \alpha) &= 0. \end{aligned}$$

Again we apply the Matrix Iterative Algorithm 2.1.1 to solve the linear system

$$\begin{bmatrix} H^T & 2B \\ 0 & H \end{bmatrix} \begin{bmatrix} \alpha \\ \mathbf{c} \end{bmatrix} = \begin{bmatrix} 2b \\ 0 \end{bmatrix}$$

where $B = \text{diag}(B_T, T \in \Delta)$ with

$$B_T = \left(\sum_{(x_l, y_l) \in T} B_{ijk}^{d,T}(x_l, y_l) B_{pqr}^{d,T}(x_l, y_l) \right)_{\substack{i+j+k=d \\ p+q+r=d}} \quad (2.61)$$

and

$$\mathbf{b} = (b_{ijk}^T, i + j + k = d, T \in \Delta) \quad (2.62)$$

with

$$b_{ijk}^T = \sum_{(x_l, y_l) \in T} f(x_l, y_l) B_{ijk}^{d,T}(x_l, y_l).$$

When we combine the minimal energy method and the discrete least squares method we form the penalized least squares method. For the penalized least squares method, let $\{(x_i, y_i, f(x_i, y_i)), i = 1, \dots, N\}$ be a scattered data set where N is a relatively large integer. Again take Ω to be the convex hull of the given data locations and Δ a triangulation of Ω . Then the penalized least squares method is to find $s_f \in \mathcal{S}$ such that for a positive weight $\lambda > 0$

$$P_\lambda(s_f) := \min_{s \in \mathcal{S}} P_\lambda(s) \quad (2.63)$$

where

$$P_\lambda(s) := \sum_{i=1}^N |s(x_i, y_i) - f(x_i, y_i)|^2 + \lambda E(s)$$

and $E(s)$ denotes the energy functional defined in equation (2.59). The existence and uniqueness criterium for the penalized least squares method is outlined in the following theorem.

Theorem 2.1.20. *Fix $\lambda > 0$ and suppose that there exist three data points that are distinct and non-collinear. Then there exists a unique $s_f \in S_d^r(\Delta)$ satisfying (2.63) with $r \geq 1$.*

Proof. For existence we need to show that $(B - \lambda K)$ is invertible. To do this we will show that $(B - \lambda K)$ is positive definite. The determinate of a positive matrix is positive and hence every positive definite matrix is invertible.

Now to show uniqueness, let s_f and \hat{s}_f be solutions to (2.63), with coefficient vectors c_f and \hat{c}_f respectively. Since P_λ is convex for any $z \in [0, 1]$ we have

$$P(zs_f + (1 - z)\hat{s}_f) \leq zP_\lambda + (1 - z)P_\lambda(\hat{s}_f) = P_\lambda(\hat{s}_f).$$

Hence $P_\lambda(\hat{s}_f + z(s_f - \hat{s}_f))$ is a constant with respect to z . Thus

$$\frac{\partial}{\partial z} P_\lambda(\hat{s}_f + z(s_f - \hat{s}_f)) = 0.$$

That is for all $z \in (0, 1)$

$$\begin{aligned} 0 &= \frac{\partial}{\partial z} P_\lambda(\hat{s}_f + z(s_f - \hat{s}_f)) \\ &= 2\lambda z(c_f - \hat{c}_f)^T K(c_f - \hat{c}_f) \\ &\quad + 2z(c_f - \hat{c}_f)^T B(c_f - \hat{c}_f) - 2b^T(c_f - \hat{c}_f). \end{aligned}$$

Hence we have

$$(c_f - \hat{c}_f)^T K(c_f - \hat{c}_f) = 0 \tag{2.64}$$

$$(c_f - \hat{c}_f)^T B(c_f - \hat{c}_f) = 0. \tag{2.65}$$

Now, (2.64) implies that $s_f - \hat{s}_f$ is a linear function. By (2.65) we know that $s_f - \hat{s}_f$ is equal to zero at three non-collinear points with C^1 conditions. Hence $s_f - \hat{s}_f \equiv 0$ and the minimizer is unique. \square

The convergence theorem for the penalized least squares method is below [Lai'07, (19)].

Theorem 2.1.21. *Let $s_{f,\lambda}$ be the penalized least squares spline in $S_d^r(\Delta)$ with $d \geq 3r + 2$. Suppose that $f \in W_\infty^{m+1}(\Omega)$ with $1 \leq m \leq d$. Suppose that $A_1 > 0$ and $A_2 < \infty$ are constants such that A_2/A_1 is independent of Δ . Then*

$$\|s_{f,\lambda} - f\|_{L_\infty(\Omega)} \leq C \left(1 + \frac{\sqrt{\lambda}}{|\Delta|} \right) \left(|\Delta|^m |f|_{m+1,\Omega} + \frac{\lambda}{|\Delta|} |f|_{2,\Omega} \right),$$

if λ is sufficiently small compared to $|\Delta|$. Here $C > 0$ is constant dependent on A_2/A_1 and β and d .

To solve the penalized least squares method, note that for $s \in \mathcal{S}$, the spline s satisfies the smoothness conditions in Theorem 2.1.8 which can be expressed as the linear system

$$H\mathbf{c} = 0.$$

The energy functional can be expressed as before in terms of \mathbf{c} as

$$E(\mathbf{c}) = \mathbf{c}^T K \mathbf{c},$$

where K is defined as before in equation (2.60). We have

$$\begin{aligned} \sum_{i=1}^N |s(x_i, y_i) - f(x_i, y_i)|^2 &= \sum_{T \in \Delta} \sum_{v \in T} \left(\sum_{i+j+k=d} c_{ijk}^T B_{ijk}^{d,T}(v) - f(v) \right)^2 \\ &= \mathbf{c}^T B \mathbf{c} - 2\mathbf{b}^T \mathbf{c} + \|\mathbf{f}\|^2 \end{aligned}$$

where $\mathbf{f} = (f(v), v = (x_l, y_l), l = 1, \dots, N)$ is the data value vector and B and \mathbf{b} are the same as (2.61) and (2.62) respectively. Thus

$$P_\lambda(s) = \lambda \mathbf{c}^T K \mathbf{c} + \mathbf{c}^T B \mathbf{c} - 2\mathbf{b}^T \mathbf{c} + \|f\|_2^2. \quad (2.66)$$

Again for the penalized least squares method, we only need to compute a local minimizer since $P_\lambda(s)$ is convex. To do this we use the Lagrange Multiplier Method by letting

$$\mathcal{F}(\mathbf{c}, \alpha) = P_\lambda(\mathbf{c}) + \alpha^T H \mathbf{c}$$

and set

$$\begin{aligned} \frac{\partial}{\partial \mathbf{c}} \mathcal{F}(\mathbf{c}, \alpha) &= 0 \\ \frac{\partial}{\partial \alpha} \mathcal{F}(\mathbf{c}, \alpha) &= 0. \end{aligned}$$

Finally by the existence and uniqueness Theorem 2.1.20 we know $(B + \lambda K)$ is positive definite. Hence we can apply the Matrix Iterative Algorithm 2.1.1 to solve the linear system

$$\begin{bmatrix} H^T & 2(B + \lambda K) \\ 0 & H \end{bmatrix} \begin{bmatrix} \alpha \\ \mathbf{c} \end{bmatrix} = \begin{bmatrix} 2\mathbf{b} \\ 0 \end{bmatrix}.$$

2.2 UNIVARIATE FUNCTIONAL LINEAR MODELS

In this section, we discuss the functional linear model as discussed in [Cardot, Ferraty and Sarda'03, (6)]. Suppose $\mathcal{C} = [0, 1]$ and let H be the separable Hilbert space of square integrable functions defined on $[0, 1]$. Let $\langle \phi, \psi \rangle$ denote the usual inner product of the functions

ϕ and ψ on H and $\|\psi\|$ the norm of ψ . Let (X, Y) be a pair of random variables defined on the same probability space, with X values in H and Y valued in \mathbb{R} . Let f be the conditional mean of Y given X , that is

$$\mathcal{E}(Y \mid \{X(t) = x(t), t \in [0, 1]\}) = f(\{x(t), t \in [0, 1]\}), \quad (2.67)$$

for $x \in H$. If the function f is linear and continuous, then by the Riesz representation theorem there is a unique function α in H such

$$\mathcal{E}(Y \mid \{X(t) = x(t), t \in [0, 1]\}) = \langle \alpha, x \rangle, \quad (2.68)$$

for $x \in H$. If f is not linear or continuous, consider the continuous linear approximation of f as the function α in H satisfying

$$\alpha = \arg \min_{\beta \in H} \mathcal{E} [(Y - \langle \beta, X \rangle)^2] = \arg \min_{\beta \in H} \mathcal{E} [(f(x) - \langle \beta, X \rangle)^2]. \quad (2.69)$$

We want to consider the model in (2.68) or equivalently (2.69), for the continuous linear function defined as

$$\Psi(x) = \langle \alpha, x \rangle, \quad (2.70)$$

for $x \in H$. In this general setting α may not exist and if it does it may not be unique. We can develop conditions for the existence and uniqueness of α based on the covariance operator of X and the cross covariance matrix of X and Y . First, we assume the H valued random variable X is centered ($\mathcal{E}(X(t)) = 0$, for all t a.e.) and has a finite second moment ($\mathcal{E}(\|X\|^2) < \infty$). Then the covariance operator Γ of the H valued random variable is defined to be

$$\Gamma x(t) = \int_0^1 \mathcal{E}[X(t)X(s)] x(s) ds, \quad (2.71)$$

for $x \in H$ and $t \in [0, 1]$. We note here that Γ is an integral operator whose kernel is the covariance function of X . It can be shown that the operator Γ is nuclear, self-adjoint, and non-negative. Similarly, we define the cross covariance operator Δ of (X, Y) to be the linear functional

$$\Delta x = \int_0^1 \mathcal{E}[X(t)Y] x(t) dt, \quad (2.72)$$

for $x \in H$. Now there is a solution to (2.69) if and only if it satisfies

$$\Delta(x) = \langle \alpha, \Gamma(x) \rangle, \quad (2.73)$$

for $x \in H$. Let λ_j for $j = 1, 2, \dots$ be the eigenvalues of Γ and v_j for $j = 1, 2, \dots$ the corresponding eigenfunctions. Then we can express

$$\alpha = \sum_{j=1}^{\infty} \langle \alpha, v_j \rangle v_j. \quad (2.74)$$

By (2.73) and (2.74) we can get the coordinates of α in terms of the functions v_j as follows

$$\langle \mathcal{E}(XY), v_j \rangle = \lambda_j \langle \alpha, v_j \rangle, \quad (2.75)$$

for $j = 1, 2, \dots$. Let $\mathcal{N}(\Gamma) = \{x \in H, \Gamma x = 0\}$, if $\mathcal{N}(\Gamma) \neq \{0\}$ then α cannot be uniquely determined. Some of the eigenvalues are null and if α satisfies (2.73), then $\alpha + \alpha_0$ satisfies (2.73) for any $\alpha_0 \in \mathcal{N}(\Gamma)$. Hence a unique solution to (2.69) can only be determined in the space $\mathcal{N}(\Gamma)^\perp$. Hence we look for a solution in the closure of $Im(\Gamma) = \{\Gamma x, x \in H\}$. By inverting (2.75) we get another expansion for α :

$$\alpha = \sum_{j=1}^{\infty} \frac{\langle \mathcal{E}(XY), v_j \rangle}{\lambda_j} v_j. \quad (2.76)$$

Now, we note that the function α will belong to H if and only if

$$\sum_{j=1}^{\infty} \frac{\langle \mathcal{E}(XY), v_j \rangle}{\lambda_j} < \infty. \quad (2.77)$$

In fact, (2.77) is satisfied if f is a continuous linear function then $f(X) = \langle \alpha, X \rangle$. We also note that the estimation of α is difficult since the eigenvalues λ_j decrease rapidly to zero.

CHAPTER 3

AUTOREGRESSIVE APPROACH FOR FUNCTIONAL LINEAR MODELS

In this chapter, we extend the functional linear model to the bivariate setting. For the autoregressive approach in the bivariate setting, we take Y to be a real valued random variable which is a functional of a random surface X over a polygonal domain $\mathcal{D} \in \mathbb{R}^2$. The functional linear model for Y is:

$$Y = f(X) + \varepsilon = \langle g, X \rangle + \varepsilon = \int_{\mathcal{D}} g(s)X(s)ds + \varepsilon, \quad (3.1)$$

where $g \in H$, such as $L^2(\mathcal{D})$, ε is a real random variable that satisfies $\mathcal{E}\varepsilon = 0$ and $\mathcal{E}X(s)\varepsilon = 0$, for all $s \in \mathcal{D}$. We rephrase the problem, by looking for the function $g \in H$ that solves the following minimization problem:

$$\min_{\beta \in H} \mathcal{E} [(f(X) + \varepsilon - \langle \beta, X \rangle)^2]. \quad (3.2)$$

We want to approximate the function, g , defined on the two dimensional spatial domain \mathcal{D} based on the observations on X from a set of design points in \mathcal{D} and the random variable Y . We cannot assume that the random surfaces at various time steps are completely independent; hence we want to write the model in terms of the covariance operator of the H -valued random variable X ,

$$\Gamma := \mathcal{E}(X(s)X(t)) \quad (3.3)$$

and the cross covariance of (X, Y) ,

$$\Delta := \mathcal{E}(X(s)Y). \quad (3.4)$$

Theorem 3.0.1. *The solution to the minimization problem (3.2) is*

$$\Gamma g = \Delta. \quad (3.5)$$

Proof. We start with the minimization problem (3.2). If g is the solution, the following function

$$F(r) = \mathcal{E} [(Y - \langle g + rf, X \rangle)^2] \quad (3.6)$$

achieves the minimum when $r = 0$ for any function $f \in H$. By taking the derivative with respect to r , we have

$$F'(r) = 2\mathcal{E} [(Y - \langle g + rf, X \rangle)(-\langle f, X \rangle)] = 0. \quad (3.7)$$

Evaluating at $r = 0$ yields

$$\mathcal{E} [(Y - \langle g, X \rangle)(\langle f, X \rangle)] = 0,$$

so

$$\mathcal{E} [\langle g, X \rangle \langle f, X \rangle] = \mathcal{E} [Y \langle f, X \rangle]. \quad (3.8)$$

Note that the left-hand side of (3.8) is

$$\mathcal{E} \left[\int_{s \in \mathcal{D}} g(s)X(s)ds \int_{t \in \mathcal{D}} f(t)X(t)dt \right] = \int_{t \in \mathcal{D}} \int_{s \in \mathcal{D}} g(s)\mathcal{E}[X(s)X(t)]f(t)dsdt \quad (3.9)$$

and the right-hand side is

$$\mathcal{E} [Y \langle f, X \rangle] = \mathcal{E} \left[\int_{t \in \mathcal{D}} f(t)X(t)Ydt \right] = \int_{t \in \mathcal{D}} f(t)\mathcal{E}[X(t)Y]dt. \quad (3.10)$$

Since the equation (3.8) holds for all $f \in H$, we have

$$\int_{t \in \mathcal{D}} \int_{s \in \mathcal{D}} g(s)\mathcal{E}[X(s)X(t)]f(t)dsdt = \int_{t \in \mathcal{D}} f(t)\mathcal{E}[X(t)Y]dt. \quad (3.11)$$

Now, let Γ be the standard covariance operator of the H -valued random variables X as defined in (3.3) and take Δ to be the cross-covariance of X and Y as defined in (3.4). Then we have

$$(\Gamma g)(t) = \int_{s \in \mathcal{D}} \mathcal{E}(X(s)X(t))g(s)ds, \quad \forall g \in H.$$

and

$$\langle \Delta, f \rangle = \int_{t \in \mathcal{D}} \mathcal{E}(X(t)Y)f(t)dt \quad \forall f \in H.$$

Now, (3.11) can be denoted by

$$\Gamma g = \Delta.$$

□

Note that Γ is a symmetric integral operator mapping H to H . Assume that Γ is a compact operator [Cardot, Ferraty, and Sarda'03, (6)]. Let $\lambda_j, j = 1, 2, \dots$, be the eigenvalues of Γ arranged in decreasing order and take $v_j \in H$ to be the eigenfunctions of Γ associated with λ_j for $j = 1, 2, \dots$. Suppose that $v_j, j = 1, 2, \dots$, form a complete orthonormal basis for H . Then we can write $\Gamma = \sum_j \lambda_j v_j(t)v_j(s)$ and $g = \sum_j \langle g, v_j \rangle v_j$ for any $g \in H$. Then (3.11) yields

$$\lambda_j \langle g, v_j \rangle = \langle g, \lambda_j v_j \rangle = \langle g, \Gamma v_j \rangle = \langle \Gamma g, v_j \rangle = \langle \Delta, v_j \rangle = \langle \mathcal{E}(X(t)Y), v_j \rangle,$$

and it follows that if $\lambda_j > 0$

$$\langle g, v_j \rangle = \langle \mathcal{E}(X(\cdot)Y), v_j \rangle / \lambda_j.$$

Thus, we get the expansion for g

$$g = \sum_{j=1}^{\infty} \frac{\langle \mathcal{E}(X(\cdot)Y), v_j \rangle}{\lambda_j} v_j.$$

Note that the function g is in H if and only if

$$\sum_{j=1}^{\infty} \left(\frac{\langle \mathcal{E}(X(\cdot)Y), v_j \rangle}{\lambda_j} \right)^2 < +\infty.$$

In general, we do not know if Γ is invertible or not. Let $\mathcal{N}(\Gamma)$ be the kernel of Γ , $\mathcal{N}(\Gamma) = \{x \in H, \Gamma x = 0\}$ and suppose that $\mathcal{N}(\Gamma) \neq \emptyset$. In this case, g can not be uniquely determined. However, g can be determined in $\mathcal{N}(\Gamma)^\perp$. So we let $H_k = \text{span}\{v_1, \dots, v_k\} \subset \mathcal{N}(\Gamma)^\perp$ be a finite dimensional approximation of the orthogonal complement of $\mathcal{N}(\Gamma)$ and \mathcal{P}_k be the orthogonal projection operator from H to H_k . Now, $\mathcal{P}_k \Gamma \mathcal{P}_k$ is invertible when $\lambda_k > 0$. Note that $\mathcal{P}_k \Gamma \mathcal{P}_k g = \sum_{j=1}^k \lambda_j \langle v_j, g \rangle v_j$. Thus, for all $f \in H$, $\mathcal{P}_k f = \sum_{j=1}^k \langle f, v_j \rangle v_j$ and (3.11) yields

$$\langle \mathcal{P}_k \Gamma \mathcal{P}_k g, \mathcal{P}_k f \rangle = \langle \Delta, \mathcal{P}_k f \rangle,$$

or

$$\sum_{j=1}^k \lambda_j \langle v_j, g \rangle \langle v_j, f \rangle = \sum_{j=1}^k \langle f, v_j \rangle \langle \Delta, v_j \rangle$$

for all $f \in H$. It follows that $\langle v_j, g \rangle = \frac{1}{\lambda_j} \langle \Delta, v_j \rangle$ for $j = 1, \dots, k$. Hence, we have the approximation of g in H_k :

$$g_k = \sum_{j=1}^k \frac{1}{\lambda_j} \langle \Delta, v_j \rangle v_j.$$

So far, we have only done a theoretical analysis. Now, we move on to an empirical estimate of g . For random samples $X_i, i = 1, \dots, n$ in H and Y_i is another random variable dependent on X_i , Γ_n be the empirical estimator of Γ is given by,

$$\Gamma_n x = \frac{1}{n} \sum_{i=1}^n \langle X_i, x \rangle X_i$$

where x is a vector in an appropriate finite dimensional space and Δ_n is the empirical estimator of Δ :

$$\Delta_n x = \frac{1}{n} \sum_{i=1}^n \langle X_i, x \rangle Y_i.$$

Then the finite dimensional operator Γ_n is a compact operator mapping H to H and hence, Γ_n can be expanded in terms of its eigenfunctions $\hat{v}_j, j = 1, 2, \dots$. That is,

$$\Gamma_n x = \sum_{j=1}^{\infty} \hat{\lambda}_j \langle \hat{v}_j, x \rangle \hat{v}_j.$$

Similar to our theoretical discussion, we have

$$\Delta_n x = \langle g_n, \Gamma_n x \rangle$$

for some $g_n \in H$. Assume that the first k_n largest eigenvalues $\hat{\lambda}_j, j = 1, \dots, k_n$ are nonzero.

Then the principal component regression estimator of g_k is

$$\hat{g}_{PCR} = \sum_{j=1}^{k_n} \frac{\Delta_n(\hat{v}_j)}{\hat{\lambda}_j} \hat{v}_j$$

which is an approximation of the empirical estimator of g .

In general, $\hat{g}_{PCR} \in H_k$ is a rough function. We smooth \hat{g}_{PCR} by approximating it with bivariate splines. Let $S_d^r(\Delta)$ be the spline space of polynomials degree d and smoothness r

over triangulation Δ with $d \geq 3r + 2$. Then we take \hat{g}_{SPCR} to be the solution of the following continuous least squares minimization:

$$\min_{f \in S_d^r(\Delta)} \int_{\mathcal{D}} |\hat{g}_{SPCR}(s) - f(s)|^2 ds.$$

In practice, the random surfaces X_i 's are not observed continuously. The only information given is the values of X_i at design points $s_k \in \mathcal{D}, k = 1, \dots, N$. That is, for the i th surface we only have $\{z_{i,k}, k = 1, \dots, N\}$ to describe X_i where $z_{i,k}$ is a random value at the design point $s_k \in \mathcal{D}$. We also have Y_i a random variable dependent on X_i . Since we only have a discrete version of the X_i we approximate it by \widetilde{X}_i by using the penalized least squares method (2.63). We use the space bivariate splines with optimal approximation order, the space $S_d^r(\Delta)$, smoothness r and degree $d \geq 3r + 2$ defined over the triangulation Δ of \mathcal{D} . Let $\widetilde{\Gamma}_n$ be an approximation of the empirical estimator Γ_n of Γ :

$$\widetilde{\Gamma}_n(x) = \frac{1}{n} \sum_{i=1}^n \langle \widetilde{X}_i, x \rangle \widetilde{X}_i \quad (3.12)$$

and $\widetilde{\Delta}_n$ be an approximation of the empirical estimator Δ_n of Δ :

$$\widetilde{\Delta}_n(x) = \frac{1}{n} \sum_{i=1}^n \langle \widetilde{X}_i, x \rangle Y_i, \quad (3.13)$$

for spline approximation of random samples $X_i, i = 1, \dots, n$.

We see that $\widetilde{\Gamma}_n$ is a bounded operator on $S_d^r(\Delta)$ and hence can be expressed as follows:

$$\widetilde{\Gamma}_n(x) = \sum_{j=1}^m \widetilde{\lambda}_j \langle \widetilde{v}_j, x \rangle \widetilde{v}_j, \quad (3.14)$$

where $\widetilde{\lambda}_j$ is an eigenvalue and its associated \widetilde{v}_j eigenvector of $\widetilde{\Gamma}_n$ and m is the dimension of the spline space $S_d^r(\Delta)$. Then

$$\langle \widetilde{\Delta}_n, x \rangle = \langle g_n, \widetilde{\Gamma}_n x \rangle \quad (3.15)$$

for some $g_n \in H$. We take the first k_n largest eigenvalues $\widetilde{\lambda}_j, j = 1, \dots, k_n$ that are nonzero and define the principal component regression estimator of g_n as

$$\widetilde{g}_{PCR} = \sum_{j=1}^{k_n} \frac{\Delta_n(\widetilde{v}_j)}{\widetilde{\lambda}_j} \widetilde{v}_j. \quad (3.16)$$

The above is an approximation of the empirical estimator of g . Finally we can use the penalized least squares fit to compute a smooth version of \tilde{g}_{PCR} and denote it by \tilde{g}_{SPCR} . We also note that instead of using H_k , one could use other finite dimensional function spaces.

CHAPTER 4

BRUTE FORCE APPROACH TO FUNCTIONAL LINEAR MODELS

In this chapter, we discuss the brute force method. The results in this chapter are from [Guillas and Lai'08, (17)] and offer an alternative approach to the autoregressive method. We include these results here to make it convenient for the reader and as a preparation for Chapter 5. The brute force method exploits the optimal approximation property of splines, Theorem 2.1.14. The general idea of this approach starts by trying to approximate a bounded and continuous functional f . By the Riesz representation theorem, the functional can be written as $f(X) = \langle g, X \rangle$ for some function $g \in H$. That is, we want to solve the same minimization problem as in Chapter 3:

$$\alpha = \arg \min_{\beta \in H} \mathcal{E} [(f(X) - \epsilon - \langle \beta, X \rangle)^2]. \quad (4.1)$$

However it is impossible to solve the above minimization problem because we have an infinite dimensional Hilbert space H . Hence we find an approximation to the solution by choosing a finite dimensional spline space $S_d^r(\Delta)$ of smoothness r and degree $d \geq 3r + 2$ which is dense in H as $|\Delta| \rightarrow 0$. This reduces the original problem (4.1) to the spline estimate

$$S_\alpha = \arg \min_{\beta \in S_d^r(\Delta)} \mathcal{E} [(f(X) - \epsilon - \langle \beta, X \rangle)^2]. \quad (4.2)$$

From the spline estimate we develop an empirical estimate for a given set of observed surfaces $\{X_1, \dots, X_n\}$

$$\widehat{S}_{\alpha, n} = \arg \min_{\beta \in S_d^r(\Delta)} \frac{1}{n} \sum_{i=1}^n (f(X_i) - \epsilon_i - \langle \beta, X_i \rangle)^2. \quad (4.3)$$

All of the theory up to this point is for given complete random surfaces but in practice we are not able to observe the entire random surface. Instead, we observe a random surface X

over design points $s_k, k = 1, \dots, N$ over \mathcal{D} . We create a surface to represent X from the given data by using splines. We create a spline S_X by finding the penalized least square fit of X . To do this we assume that $s_k, k = 1, \dots, N$ are evenly distributed over Δ of \mathcal{D} with respect to $S_d^r(\Delta)$. Then we repeat the above theory using our approximated random surfaces. We start with the original problem (4.1) using S_X instead of X :

$$\alpha_D = \arg \min_{\beta \in H} \mathcal{E} [(f(X) - \epsilon - \langle \beta, S_X \rangle)^2]. \quad (4.4)$$

Again we have the same issue, that the Hilbert space H is infinite and we cannot find the minimum but we can find an approximate solution in the finite spline space $S_d^r(\Delta)$. Hence we obtain a spline estimate based on the approximated random surfaces:

$$S_{\alpha_D} = \arg \min_{\beta \in S_d^r(\Delta)} \mathcal{E} [(f(X) - \epsilon - \langle \beta, S_X \rangle)^2]. \quad (4.5)$$

From this spline estimate we finally reach something we can compute from real data, the empirical estimate based the approximated random surfaces:

$$\widetilde{S}_{\alpha, n} = \arg \min_{\beta \in S_d^r(\Delta)} \frac{1}{n} \sum_{i=1}^n (f(X_i) - \epsilon_i - \langle \beta, S_{X_i} \rangle)^2. \quad (4.6)$$

The first theorem in this section states when there exists a unique solution to the original minimization problem over $S_d^r(\Delta)$, (4.2).

Theorem 4.0.2. *Suppose that only the zero spline in $S_d^r(\Delta)$ is orthogonal to the collection $\mathcal{X} = \{X(s), s \in \mathcal{D}\} \subset H$. Then the minimization problem (4.2) has a unique solution in $S_d^r(\Delta)$.*

Proof. We want to rewrite the minimization problem in terms of a linear system. Let $\{\phi_1, \dots, \phi_m\}$ be a basis for $S_d^r(\Delta)$. First we note that if $\beta \in S_d^r(\Delta)$ we can write $\beta = \sum_{j=1}^m c_j \phi_j$ and then

$$\langle \beta, X \rangle = \left\langle \sum_{j=1}^m c_j \phi_j, X \right\rangle = \sum_{j=1}^m c_j \langle \phi_j, X \rangle.$$

Hence we can write the difference in the minimization problem as the following function of the coefficient vector:

$$\mathcal{F}(c_j) = \mathcal{E} \left[\left(f(X) - \sum_{j=1}^m c_j \langle \phi_j, X \rangle \right)^2 \right]. \quad (4.7)$$

Differentiation yields

$$\begin{aligned}\frac{\partial \mathcal{F}}{\partial c_l} &= 2\mathcal{E} \left[\left(f(X) - \sum_{j=1}^m c_j \langle \phi_j, X \rangle \right) \sum_{j=1}^m \langle \phi_j, X \rangle \right] \\ &= 2\mathcal{E} \left[f(X) \sum_{j=1}^m \langle \phi_j, X \rangle - \sum_{j=1}^m c_j \langle \phi_j, X \rangle \sum_{j=1}^m \langle \phi_j, X \rangle \right].\end{aligned}$$

Then $\frac{\partial \mathcal{F}}{\partial c_l} = 0$ implies

$$\mathcal{E} \left[f(X) \sum_{j=1}^m \langle \phi_j, X \rangle \right] = \mathcal{E} \left[\sum_{j=1}^m c_j \langle \phi_j, X \rangle \sum_{j=1}^m \langle \phi_j, X \rangle \right]. \quad (4.8)$$

We can rewrite this as a linear system

$$A\mathbf{c} = \mathbf{b}, \quad (4.9)$$

where A is an $m \times m$ matrix with entries $\mathcal{E}(\langle \phi_i, X \rangle \langle \phi_j, X \rangle)$ for $i, j = 1, \dots, m$ and the vector \mathbf{b} is of length m with entries $\mathcal{E}((f(X) + \epsilon) \langle \phi_j, X \rangle) = \mathcal{E}(f(X) \langle \phi_j, X \rangle)$ for $j = 1, \dots, m$ and the coefficient vector of S_α is the vector $\mathbf{c} = (c_1, \dots, c_m)^T$ which satisfies (4.9). Here we note that the matrix A is the same A matrix in the previous chapter, the representation of the covariance function of X expanded with respect to the spline basis $\phi_j, j = 1, \dots, m$.

To have a unique solution to (4.2) we need to solve the linear system (4.9). We know that A is invertible if it is full rank and the only solution to $\mathbf{c}^T A \mathbf{c} = 0$ is $\mathbf{c} = 0$. That is for any vector \mathbf{c} we have

$$\mathbf{c}^T A \mathbf{c} = \sum_{i=1}^m \sum_{j=1}^m c_i \mathcal{E}(\langle \phi_i, X \rangle \langle \phi_j, X \rangle) c_j \quad (4.10)$$

$$\mathbf{c} = \mathcal{E} \left(\left\langle \sum_{i=1}^m c_i \phi_i, X \right\rangle \left\langle \sum_{j=1}^m c_j \phi_j, X \right\rangle \right) \quad (4.11)$$

$$= \mathcal{E} \left(\left\langle \sum_{i=1}^m c_i \phi_i, X \right\rangle^2 \right) = 0, \quad (4.12)$$

for all $X \in \mathcal{X}$. The above requires

$$\left\langle \sum_{i=1}^m c_i \phi_i, X \right\rangle = \sum_{i=1}^m c_i \langle \phi_i, X \rangle = 0 \quad (4.13)$$

which implies that $\mathbf{c} = 0$. Therefore if we assume that the zero spline function in $S_d^r(\Delta)$ is the only one orthogonal to all $X \in \mathcal{X}$ then A is invertible and (4.2) has a solution. \square

Now that we know when there exists a unique S_α , we want to know how well S_α approximates α in terms of, $|\Delta|$, the size of triangulation.

Theorem 4.0.3. *Suppose that $\mathcal{E}(\|X\|^2) < \infty$ and suppose $\alpha \in C^\nu(\mathcal{D})$ for $r \leq \nu \leq d + 1$. Then the solution S_α from the minimization problem (4.2) approximates α in the sense:*

$$\mathcal{E}(\langle \alpha - S_\alpha, X \rangle^2) \leq C|\Delta|^{2\nu} \mathcal{E}(\|X\|^2), \quad (4.14)$$

where $|\Delta|$ is the maximal length of the edges of Δ .

Proof. Let $\{\phi_1, \dots, \phi_m\}$ be a basis for $S_d^r(\Delta)$ and take $\{\phi_j, j = m + 1, m + 2, \dots\}$ to be a basis of the orthogonal complement space of $S_d^r(\Delta)$ in H . Then write $\alpha = \sum_j c_j \phi_j$. The minimization in (3.2) yields

$$\mathcal{E}(\langle \alpha, X \rangle \langle \phi_j, X \rangle) = \mathcal{E}(f(X) \langle \phi_j, X \rangle) \quad (4.15)$$

for all $j = 1, 2, \dots$ while the minimization in (4.2) gives

$$\mathcal{E}(\langle S_\alpha, X \rangle \langle \phi_j, X \rangle) = \mathcal{E}(f(X) \langle \phi_j, X \rangle) \quad (4.16)$$

for $j = 1, 2, \dots, m$. Now by subtracting (4.15) and (4.16) we obtain

$$\mathcal{E}(\langle \alpha - S_\alpha, X \rangle \langle \phi_j, X \rangle) = 0 \quad (4.17)$$

for $j = 1, 2, \dots, m$. Let $Q_\alpha = \sum_{j=1}^m a_j \phi_j$ be the quasi-interpolatory spline in $S_d^r(\Delta)$ which achieves the optimal order of approximation of α from $S_d^r(\Delta)$. Then by (4.17) and the Cauchy

Schwartz inequality we have:

$$\begin{aligned}
\mathcal{E}((\langle \alpha - S_\alpha, X \rangle)^2) &= \mathcal{E}(\langle \alpha - S_\alpha, X \rangle \langle \alpha - S_\alpha, X \rangle) \\
&= \mathcal{E}(\langle \alpha - S_\alpha, X \rangle \langle \alpha - S_\alpha + Q_\alpha - Q_\alpha, X \rangle) \\
&= \mathcal{E}((\langle \alpha - S_\alpha, X \rangle)(\langle \alpha - Q_\alpha, X \rangle + \langle Q_\alpha - S_\alpha, X \rangle)) \\
&= \mathcal{E} \left((\langle \alpha - S_\alpha, X \rangle) \left(\langle \alpha - Q_\alpha, X \rangle + \left\langle \sum_{j=1}^m (a_j - c_j) \phi_j, X \right\rangle \right) \right) \\
&= \mathcal{E} \left((\langle \alpha - S_\alpha, X \rangle) \left(\langle \alpha - Q_\alpha, X \rangle + \sum_{j=1}^m (a_j - c_j) \langle \phi_j, X \rangle \right) \right) \\
&= \mathcal{E}(\langle \alpha - S_\alpha, X \rangle \langle \alpha - Q_\alpha, X \rangle) \\
&\leq (\mathcal{E}((\langle \alpha - S_\alpha, X \rangle)^2))^{1/2} \mathcal{E}((\langle \alpha - Q_\alpha, X \rangle)^2)^{1/2}.
\end{aligned}$$

Squaring both sides an applying Theorem 2.1.14 yields the result:

$$\mathcal{E}((\langle \alpha - S_\alpha, X \rangle)^2) \leq \mathcal{E}((\langle \alpha - Q_\alpha, X \rangle)^2) \leq \|\alpha - Q_\alpha\|^2 \mathcal{E}(\|X\|^2). \quad (4.18)$$

□

Now, we consider the empirical estimate of S_α for given a sample of independent and identically distributed (i.i.d) random surfaces X_i , $i = 1, \dots, n$. The empirical estimate $\widehat{S}_{\alpha,n} \in S_d^r(\Delta)$ is the solution of

$$\widehat{S}_{\alpha,n} = \arg \min_{\beta \in S_d^r(\Delta)} \frac{1}{n} \sum_{i=1}^n (f(X_i) + \epsilon_i - \langle \beta, X_i \rangle)^2. \quad (4.19)$$

The following is theorem for the existence and uniqueness of the empirical estimate.

Theorem 4.0.4. *Suppose that only the zero spline function in the spline space $S_d^r(\Delta)$ is perpendicular to the subspace $\text{span}\{X_1, \dots, X_n\}$ except on an event whose probability p_n goes to zero as $n \rightarrow +\infty$. Then, with probability $1 - p_n$, there exists a unique $\widehat{S}_{\alpha,n} \in S_d^r(\Delta)$ minimizing (4.19).*

Proof. Similar to the proof of Theorem 4.0.2, we will start be writing the minimization problem in to a linear system. Let $\{\phi_1, \dots, \phi_m\}$ be a basis for $S_d^r(\Delta)$. The difference in the

minimization problem can be written as a function of the coefficient vector:

$$\mathcal{F}(c_j) = \frac{1}{n} \sum_{i=1}^n \left(f(X_i) - \sum_{j=1}^m c_j \langle \phi_j, X_i \rangle \right)^2. \quad (4.20)$$

Differentiation yields

$$\begin{aligned} \frac{\partial \mathcal{F}}{\partial c_l} &= 2 \frac{1}{n} \sum_{i=1}^n \left(f(X_i) - \sum_{j=1}^m c_j \langle \phi_j, X_i \rangle \right) \sum_{j=1}^m \langle \phi_j, X_i \rangle \\ &= 2 \frac{1}{n} \sum_{i=1}^n f(X_i) \sum_{j=1}^m \langle \phi_j, X_i \rangle - \sum_{j=1}^m c_j \langle \phi_j, X \rangle \sum_{j=1}^m \langle \phi_j, X_i \rangle. \end{aligned}$$

Then $\frac{\partial \mathcal{F}}{\partial c_l} = 0$ implies

$$\frac{1}{n} \sum_{i=1}^n f(X_i) \sum_{j=1}^m \langle \phi_j, X_i \rangle = \frac{1}{n} \sum_{i=1}^n \sum_{j=1}^m c_j \langle \phi_j, X_i \rangle \sum_{j=1}^m \langle \phi_j, X_i \rangle. \quad (4.21)$$

Now, we see the solution of the above minimization is given by $\widehat{S}_{\alpha, n} = \sum_{i=1}^m c_{n,i} \phi_i$ with coefficient vector $\mathbf{c}_n = (c_{n,i}, i = 1, \dots, m)$ satisfies the linear system

$$\widehat{A}_n \mathbf{c}_n = \widehat{b}_n, \quad (4.22)$$

where

$$\widehat{A}_n = \left[\frac{1}{n} \sum_{\ell=1}^n \langle \phi_i, X_\ell \rangle \langle \phi_j, X_\ell \rangle \right]_{i,j=1,\dots,m} \quad (4.23)$$

and

$$\widehat{b}_n = \left[\frac{1}{n} \sum_{\ell=1}^n f(X_\ell) \langle \phi_j, X_\ell \rangle + \frac{1}{n} \sum_{\ell=1}^n \langle \phi_j, \epsilon_\ell X_\ell \rangle \right]_{j=1,\dots,m}. \quad (4.24)$$

To see that (4.22) has a unique solution, we claim that if $\widehat{A}_n c' = 0$, then $c' = 0$. It follows that $(c')^T \widehat{A}_n c' = 0$, that is $\sum_{\ell=1}^n (\langle \sum_{i=1}^m c'_i \phi_i, X_\ell \rangle)^2 = 0$. So, $\sum_{i=1}^m c'_i \phi_i$ is orthogonal to $X_\ell, \ell = 1, \dots, n$. Now, by the assumption, $c' = 0$ except for an event whose probability p_n goes to zero when $n \rightarrow +\infty$. \square

We want to show that \widehat{A}_n converges to A , componentwise. Assume that the finite sequence $\{\langle \phi_i, X_\ell \rangle \langle \phi_j, X_\ell \rangle, \ell = 1, 2, \dots, n\}$ is i.i.d. and the infinite the sequence $(\langle \phi_i, X_\ell \rangle \langle \phi_j, X_\ell \rangle), \ell =$

$1, 2, \dots$ is integrable. Now, further assume that $\mathcal{E}(\|X_l\|^2) \leq B < \infty$. Then by Cauchy-Schwartz we have

$$\mathcal{E}(\langle \phi_i, X_l \rangle \langle \phi_j, X_l \rangle) \leq \mathcal{E}(\|\phi_i\| \|\phi_j\| \|X_l\|^2) \leq B^2 \|\phi_i\| \|\phi_j\| < \infty.$$

The last inequality follows because all of the basis functions ϕ_j can be chosen such that they are bounded in $L_2(\mathcal{D})$ independently of the triangulation [Lai and Schumaker'07, (21)].

Hence by the Strong Law of Large Numbers we have

$$\frac{1}{n} \sum_{\ell=1}^n \langle \phi_i, X_\ell \rangle \langle \phi_j, X_\ell \rangle - \mathcal{E}(\langle \phi_i, X \rangle \langle \phi_j, X \rangle) \rightarrow 0$$

almost surely for all i and j . To obtain the theorem for a global rate of convergence we need the following lemma [Golub and Van Loan'89, (18)].

Lemma 4.0.1. *Let A be an invertible matrix and \tilde{A} be a perturbation of A satisfying $\|A^{-1}\| \|A - \tilde{A}\| < 1$. Suppose that x and \tilde{x} are the exact solutions of $Ax = b$ and $\tilde{A}\tilde{x} = \tilde{b}$, respectively. Then*

$$\frac{\|x - \tilde{x}\|}{\|x\|} \leq \frac{\kappa(A)}{1 - \kappa(A) \frac{\|A - \tilde{A}\|}{\|A\|}} \left[\frac{\|A - \tilde{A}\|}{\|A\|} + \frac{\|b - \tilde{b}\|}{\|b\|} \right].$$

Here, $\kappa(A)$ denotes the condition number of matrix A .

We also need Hoeffding's exponential inequality [Bosq'98, (4)].

Lemma 4.0.2 (Hoeffding). *Let $\{\xi_l\}_{l=1}^n$ be n independent random variables. Suppose that there exists a positive number M such that for each i , $|\xi_l| \leq M < \infty$ almost surely. Then*

$$P \left(\left| \frac{1}{n} \sum_{\ell=1}^n (\xi_l - \mathcal{E}(\xi_l)) \right| \geq \delta \right) \leq 2 \exp \left(-\frac{n\delta^2}{2M^2} \right) \quad (4.25)$$

for $\delta > 0$.

Theorem 4.0.5. *Suppose that X_ℓ , $\ell = 1, \dots, n$ are independent and identically distributed and X_ℓ is bounded almost surely. Suppose that the ϵ_ℓ are independent and bounded almost*

surely. Assume that $f(X)$ is a bounded linear functional. Then $\widehat{S}_{\alpha,n}$ converges to S_α in probability with convergence rate in

$$P\left(\frac{\|S_\alpha - \widehat{S}_{\alpha,n}\|}{\|S_\alpha\|} \geq \delta\right) \leq 4m^2 \exp\left(-\frac{n\gamma^2\delta^2}{32\kappa(A)^2m^2M^2}\right) + 2m \exp\left(-\frac{n\gamma^2\delta^2}{128\kappa(A)^2M_b^2}\right) + 2m \exp\left(-\frac{n\gamma^2\delta^2}{128\kappa(A)^2M_\epsilon^2}\right). \quad (4.26)$$

Proof. The we find the rate of convergence by applying Lemma 4.0.2, Hoeffding's exponential inequality. To implement Lemma 4.0.1, we use the maximum norm for the matrix $A - \widehat{A}_n$ and the vector $b - \widehat{b}_n$. We start with $A - \widehat{A}_n$. Define $\xi_l = \langle \phi_i, X_l \rangle \langle \phi_j, X_l \rangle$ then the ξ_l are i.i.d random variables bounded by

$$M = \max_{ij} \max_{\ell} |\langle \phi_i, X_\ell \rangle \langle \phi_j, X_\ell \rangle| \leq \max_{ij} \max_{\ell} \|\phi_i\| \|\phi_j\| \|X_\ell\|^2.$$

That is, for each i , $|\xi_l| \leq M < \infty$ almost surely. We write

$$\widehat{A}_n - A = [a_{ij}]_{1 \leq i, j \leq m} = \left[\frac{1}{n} \sum_{\ell=1}^n \langle \phi_i, X_\ell \rangle \langle \phi_j, X_\ell \rangle - \mathcal{E}(\langle \phi_i, X \rangle \langle \phi_j, X \rangle) \right]_{i, j=1, \dots, m}$$

and then by Lemma 4.0.2,

$$\begin{aligned} P(\| [a_{ij}]_{1 \leq i, j \leq m} \|_\infty \geq \delta) &= P\left(\max_{1 \leq i \leq m} \sum_{j=1}^m |a_{ij}| \geq \delta\right) \\ &\leq \sum_{i=1}^m P\left(\sum_{j=1}^m |a_{ij}| \geq \delta\right) \\ &\leq \sum_{i=1}^m \sum_{j=1}^m P(|a_{ij}| \geq \delta/m) \\ &\leq 2m^2 \exp\left(-\frac{n\delta^2}{2m^2M^2}\right). \end{aligned} \quad (4.27)$$

We estimate the entries of $\mathbf{b} - \widehat{b}_n$ in a similar way, by letting $b_j = b_j^1 + b_j^2$ with

$$b_j^1 = \frac{1}{n} \sum_{\ell=1}^n f(X_\ell) \langle \phi_j, X_\ell \rangle - \mathcal{E}(f(X) \langle \phi_j, X \rangle)$$

and

$$b_j^2 = \frac{1}{n} \sum_{\ell=1}^n \langle \phi_j, \epsilon_\ell X_\ell \rangle.$$

Then we can break up the probability by

$$P(|b_j| \geq \delta) \leq P(|b_j^1| \geq \delta/2) + P(|b_j^2| \geq \delta/2).$$

We know that the functional f is bounded, and thus $|f(X_\ell)| \leq F\|X_\ell\|$ for some constant F .

By Lemma 4.0.2, we have

$$P(|b_j^1| \geq \delta/2) \leq 2 \exp\left(-\frac{n\delta^2}{8M_b^2}\right),$$

where

$$M_b = \max_j |f(X_\ell)\langle\phi_j, X_\ell\rangle| \leq F\|X_\ell\|\|\phi_j\|\|X_\ell\|$$

which is a finite quantity since $\|X_\ell\|$ is bounded almost surely. For b_j^2 , we recall that the random noises ϵ_ℓ are bounded almost surely and let $\xi_\ell = \langle\phi_j, \epsilon_\ell X_\ell\rangle$. Then we apply Lemma 4.0.2 to have

$$P(|b_j^2| \geq \delta/2) \leq 2 \exp\left(-\frac{n\delta^2}{8M_\epsilon^2}\right)$$

where

$$M_\epsilon = \max_j |\langle\phi_j, \epsilon_\ell X_\ell\rangle| \leq \max_j \|\phi_j\|\|\epsilon_\ell\|\|X_\ell\|$$

which is finite under the assumption that both $\|X_\ell\|$ and $|\epsilon_\ell|$ are bounded almost surely.

Thus we have

$$P\left(\|\mathbf{b} - \widehat{\mathbf{b}}_n\|_\infty \geq \delta\right) \leq \sum_{j=1}^m P(|b_j| \geq \delta) \leq 2m \exp\left(-\frac{n\delta^2}{8M_b^2}\right) + 2m \exp\left(-\frac{n\delta^2}{8M_\epsilon^2}\right). \quad (4.28)$$

Now that we have bounds on $\|\widehat{A} - A\|$ and $\|\widehat{\mathbf{b}} - \mathbf{b}\|$, use Lemma 2.1.4 to obtain

$$P\left(\frac{\|S_\alpha - \widetilde{S}_{\alpha,n}\|}{\|S_\alpha\|} \geq \delta\right) \leq P\left(\frac{\|\mathbf{c} - \widetilde{\mathbf{c}}_n\|}{\|\mathbf{c}\|} \geq \gamma\delta\right)$$

where $\gamma = \sqrt{\frac{C_1}{C_2}}$. Let $\beta = \frac{\|\mathbf{c} - \widetilde{\mathbf{c}}_n\|}{\|\mathbf{c}\|}$, $\eta = \frac{\|A - \widehat{A}_n\|}{\|A\|}$ and $\theta = \frac{\|\mathbf{b} - \widehat{\mathbf{b}}_n\|}{\|\mathbf{b}\|}$ then Lemma 4.0.1 yields

$$\beta \leq \frac{\kappa(A)}{1 - \kappa(A)\eta}(\eta + \theta). \quad (4.29)$$

We also note that for $\kappa(A)\eta \leq \frac{1}{2}$, we have $1 - \kappa(A)\eta \geq 1 - \frac{1}{2}$ which implies

$$\frac{\kappa(A)}{1 - \kappa(A)\eta} \leq 2\kappa(A). \quad (4.30)$$

Now,

$$\begin{aligned}
P(\beta \geq \gamma\delta) &\leq P(\beta \geq \gamma\delta, \kappa(A)\eta \leq 1/2) + P(\beta \geq \gamma\delta, \kappa(A)\eta \geq 1/2) \\
&\leq P\left(\frac{\kappa(A)}{1 - \kappa(A)\eta}(\eta + \theta) \geq \gamma\delta, \kappa(A)\eta \leq 1/2\right) + P(\kappa(A)\eta \geq 1/2) \\
&\leq P\left((\eta + \theta) \geq \frac{\gamma\delta}{2\kappa(A)}\right) + P(\kappa(A)\eta \geq 1/2) \\
&\leq P\left(\eta \geq \frac{\gamma\delta}{4\kappa(A)}\right) + P\left(\theta \geq \frac{\gamma\delta}{4\kappa(A)}\right) + P\left(\eta \geq \frac{\gamma\delta}{2\kappa(A)}\right) \\
&\leq 2P\left(\eta \geq \frac{\gamma\delta}{4\kappa(A)}\right) + P\left(\theta \geq \frac{\gamma\delta}{4\kappa(A)}\right)
\end{aligned}$$

for all $\delta \leq 1$. By (4.27) and (4.28) we have

$$\begin{aligned}
P\left(\frac{\|S_\alpha - \widetilde{S}_{\alpha,n}\|}{\|S_\alpha\|} \geq \delta\right) &\leq 2P\left(\eta \geq \frac{\gamma\delta}{4\kappa(A)}\right) + P\left(\theta \geq \frac{\gamma\delta}{4\kappa(A)}\right) \\
&= 2P\left(\frac{\|A - \widehat{A}_n\|}{\|A\|} \geq \frac{\gamma\delta}{4\kappa(A)}\right) + P\left(\frac{\|\mathbf{b} - \widehat{b}_n\|}{\|\mathbf{b}\|} \geq \frac{\gamma\delta}{4\kappa(A)}\right) \\
&= 2\left(2m^2 \exp\left(-\frac{n\left(\frac{\gamma\delta}{4\kappa(A)}\right)^2}{2m^2 M^2}\right)\right) + 2m \exp\left(-\frac{n\left(\frac{\gamma\delta}{4\kappa(A)}\right)^2}{8M_b^2}\right) \\
&\quad + 2m \exp\left(-\frac{n\left(\frac{\gamma\delta}{4\kappa(A)}\right)^2}{8M_\epsilon^2}\right) \\
&= 4m^2 \exp\left(-\frac{n\gamma^2\delta^2}{32\kappa(A)^2 m^2 M^2}\right) + 2m \exp\left(-\frac{n\gamma^2\delta^2}{128\kappa(A)^2 M_b^2}\right) \\
&\quad + 2m \exp\left(-\frac{n\gamma^2\delta^2}{128\kappa(A)^2 M_\epsilon^2}\right).
\end{aligned}$$

□

We also want to consider the case where ϵ_ℓ 's are Gaussian noise. We will need the following lemma.

Lemma 4.0.3. *Suppose that ϵ_ℓ is a Gaussian noise $N(0, \sigma_\ell^2)$ for $\ell = 1, \dots, n$. Then*

$$P\left(\left|\frac{1}{n} \sum_{\ell=1}^n \epsilon_\ell\right| > \delta\right) \leq 2 \exp\left(-\frac{n^2\delta^2}{2\sum_{\ell=1}^n \sigma_\ell^2}\right). \quad (4.31)$$

Now, we have a theorem for Gaussian noise similar to Theorem 4.0.5.

Theorem 4.0.6. *Suppose that X_ℓ , $\ell = 1, \dots, n$ are independent and identically distributed random variables and $\|X_\ell\|$ are bounded almost surely. Suppose ϵ_ℓ are independent and identically distributed Gaussian noise $N(0, \sigma^2)$ and $f(X)$ is a bounded linear functional. Then $\widehat{S}_{\alpha, n}$ converges to S_α in probability with convergence rate*

$$P\left(\frac{\|S_\alpha - \widehat{S}_{\alpha, n}\|}{\|S_\alpha\|} \geq \delta\right) \leq 4m^2 \exp\left(-\frac{n\gamma^2\delta^2}{32\kappa(A)^2 m^2 M^2}\right) + 2m \exp\left(-\frac{n\gamma^2\delta^2}{128\kappa(A)^2 M_b^2}\right) + 2m \exp\left(-\frac{n\gamma^2\delta^2}{128\kappa(A)^2 \sigma^2 C^2}\right). \quad (4.32)$$

Proof. Using Lemma 4.0.3 when the ϵ_ℓ are i.i.d Gaussian noises $N(0, \sigma^2)$, we have

$$P\left(\left|\frac{1}{n} \sum_{\ell=1}^n (\epsilon_\ell Y_\ell)\right| \geq \delta\right) \leq 2 \exp\left(-\frac{n\delta^2}{2\sigma^2 C^2}\right)$$

for $\delta > 0$ with the assumption that Y_ℓ are independent random variables which are bounded by C , $\|Y_\ell\| \leq C$. Now to obtain the result (4.32), repeat the proof of Theorem 4.0.5 with

$$P\left(\|\mathbf{b} - \widehat{\mathbf{b}}_n\|_\infty \geq \delta\right) \leq \sum_{j=1}^m P(|b_j| \geq \delta) \leq 2m \exp\left(-\frac{n\delta^2}{8M_b^2}\right) + 2 \exp\left(-\frac{n\delta^2}{2\sigma^2 C^2}\right). \quad (4.33)$$

instead of (4.28). \square

Now we consider the cases where we observe X over a set of design points $s_k, k = 1, \dots, N$ in \mathcal{D} . We create a surface to represent X from the given data by constructing S_X , the penalized least square fit of X . To do this we assume that s_k are evenly distributed over Δ of \mathcal{D} with respect to $S_d^r(\Delta)$. We look for the α_D that solves the minimization problem (4.4):

$$\alpha_D = \arg \min_{\beta \in H} \mathcal{E} [(f(X) + \epsilon - \langle \beta, S_X \rangle)^2].$$

First, we note that α_D approximates α . We can see this by defining the strictly convex and continuous function

$$F(\beta) = \mathcal{E} [(f(X) + \epsilon - \langle \beta, X \rangle)^2]$$

and an approximation to F , as $|\Delta| \rightarrow 0$:

$$F_D(\beta) = \mathcal{E} [(f(X) + \epsilon - \langle \beta, S_X \rangle)^2].$$

Since strictly convex functions have unique minimizers we have α_D approximating α . Indeed, if $\alpha_D \rightarrow \beta \neq \alpha$, then

$$F(\alpha) < F(\beta) = F_D(\beta) + \eta_1 = F_D(\alpha_D) + \eta_1 + \eta_2 \leq F_D(\alpha) + \eta_1 + \eta_2 = F(\alpha_D) + \eta_1 + \eta_2 + \eta_3$$

for arbitrary small $\eta_1 + \eta_2 + \eta_3$. We would get the contradiction $F(\alpha) < F(\alpha)$.

Again we are trying to find a minimum in the infinite dimensional Hilbert space H so we approximate solution in the finite spline space $S_d^r(\Delta)$. We approximate the solution $S_{\alpha_D} \in S_d^r(\Delta)$ of α_S by solving (4.5)

$$S_{\alpha_D} = \arg \min_{\beta \in S_d^r(\Delta)} \mathcal{E} [(f(X) + \epsilon - \langle \beta, S_X \rangle)^2].$$

Let $\{\phi_1, \dots, \phi_m\}$ be a basis for $S_d^r(\Delta)$, then we $S_{\alpha_D} = \sum_{j=1}^m c_{S,j} \phi_j$ where the coefficient vector $\mathbf{c}_D = (c_{S,1}, \dots, c_{S,m})^T$ satisfies the linear system

$$A_D \mathbf{c}_D = \mathbf{b}_D$$

where A_D is the matrix A in the continuous case evaluated at S_X instead of X . That is, A_D is an $m \times m$ matrix with entries $\mathcal{E}(\langle \phi_i, S_X \rangle \langle \phi_j, S_X \rangle)$ for $i, j = 1, \dots, m$. Similarly, \mathbf{b}_D is a vector of length m with entries $\mathcal{E}((f(X) + \epsilon) \langle \phi_j, S_X \rangle)$ for $j = 1, \dots, m$. The matrix, A_D converges to the matrix A as $|\Delta| \rightarrow 0$ by Theorem 2.1.14:

$$\|S_X - X\|_{\infty, \mathcal{D}} \leq C |\Delta|^\nu |X|_{\nu, \infty, \mathcal{D}}$$

for $X \in W_2^\nu(\mathcal{D})$ with $\nu \geq r > 0$, and thus

$$\mathcal{E}(\langle \phi_i, S_X \rangle \langle \phi_j, S_X \rangle) \rightarrow \mathcal{E}(\langle \phi_i, X \rangle \langle \phi_j, X \rangle)$$

as $S_X \rightarrow X$.

The next theorem states how well S_{α_D} approximates α_D in terms of $|\Delta|$, the size of triangulation.

Theorem 4.0.7. *Suppose that $\mathcal{E}(\|X\|^2) < \infty$ and suppose $\alpha \in C^r(\mathcal{D})$ for $r \geq 0$. Then the solution S_{α_D} from the minimization problem (4.5) approximates α_S in the following sense:*

$$\mathcal{E}(\langle \alpha_D - S_{\alpha_D}, S_X \rangle^2) \leq C |\Delta|^{2r} \tag{4.34}$$

for a constant C dependent on $\mathcal{E}(\|X\|^2)$, where $|\Delta|$ is the maximal length of the edges of Δ .

Proof. Similar to the proof of Theorem 4.0.3, we let $\{\phi_1, \dots, \phi_m\}$ denote a basis for $S_d^r(\Delta)$ and take $\{\phi_j, j = m+1, m+2, \dots\}$ to be a basis of the orthogonal complement space of $S_d^r(\Delta)$ in H as before. Then we can write

$$\alpha_D = \sum_{j=1}^{\infty} c_{D,j} \phi_j.$$

Note that the minimization in (4.4) yields

$$\mathcal{E}(\langle \alpha_D, S_X \rangle \langle \phi_j, S_X \rangle) = \mathcal{E}((f(X) + \epsilon) \langle \phi_j, S_X \rangle)$$

for all $j = 1, 2, \dots$ while the minimization in (4.5) gives

$$\mathcal{E}(\langle S_{\alpha_S}, S_X \rangle \langle \phi_j, S_X \rangle) = \mathcal{E}((f(X) + \epsilon) \langle \phi_j, S_X \rangle)$$

for all $j = 1, 2, \dots, m$. Subtraction yields,

$$\mathcal{E}(\langle \alpha_D - S_{\alpha_D}, S_X \rangle \langle \phi_j, S_X \rangle) = 0 \tag{4.35}$$

for all $j = 1, 2, \dots, m$. Let Q_{α_D} be the quasi-interpolatory spline in $S_d^r(\Delta)$ which achieves the optimal order of approximation of α_D from $S_d^r(\Delta)$. Then by (4.35) and the Cauchy Schwartz inequality we have

$$\begin{aligned} \mathcal{E}(\langle \alpha_D - S_{\alpha_D}, S_X \rangle^2) &= \mathcal{E}(\langle \alpha_D - S_{\alpha_D}, S_X \rangle \langle \alpha_D - S_{\alpha_D}, S_X \rangle) \\ &= \mathcal{E}(\langle \alpha_D - S_{\alpha_D}, S_X \rangle \langle \alpha_D - S_{\alpha_D} + Q_{\alpha_D} - Q_{\alpha_D}, S_X \rangle) \\ &= \mathcal{E}(\langle \alpha_D - S_{\alpha_D}, S_X \rangle (\langle \alpha_D - Q_{\alpha_D}, S_X \rangle + \langle Q_{\alpha_D} - S_{\alpha_D}, S_X \rangle)) \\ &= \mathcal{E} \left(\langle \alpha_D - S_{\alpha_D}, S_X \rangle \left(\langle \alpha_D - Q_{\alpha_D}, S_X \rangle + \left\langle \sum_{j=1}^m (a_j - c_j) \phi_j, S_X \right\rangle \right) \right) \\ &= \mathcal{E} \left(\langle \alpha_D - S_{\alpha_D}, S_X \rangle \left(\langle \alpha_D - Q_{\alpha_D}, S_X \rangle + \sum_{j=1}^m (a_j - c_j) \langle \phi_j, S_X \rangle \right) \right) \\ &= \mathcal{E}(\langle \alpha_D - S_{\alpha_D}, S_X \rangle \langle \alpha_D - Q_{\alpha_D}, S_X \rangle) \\ &\leq (\mathcal{E}(\langle \alpha_D - S_{\alpha_D}, S_X \rangle^2))^{1/2} \mathcal{E}(\langle \alpha_D - Q_{\alpha_D}, S_X \rangle^2)^{1/2}. \end{aligned}$$

Yielding

$$\mathcal{E}(\langle \alpha_D - S_{\alpha_D}, S_X \rangle)^2 \leq \mathcal{E}(\langle \alpha_D - Q_{\alpha_D}, S_X \rangle)^2 \leq \|\alpha_D - Q_{\alpha_D}\|^2 \mathcal{E}(\|S_X\|^2).$$

The convergence of S_X to X implies that $\mathcal{E}(\|S_X\|^2)$ is bounded by a constant dependent on $\mathcal{E}(\|X\|^2)$. The approximation of the quasi-interpolant Q_{α_S} of α_S in Theorem 2.1.14 yields (4.34). \square

The empirical estimate of S_{α_D} based on discrete observations of random surfaces $X_i, i = 1, \dots, n$, is given by solving the minimization problem:

$$\widetilde{S}_{\alpha_D, n} = \arg \min_{\beta \in S_d^r(\Delta)} \frac{1}{n} \sum_{i=1}^n (f(X_i) + \epsilon_i - \langle \beta, S_{X_i} \rangle)^2.$$

Again, we can expand $\widetilde{S}_{\alpha, n}$ in terms of the basis functions of $S_d^r(\Delta)$ as $\widetilde{S}_{\alpha, n} = \sum_{i=1}^m \widetilde{c}_{n, i} \phi_i$ where the coefficient vector $\widetilde{\mathbf{c}}_n = (\widetilde{c}_{n, i}, i = 1, \dots, m)$ satisfies the linear system

$$\widetilde{A}_n \widetilde{\mathbf{c}}_n = \widetilde{\mathbf{b}}_n,$$

where

$$\widetilde{A}_n = \left[\frac{1}{n} \sum_{\ell=1}^n \langle \phi_i, S_{X_\ell} \rangle \langle \phi_j, S_{X_\ell} \rangle \right]_{i, j=1, \dots, m}$$

where S_{X_ℓ} is the penalized least squares fit of X_ℓ and

$$\widetilde{\mathbf{b}}_n = \left[\frac{1}{n} \sum_{\ell=1}^n f(X_\ell) \langle \phi_j, S_{X_\ell} \rangle + \frac{1}{n} \sum_{\ell=1}^n \langle \phi_j, \epsilon_\ell S_{X_\ell} \rangle \right]_{j=1, \dots, m}.$$

Now we argue that $\widetilde{S}_{\alpha, n}$ converges to $\widehat{S}_{\alpha, n}$. To do this, we implement Lemma 4.0.1, we use the maximum norm for the matrix $\widehat{A}_n - \widetilde{A}_n$ and the vector $\widehat{\mathbf{b}}_n - \widetilde{\mathbf{b}}_n$. We start with $\widehat{A}_n - \widetilde{A}_n$:

$$\begin{aligned} \widehat{A}_n - \widetilde{A}_n &= \left[\frac{1}{n} \sum_{\ell=1}^n \langle \phi_i, S_{X_\ell} \rangle \langle \phi_j, S_{X_\ell} \rangle - \frac{1}{n} \sum_{\ell=1}^n \langle \phi_i, X_\ell \rangle \langle \phi_j, X_\ell \rangle \right]_{i, j=1, \dots, m} \\ &= \left[\frac{1}{n} \sum_{\ell=1}^n \langle \phi_i, S_{X_\ell} \rangle \langle \phi_j, S_{X_\ell} \rangle - \langle \phi_i, X_\ell \rangle \langle \phi_j, X_\ell \rangle \right]_{i, j=1, \dots, m} \\ &= \left[\frac{1}{n} \sum_{\ell=1}^n \langle \phi_i, S_{X_\ell} - X_\ell \rangle \langle \phi_j, S_{X_\ell} - X_\ell \rangle \right]_{i, j=1, \dots, m} \end{aligned}$$

Taking the norm yields,

$$\begin{aligned}
\|\widetilde{A}_n - \widehat{A}_n\|_\infty &= \max_i \sum_{j=1}^m \left| \frac{1}{n} \sum_{\ell=1}^n \langle \phi_i, S_{X_\ell} - X_\ell \rangle \langle \phi_j, S_{X_\ell} - X_\ell \rangle \right| \\
&\leq \max_i \sum_{j=1}^m \frac{1}{n} \sum_{\ell=1}^n |\langle \phi_i, S_{X_\ell} - X_\ell \rangle \langle \phi_j, S_{X_\ell} - X_\ell \rangle| \\
&\leq \max_i \sum_{j=1}^m \max_\ell |\langle \phi_i, S_{X_\ell} - X_\ell \rangle \langle \phi_j, S_{X_\ell} - X_\ell \rangle| \\
&\leq m \max_{i,j} \max_\ell |\langle \phi_i, S_{X_\ell} - X_\ell \rangle \langle \phi_j, S_{X_\ell} - X_\ell \rangle| \\
&\leq m \max_{i,j} \max_\ell \|\phi_i\| \|\phi_j\| \|S_{X_\ell} - X_\ell\|^2.
\end{aligned}$$

Hence $\|\widetilde{A}_n - \widehat{A}_n\|_\infty = O(|\Delta|^{\nu-2})$ since $S_{X_\ell} - X_\ell = O(|\Delta|^\nu)$ by Theorem 2.1.14. So if ν is sufficiently large then $\|\widetilde{A}_n - \widehat{A}_n\|_\infty \rightarrow 0$ as $\|\Delta\| \rightarrow 0$.

Similarly, we estimate the entries of $\widehat{b}_n - \widetilde{b}_n$

$$\begin{aligned}
\|\widehat{b}_n - \widetilde{b}_n\|_\infty &= \left\| \frac{1}{n} \sum_{\ell=1}^n f(X_\ell) \langle \phi_j, X_\ell \rangle - \frac{1}{n} \sum_{\ell=1}^n f(X_\ell) \langle \phi_j, S_{X_\ell} \rangle \right\|_\infty \\
&= \left\| \frac{1}{n} \sum_{\ell=1}^n f(X_\ell) \langle \phi_j, X_\ell - S_{X_\ell} \rangle \right\|_\infty \\
&\leq \max_{j,\ell} |f(X_\ell) \langle \phi_j, X_\ell - S_{X_\ell} \rangle| \\
&\leq \max_{j,\ell} F \|X_\ell\| \|\phi_j\| \|X_\ell - S_{X_\ell}\|.
\end{aligned}$$

Thus $\widehat{b}_n - \widetilde{b}_n$ also converges to 0. Now, we apply Lemma 4.0.1 as we did in the proof of Theorem 4.26 to see that $\widetilde{S}_{\alpha,n}$ converges to $\widehat{S}_{\alpha,n}$ as $|\Delta| \rightarrow 0$.

CHAPTER 5

BRUTE FORCE EXTENSION

So far we have discussed functional linear models, a regression model where the explanatory variable is a random function and the response is a real random variable. There are many cases where we may want to predict values for locations where there are no measurements. In this chapter, we consider the case when the explanatory and response variables are both random surfaces. We define the model by convolution:

$$Y(s) = G(s, t) * X(t) = \int_{\mathcal{D}} G(s, t) X(t) dt, \quad (5.1)$$

where \mathcal{D} a polygonal domain in \mathbb{R}^2 and $G(s, t)$ is some function in $H \times H$. We usually take H to be $L^2(\mathcal{D})$. For this application, we assume we are given a function F such that $F = G * X$ for some function G . The objective is to recover the function G .

For our research, we will need a tensor product version of Theorem 2.1.14. For convenience, we use a special instance of the quasi-interpolatory operator to illustrate the main ideas. That is, when

$$a_{\nu}^{ijk} = \begin{cases} 1 & \text{if } \nu = ijk \\ 0 & \text{otherwise} \end{cases}$$

in (2.58), we have the following quasi-interpolatory operator

$$Qf := \sum_{T \in \Delta} \sum_{i+j+k=d} f(\xi_{ijk}) B_{ijk}^T. \quad (5.2)$$

We will need the following lemma for the proof of the analog of Theorem 2.1.14.

Lemma 5.0.4. *Let $F(s, t)$ be a function in $H \times H$ and define for a fixed $s \in \mathbb{R}^2$,*

$$RF(s, t) = \sum_{T \in \Delta} \sum_{i+j+k=d} F(\xi_{ijk}, s) B_{ijk}^T(t). \quad (5.3)$$

Then

$$|F(s, t) - RF(s, t)| \leq |\Delta|^{d+1} |F(s, \cdot)|_{d+1}. \quad (5.4)$$

Proof. First note that by Theorem 2.1.14 we have

$$\|Qf - f\| \leq |\Delta|^{d+1} |f|_{d+1} \quad (5.5)$$

for a quasi-interpolatory spline defined in (2.52). We can utilize the inequality in (5.5) since for a fixed s we are only comparing the difference in one variable. To see how well we are approximating in t , we consider the following difference for a fixed s , and apply Theorem 2.1.14

$$\begin{aligned} |F(s, t) - RF(s, t)| &= \left| F(s, t) - \sum_{T \in \Delta} \sum_{i+j+k=d} F(\xi_{ijk}, s) B_{ijk}^T(t) \right| \\ &\leq |\Delta|^{d+1} |F_t(s, \cdot)|_{d+1}. \end{aligned}$$

□

With the above lemma, we are ready for the analog of Theorem 2.1.14.

Theorem 5.0.8. *Let $F(s, t) \in H \times H$ and let $Q_F(s, t)$ be the special case of quasi-interpolatory spline defined for the tensor product of two splines:*

$$Q_F = \sum_{T'} \sum_{i'+j'+k'=d} \sum_T \sum_{i+j+k=d} F(\xi_{ijk}, \xi'_{i'j'k'}) B_{ijk}^T(t) B_{i'j'k'}^{T'}(s). \quad (5.6)$$

Then

$$|F(s, t) - Q_F(s, t)| \leq 2|\Delta|^{d+1} \max\{|F(s, \cdot)|_{d+1}, |F(\cdot, t)|_{d+1}\}. \quad (5.7)$$

Proof. Define the function RF as in (5.3). First, note that

$$\begin{aligned} &|RF(s, t) - Q_F(s, t)| \\ &= \left| \sum_{T \in \Delta} \sum_{i+j+k=d} F(\xi_{ijk}, s) B_{ijk}^T(t) - \sum_{T'} \sum_{i'+j'+k'=d} \sum_T \sum_{i+j+k=d} F(\xi_{ijk}, \xi'_{i'j'k'}) B_{ijk}^T(t) B_{i'j'k'}^{T'}(s) \right| \\ &= \left| \sum_{T \in \Delta} \sum_{i+j+k=d} B_{ijk}^T(t) \left(F(\xi_{ijk}, s) - \sum_{T'} \sum_{i'+j'+k'=d} F(\xi_{ijk}, \xi'_{i'j'k'}) B_{i'j'k'}^{T'}(s) \right) \right| \end{aligned} \quad (5.8)$$

$$\begin{aligned} &\leq \left| F(\xi_{ijk}, s) - \sum_{T'} \sum_{i'+j'+k'=d} F(\xi_{ijk}, \xi'_{i'j'k'}) B_{i'j'k'}^{T'}(s) \right| \\ &= |\Delta|^{d+1} |F(\cdot, t)|_{d+1, s}. \end{aligned} \quad (5.9)$$

In (5.8), we used the partition of unity property of splines and for (5.9) we applied Lemma 5.0.4. We apply Lemma 5.0.4 again to obtain:

$$\begin{aligned}
|F(s, t) - Q_F(s, t)| &= |F(s, t) - RF(s, t) + RF(s, t) - Q_F(s, t)| \\
&\leq |F(s, t) - RF(s, t)| + |RF(s, t) - Q_F(s, t)| \\
&\leq |\Delta|^{d+1} |F(s, \cdot)|_{d+1, t} + |\Delta|^{d+1} |F(\cdot, t)|_{d+1, s} \\
&\leq 2|\Delta|^{d+1} \max\{|F(s, \cdot)|_{d+1, t}, |F(\cdot, t)|_{d+1, s}\}.
\end{aligned}$$

□

Now, consider the model given in (5.1). The solution to the model, G , is given by solving the following minimization problem:

$$G = \arg \min_{\beta \in H \times H} \mathcal{E} \left(\int_{s \in \mathcal{D}} (F(X)(s) - \beta(s, \cdot) * X(\cdot))^2 ds \right). \quad (5.10)$$

However, it is impossible solve the above minimization problem because we have an infinite dimensional Hilbert space H . To find an approximation to the solution, we can choose a spline space $S_d^r(\Delta)$ for some integers r and d with $r < d$. By Theorem 2.1.14, it is dense in H as $|\Delta| \rightarrow 0$ and $S_d^r(\Delta) \times S_d^r(\Delta)$ is dense in $H \times H$ by Theorem 5.5. Hence we look for an approximation to G , in the finite dimensional space $S_G \in S_d^r(\Delta) \times S_d^r(\Delta)$, such that

$$S_G = \arg \min_{\beta \in S_d^r(\Delta) \times S_d^r(\Delta)} \mathcal{E} \left(\int_{s \in \mathcal{D}} (F(X)(s) - \beta(s, \cdot) * X(\cdot))^2 ds \right). \quad (5.11)$$

Theorem 5.0.9. *Suppose that only the zero spline in $S_d^r(\Delta)$ is orthogonal to the collection $\mathcal{X} \subset H$. Then solution to (5.11) has a unique solution in $S_d^r(\Delta) \times S_d^r(\Delta)$.*

Proof. We start by simplifying $S_G * X$:

$$\begin{aligned}
S_G * X &= \int_{\mathcal{D}} X(t) S_G(s, t) dt \\
&= \int_{\mathcal{D}} X(t) \sum_{i, j} c_{i, j} \phi_i(s) \phi_j(t) dt \\
&= \sum_{i, j} c_{i, j} \phi_i(s) \int_{\mathcal{D}} X(t) \phi_j(t) dt \\
&= \sum_{i, j} c_{i, j} \phi_i(s) \langle X, \phi_j \rangle.
\end{aligned}$$

We want to find the coefficient vector that minimizes the difference in (5.11). For simplicity, we write the difference as a function of the coefficient vector:

$$\mathcal{F}(c_{i,j}) = \mathcal{E} \left(\int_{\mathcal{D}} \left(F(X)(s) - \sum_{i,j} c_{i,j} \phi_i(s) \langle X, \phi_j \rangle \right)^2 ds \right). \quad (5.12)$$

Hence by differentiation we have

$$\begin{aligned} \frac{\partial \mathcal{F}}{\partial c_{l,k}} &= 2\mathcal{E} \left(\int_{\mathcal{D}} \left(F(X)(s) - \sum_{i,j} c_{i,j} \phi_i(s) \langle X, \phi_j \rangle \right) (\phi_l(s) \langle X, \phi_k \rangle) ds \right) \\ &= 2\mathcal{E} \left(\int_{\mathcal{D}} \left(F(X)(s) \phi_l(s) \langle X, \phi_k \rangle - \sum_{i,j} c_{i,j} \phi_i(s) \langle X, \phi_j \rangle \phi_l(s) \langle X, \phi_k \rangle \right) ds \right). \end{aligned}$$

Then $\frac{\partial \mathcal{F}}{\partial c_{l,k}} = 0$ implies

$$\mathcal{E} \left(\int_{\mathcal{D}} (F(X_J)(s) \phi_l(s) \langle X_J, \phi_k \rangle) ds \right) = \mathcal{E} \left(\int_{\mathcal{D}} \left(\sum_{i,j} c_{i,j} \phi_i(s) \langle X_J, \phi_j \rangle \phi_l(s) \langle X_J, \phi_k \rangle \right) ds \right) \quad (5.13)$$

for all $0 \leq l, k \leq m$. We rewrite this as a linear system $Ac = b$ where c is the vector of coefficients, A is an $m^2 \times m^2$ matrix with entries

$$\mathcal{E} \left(\int_{\mathcal{D}} (\phi_i(s) \langle X, \phi_j \rangle \phi_l(s) \langle X, \phi_k \rangle) ds \right)$$

and b is a vector of the form

$$\mathcal{E} \left(\int_{\mathcal{D}} (F(X)(s) \phi_l(s) \langle X, \phi_k \rangle) ds \right).$$

To solve the linear system, we need to find the conditions for which A is invertible. We know that A is invertible, if it is of full rank and the only solution to $v^T Av = 0$ is $v = 0$. Let v be an arbitrary vector then we have

$$\begin{aligned} v^T Av &= \mathcal{E} \left(\int_{\mathcal{D}} \left(\sum_{l,k} \sum_{i,j} v_{i,j} (\phi_i(s) \langle X, \phi_j \rangle \phi_l(s) \langle X, \phi_k \rangle) v_{l,k} \right) ds \right) \\ &= \mathcal{E} \left(\int_{\mathcal{D}} \left(\sum_{l,k} \phi_l(s) \langle X, \phi_k \rangle v_{l,k} \sum_{i,j} v_{i,j} \phi_i(s) \langle X, \phi_j \rangle \right) ds \right) \\ &= \mathcal{E} \left(\int_{\mathcal{D}} \left(\sum_{i,j} v_{i,j} \phi_i(s) \langle X, \phi_j \rangle \right)^2 ds \right) = 0. \end{aligned}$$

To have $v^T Av = 0$ then for all $s \in \mathcal{D}$ we have

$$\sum_{i,j} v_{i,j} \phi_i(s) \langle X, \phi_j \rangle = \sum_i \left(\sum_j v_{i,j} \langle X, \phi_j \rangle \right) \phi_i(s) = 0. \quad (5.14)$$

The $\{\phi_i\}$ form a basis for the spline space $S_d^r(\Delta) \times S_d^r(\Delta)$ hence the only solution (5.14) is for all the coefficients to be zero, that is

$$\sum_j v_{i,j} \langle X, \phi_j \rangle = 0 \quad (5.15)$$

for all $X \in \mathcal{X}$. By our assumption that only the zero spline is orthogonal to X therefore $\langle X, \phi_j \rangle \neq 0$ which implies that the only way $vAv^T = 0$ is for $v = 0$. \square

Now that we know when there exists a unique solution to (5.11), we want to know how well S_G approximates G in terms of $|\Delta|$.

Theorem 5.0.10. *Suppose that $\mathcal{E}(\|X\|^2) < \infty$ and $G \in \mathcal{C}^{d+1}(\mathcal{D})$. Then the solution S_G from the minimization problem (5.11) approximates G in the following sense*

$$\mathcal{E} \left(\int ((G - S_G) * X)^2 ds \right) \leq (2|\Delta|^{d+1} \max\{|G(s, \cdot)|_{d+1}, |G(\cdot, t)|_{d+1}\})^2 \mathcal{E}(\|X\|^2). \quad (5.16)$$

Proof. Since we choose $S_d^r(\Delta) \times S_d^r(\Delta)$ to be dense in $H \times H$ as $|\Delta| \rightarrow 0$ based on Theorem 5.0.11, we look for an approximation S_G of G that satisfies (5.11). We need to show that S_G approximates G . Let $\{\phi_1, \dots, \phi_m\}$ be a basis for $S_d^r(\Delta)$, and $\{\phi_j, j = m+1, m+2, \dots\}$ be a basis of the orthogonal complement space of $S_d^r(\Delta)$ in H . Then for any function $G \in H \times H$ we can express G by

$$\begin{aligned} G &= \sum_{i,j=1}^{m \times m} c_{ij} \phi_i(t) \phi_j(s) + \sum_{i=1}^m \sum_{j \geq m+1} d_{ij} \phi_i(t) \phi_j(s) \\ &\quad + \sum_{i \geq m+1} \sum_{j=1}^m d_{ij} \phi_i(t) \phi_j(s) + \sum_{i \geq m+1} \sum_{j \geq m+1} d_{ij} \phi_i(t) \phi_j(s). \end{aligned} \quad (5.17)$$

To simplify (5.17), let $\{\varphi_i(s, t), i = 1, \dots, m^2\}$ be the basis elements for $S_d^r(\Delta) \times S_d^r(\Delta)$ and let $\{\varphi_i(s, t), i = m^2 + 1, m^2 + 2, \dots\}$ be a basis of the orthogonal complement space of

$S_d^r(\Delta) \times S_d^r(\Delta)$ in $H \times H$ then we expand G in terms of the basis elements $\{\varphi_i(s, t), i = 1, 2, \dots\}$. By minimizing (5.10) we have

$$\mathcal{E} \left(\int_{s \in \mathcal{D}} f(X)(s)(X * \varphi_i(s, t)) ds \right) = \mathcal{E} \left(\int_{s \in \mathcal{D}} (X * G(s, t))(X * \varphi_i(s, t)) ds \right) \quad (5.18)$$

for all i . Similarly when we minimize (5.11) we obtain

$$\mathcal{E} \left(\int_{s \in \mathcal{D}} f(X)(s)(X * \varphi_i(s, t)) ds \right) = \mathcal{E} \left(\int_{s \in \mathcal{D}} (X * S_G(s, t))(X * \varphi_i(s, t)) ds \right) \quad (5.19)$$

for $i = 1, \dots, m^2$. Subtraction of (5.19) from (5.18) yields:

$$0 = \mathcal{E} \int X * (G(s, t) - S_G(s, t))(X * \varphi_i(s, t)) ds \quad (5.20)$$

for $i = 1, \dots, m^2$. Let $Q_G = \sum_{j=1}^{m^2} a_j \varphi_j(s, t)$ be the quasi-interpolatory spline in $S_d^r(\Delta) \times S_d^r(\Delta)$ which achieves the optimal order of approximation of G from $S_d^r(\Delta) \times S_d^r(\Delta)$. Then

$$\begin{aligned} & \mathcal{E} \left(\int ((G - S_G) * X)^2 ds \right) \\ &= \mathcal{E} \left(\int (X * (G - S_G))(X * (G - S_G)) ds \right) \\ &= \mathcal{E} \left(\int (X * (G - S_G))(X * (G - Q_G + Q_G - S_G)) ds \right) \\ &= \mathcal{E} \left(\int (X * (G - S_G))(X * (G - Q_G)) ds \right) \quad \text{By (5.20)} \\ &\leq \mathcal{E} \left(\sqrt{\int ((G - S_G) * X)^2 ds} \sqrt{\int ((G - Q_G) * X)^2 ds} \right) \\ &\leq \sqrt{\mathcal{E} \left(\int ((G - S_G) * X)^2 ds \right) \mathcal{E} \left(\int ((G - Q_G) * X)^2 ds \right)}. \end{aligned}$$

Squaring both sides yields,

$$\mathcal{E} \left(\int ((G - S_G) * X)^2 ds \right)^2 \leq \mathcal{E} \left(\int ((G - S_G) * X)^2 ds \right) \mathcal{E} \left(\int ((G - Q_G) * X)^2 ds \right)$$

and thus we have

$$\begin{aligned}
\mathcal{E} \left(\int ((G - S_G) * X)^2 ds \right) &\leq \mathcal{E} \left(\int ((G - Q_G) * X)^2 ds \right) \\
&= \mathcal{E} (\|(G - Q_G) * X\|^2) \\
&\leq \mathcal{E} (\|(G - Q_G)\|^2 \|X\|^2) \\
&= \int_{\mathcal{D}} \|(G - Q_G)\|^2 \|X\|^2 P(X) dX \\
&= \|(G - Q_G)\|^2 \int_{\mathcal{D}} \|X\|^2 P(X) dX \\
&= \|(G - Q_G)\|^2 \mathcal{E} (\|X\|^2)
\end{aligned}$$

where $P(X)$ is the probability density function for the random surfaces in \mathcal{X} . Therefore by Theorem 5.0.8 we have

$$\begin{aligned}
\mathcal{E} \left(\int ((G - S_G) * X)^2 ds \right) &\leq \|(G - Q_G)\|^2 \mathcal{E} (\|X\|^2) \\
&\leq (2|\Delta|^{d+1} \max\{|G(s, \cdot)|_{d+1}, |G(\cdot, t)|_{d+1}\})^2 \mathcal{E} (\|X\|^2).
\end{aligned}$$

□

Now we consider the empirical estimate of S_G . Let X_ℓ , $\ell = 1, \dots, n$ a sample of be random surfaces in \mathcal{X} such that only the zero spline function in the space $S_d^r(\Delta) \times S_d^r(\Delta)$ is orthogonal to the subspace spanned by $\{X_1, \dots, X_n\}$. Then the empirical estimate of S_G is

$$\widehat{S}_{G,n} = \arg \min_{\beta \in S_d^r(\Delta) \times S_d^r(\Delta)} \frac{1}{n} \sum_{\ell=1}^n \left(\int_{s \in \mathcal{D}} (F(X_\ell(\cdot))(s) - \beta(s, \cdot) * X_\ell)^2 ds \right). \quad (5.21)$$

Theorem 5.0.11. *Suppose that only the zero spline function in the spline space $S_d^r(\Delta)$ is perpendicular to the subspace $\text{span}\{X_1, \dots, X_n\}$ except on an event whose probability p_n goes to zero as $n \rightarrow +\infty$. Then, with probability $1 - p_n$, there exists a unique $\widehat{S}_{\alpha,n} \in S_d^r(\Delta)$ minimizing (5.21).*

Proof. Again, we can write

$$\widehat{S}_{G,n} * X = \sum_{i,j} \hat{c}_{i,j} \phi_i(s) \langle X, \phi_j \rangle.$$

We want to find the coefficient vector that minimizes the difference in (5.21). For simplicity, we write the difference as a function of the coefficient vector:

$$\mathcal{F}(\hat{c}_{i,j}) = \frac{1}{n} \sum_{\ell=1}^n \int_{s \in \mathcal{D}} \left(F(X_\ell)(s) - \sum_{i,j} \hat{c}_{i,j} \phi_i(s) \langle X_\ell, \phi_j \rangle \right)^2 ds. \quad (5.22)$$

Hence by differentiation we have

$$\begin{aligned} \frac{\partial \mathcal{F}}{\partial \hat{c}_{l,k}} &= 2 \frac{1}{n} \sum_{\ell=1}^n \int_{s \in \mathcal{D}} \left(F(X_\ell)(s) - \sum_{i,j} \hat{c}_{i,j} \phi_i(s) \langle X_\ell, \phi_j \rangle \right) (\phi_l(s) \langle X_\ell, \phi_k \rangle) ds \\ &= 2 \frac{1}{n} \sum_{\ell=1}^n \int_{s \in \mathcal{D}} \left(F(X_\ell)(s) \phi_l(s) \langle X_\ell, \phi_k \rangle - \sum_{i,j} \hat{c}_{i,j} \phi_i(s) \langle X_\ell, \phi_j \rangle \phi_l(s) \langle X_\ell, \phi_k \rangle \right) ds. \end{aligned}$$

Then $\frac{\partial \mathcal{F}}{\partial \hat{c}_{l,k}} = 0$ implies

$$\frac{1}{n} \sum_{\ell=1}^n \int_{s \in \mathcal{D}} (F(X_\ell)(s) \phi_l(s) \langle X_\ell, \phi_k \rangle) ds = \frac{1}{n} \sum_{\ell=1}^n \int_{s \in \mathcal{D}} \left(\sum_{i,j} \hat{c}_{i,j} \phi_i(s) \langle X_\ell, \phi_j \rangle \phi_l(s) \langle X_\ell, \phi_k \rangle \right) ds \quad (5.23)$$

for all $0 \leq l, k \leq m$. We rewrite the above as a linear system $Ac = b$ where c is the vector of coefficients, A is an $m^2 \times m^2$ matrix with entries

$$\frac{1}{n} \sum_{\ell=1}^n \int_{s \in \mathcal{D}} (\phi_i(s) \langle X_\ell, \phi_j \rangle \phi_l(s) \langle X_\ell, \phi_k \rangle) ds$$

and b is a vector of the form

$$\frac{1}{n} \sum_{\ell=1}^n \int_{s \in \mathcal{D}} (F(X_\ell)(s) \phi_l(s) \langle X_\ell, \phi_k \rangle) ds.$$

To solve the linear system, we need to find the conditions for which A is invertible. We know that A is invertible if it is of full rank and the only solution to $v^T A v = 0$ is $v = 0$. Let v be an arbitrary vector then we have

$$\begin{aligned} v^T A v &= \frac{1}{n} \sum_{\ell=1}^n \int_{s \in \mathcal{D}} \left(\sum_{l,k} \sum_{i,j} v_{i,j} (\phi_i(s) \langle X_\ell, \phi_j \rangle \phi_l(s) \langle X_\ell, \phi_k \rangle) v_{l,k} \right) ds \\ &= \frac{1}{n} \sum_{\ell=1}^n \int_{s \in \mathcal{D}} \left(\sum_{l,m} \phi_l(s) \langle X_\ell, \phi_m \rangle v_{l,m} \sum_{i,j} v_{i,j} \phi_i(s) \langle X_\ell, \phi_j \rangle \right) ds \\ &= \frac{1}{n} \sum_{\ell=1}^n \int_{s \in \mathcal{D}} \left(\sum_{i,j} v_{i,j} \phi_i(s) \langle X_\ell, \phi_j \rangle \right)^2 ds = 0. \end{aligned}$$

To have $v^T Av = 0$ then for all $s \in \mathcal{D}$ we have

$$\sum_{i,j} v_{i,j} \phi_i(s) \langle X_\ell, \phi_j \rangle = \sum_i \left(\sum_j v_{i,j} \langle X_\ell, \phi_j \rangle \right) \phi_i(s) = 0. \quad (5.24)$$

The $\{\phi_i\}$ form a basis for the spline space $S_d^r(\Delta) \times S_d^r(\Delta)$ hence the only solution (5.24) is for all the coefficients to be zero, that is

$$\sum_j v_{i,j} \langle X_\ell, \phi_j \rangle = 0 \quad (5.25)$$

for all ℓ . By our assumption that only the zero spline is orthogonal to X except for an even whose probability p_n goes to zero as $n \rightarrow +\infty$. Therefore $\langle X_\ell, \phi_j \rangle \neq 0$ which implies that the only way $vAv^T = 0$ is for $v = 0$. \square

Now, we consider the case when we approximate linear functions based on discrete observations. For applications, we will only know X over some given points in the domain \mathcal{D} . That is, we will have observations of X over designated points s_k , $k = 1, \dots, N$ in \mathcal{D} . Let S_X be the penalized least squares fit of X over the designated points s_k . We consider G_D that solves the following minimization problem:

$$G_D = \arg \min_{\beta \in H \times H} \mathcal{E} \left(\sum_{k=1}^N (F(X)(s_k) - \beta(s_k, \cdot) * S_X(\cdot))^2 \right). \quad (5.26)$$

Heuristically we can see that G_D converges to G as the observation locations become dense in \mathcal{D} and as $|\Delta| \rightarrow 0$. We also look for an approximation $S_{G_D} \in S_d^r(\Delta) \times S_d^r(\Delta)$ of G_D such that

$$S_{G_D} = \arg \min_{\beta \in S_d^r(\Delta) \times S_d^r(\Delta)} \mathcal{E} \left(\sum_{k=1}^N (F(X)(s_k) - \beta(s_k, \cdot) * S_X(\cdot))^2 \right). \quad (5.27)$$

Now, we can write S_{G_D} as $S_{G_D} = \sum_{j=1}^{m^2} c_D \varphi_j(s, t)$ where $\{\varphi_i(s, t), i = 1, \dots, m^2\}$ is a basis for $S_d^r(\Delta) \times S_d^r(\Delta)$. Then the coefficient vector c_D satisfies the following relation:

$$A_D c_D = b_D$$

where A_D is an $m^2 \times m^2$ matrix with entries

$$\mathcal{E} \left(\sum_{k=1}^N (\phi_i(s_k) \langle S_X, \phi_j \rangle \phi_l(s_k) \langle S_X, \phi_m \rangle) ds \right)$$

and b_D is a vector of the form

$$\mathcal{E} \left(\sum_{k=1}^N (F(X)(s) \phi_l(s) \langle S_X, \phi_m \rangle) ds \right).$$

We want to show that $A_D \rightarrow A$ that is

$$\mathcal{E} \left(\sum_{k=1}^N (\phi_i(s) \langle S_X, \phi_j \rangle \phi_l(s) \langle S_X, \phi_m \rangle) ds \right) \rightarrow \mathcal{E} \left(\int_{s \in \mathcal{D}} (\phi_i(s) \langle X, \phi_j \rangle \phi_l(s) \langle X, \phi_m \rangle) ds \right)$$

We know that $S_X \rightarrow X$ as $|\Delta| \rightarrow 0$ by Theorem 2.1.14.

In the following theorem we show that S_{G_D} is a good approximation for G_D .

Theorem 5.0.12. *Suppose that $\mathcal{E}(\|S_X\|^2) < \infty$ and $G_D \in \mathcal{C}^{d+1}(\mathcal{D})$. Then the solution S_{G_D} from the minimization problem (5.27) approximates G_D in the following sense*

$$\mathcal{E} \left(\sum_{k=1}^N ((G_D - S_{G_D}) * S_X)^2 ds \right) \leq C (2|\Delta|^{d+1} \max\{|G(s, \cdot)|_{d+1}, |G(\cdot, t)|_{d+1}\})^2 \quad (5.28)$$

where C is a constant dependent on $\mathcal{E}(\|X\|^2)$.

Proof. By Theorem 5.0.11, we choose $S_d^r(\Delta) \times S_d^r(\Delta)$ to be dense in $H \times H$ as $|\Delta| \rightarrow 0$ and look for an approximation S_{G_D} of G_D that satisfies (5.27). To show that S_{G_D} approximates G_D we simplify (5.17) by letting $\{\varphi_i(s, t), i = 1, \dots, m^2\}$ be the basis elements for $S_d^r(\Delta) \times S_d^r(\Delta)$ and let $\{\varphi_i(s, t), i = m^2 + 1, m^2 + 2, \dots\}$ be a basis of the orthogonal complement space of $S_d^r(\Delta) \times S_d^r(\Delta)$ in $H \times H$. By minimizing (5.26) we have

$$\mathcal{E} \left(\sum_{k=1}^N f(X)(s_k) (S_X * \varphi_i(s_k, t)) \right) = \mathcal{E} \left(\sum_{k=1}^N (S_X * G_D(s_k, t)) (S_X * \varphi_i(s_k, t)) \right) \quad (5.29)$$

for all i . Similarly when we minimize (5.27) we obtain

$$\mathcal{E} \left(\sum_{k=1}^N f(X)(s_k) (S_X * \varphi_i(s_k, t)) \right) = \mathcal{E} \left(\sum_{k=1}^N (S_X * S_{G_D}(s_k, t)) (S_X * \varphi_i(s_k, t)) \right) \quad (5.30)$$

for $i = 1, \dots, m^2$. Subtraction of (5.30) from (5.29) yields:

$$0 = \mathcal{E} \left(\sum_{k=1}^N (S_X * (G_D(s_k, t) - S_{G_D}(s_k, t))) (S_X * \varphi_i(s_k, t)) \right) \quad (5.31)$$

for $i = 1, \dots, m^2$. Let $Q_{G_D} = \sum_{j=1}^{m^2} a_j \varphi_j(s, t)$ be the quasi-interpolatory spline in $S_d^r(\Delta) \times S_d^r(\Delta)$ which achieves the optimal order of approximation of G_D from $S_d^r(\Delta) \times S_d^r(\Delta)$. Then

$$\begin{aligned}
& \mathcal{E} \left(\sum_{k=1}^n ((G_D(s_k, t) - S_{G_D}(s_k, t)) * S_X)^2 \right) \\
&= \mathcal{E} \left(\sum_{k=1}^n ((G_D - S_{G_D}) * S_X)(G_D - S_{G_D}) * S_X \right) \\
&= \mathcal{E} \left(\sum_{k=1}^n ((G_D - S_{G_D}) * S_X)((G_D - Q_{G_D} + Q_{G_D} - S_{G_D}) * S_X) \right) \\
&= \mathcal{E} \left(\sum_{k=1}^n ((G_D - S_{G_D}) * S_X)((G_D - Q_{G_D}) * S_X) \right) \quad \text{By (5.31)} \\
&\leq \mathcal{E} \left(\sqrt{\sum_{k=1}^n ((G_D - S_{G_D}) * S_X)^2} \sqrt{\sum_{k=1}^n ((G_D - Q_{G_D}) * S_X)^2} \right) \\
&\leq \sqrt{\mathcal{E} \left(\sum_{k=1}^n ((G_D - S_{G_D}) * S_X)^2 \right) \mathcal{E} \left(\sum_{k=1}^n ((G_D - Q_{G_D}) * S_X)^2 \right)}.
\end{aligned}$$

Squaring both sides yields,

$$\begin{aligned}
& \mathcal{E} \left(\sum_{k=1}^n ((G_D(s_k, t) - S_{G_D}(s_k, t)) * S_X)^2 \right)^2 \\
&\leq \mathcal{E} \left(\sum_{k=1}^n ((G_D - S_{G_D}) * S_X)^2 \right) \mathcal{E} \left(\sum_{k=1}^n ((G_D - Q_{G_D}) * S_X)^2 \right).
\end{aligned}$$

Hence we have

$$\begin{aligned}
\mathcal{E} \left(\sum_{k=1}^N ((G_D(s_k, t) - S_{G_D}(s_k, t)) * S_X)^2 \right) &\leq \mathcal{E} \left(\sum_{k=1}^N ((G_D - Q_{G_D}) * S_X)^2 \right) \\
&= \mathcal{E} (\|(G_D - Q_{G_D}) * S_X\|^2) \\
&\leq \mathcal{E} (\|(G_D - Q_{G_D})\|^2 \|S_X\|^2) \\
&= \|(G_D - Q_{G_D})\|^2 \mathcal{E} (\|S_X\|^2).
\end{aligned}$$

Therefore by Theorem 5.0.8 we have

$$\begin{aligned}
\mathcal{E} \left(\sum_{k=1}^N ((G_D - S_{G_D}) * S_X)^2 ds \right) &\leq \|(G_D - Q_{G_D})\|^2 \mathcal{E} (\|S_X\|^2) \\
&\leq (2|\Delta|^{d+1} \max\{|G(s, \cdot)|_{d+1}, |G(\cdot, t)|_{d+1}\})^2 \mathcal{E} (\|S_X\|^2).
\end{aligned}$$

Since S_X converges to X implies that $\mathcal{E}(\|S_X\|^2)$ is bounded by a constant dependent on $\mathcal{E}(\|X\|^2)$, this yields the result

$$\mathcal{E} \left(\sum_{k=1}^N ((G_D - S_{G_D}) * S_X)^2 ds \right) \leq C (2|\Delta|^{d+1} \max\{|G(s, \cdot)|_{d+1}, |G(\cdot, t)|_{d+1}\})^2.$$

□

Now we consider the empirical estimate of S_{G_D} . Let X_ℓ , $\ell = 1, \dots, n$ a sample of be random surfaces in \mathcal{X} such that only the zero spline function in the space $S_d^r(\Delta) \times S_d^r(\Delta)$ is orthogonal to the subspace spanned by $\{X_1, \dots, X_n\}$. Then the empirical estimate of S_{G_D} is

$$\widetilde{S_{G_D, n}} = \arg \min_{\beta \in S_d^r(\Delta) \times S_d^r(\Delta)} \frac{1}{n} \sum_{\ell=1}^n \sum_{k=1}^N (F(X_\ell(\cdot))(s_k) - \beta(s_k, \cdot) * S_{X_\ell}(\cdot))^2. \quad (5.32)$$

Theorem 5.0.13. *Suppose that only the zero spline in $S_d^r(\Delta)$ is orthogonal to the collection of approximations of $X \in H$. Then solution to (5.32) has a unique solution in $S_d^r(\Delta) \times S_d^r(\Delta)$.*

Proof. We start by writing $\widetilde{S_{G_D, n}} * X = \sum_{i,j} \tilde{c}_{i,j} \phi_i(s) \langle X, \phi_j \rangle$. We want to find the coefficient vector the minimizes the difference in (5.32). As we have done before, we write the difference as a function of the coefficient vector:

$$\mathcal{F}(\tilde{c}_{i,j}) = \frac{1}{n} \sum_{\ell=1}^n \sum_{k=1}^N \left(F(X_\ell)(s_k) - \sum_{i,j} c_{i,j} \phi_i(s_k) \langle S_{X_\ell}, \phi_j \rangle \right)^2. \quad (5.33)$$

Hence by differentiation we have

$$\begin{aligned} \frac{\partial \mathcal{F}}{\partial c_{l,t}} &= 2 \frac{1}{n} \sum_{\ell=1}^n \sum_{k=1}^N \left(F(X_\ell)(s_k) - \sum_{i,j} c_{i,j} \phi_i(s_k) \langle S_{X_\ell}, \phi_j \rangle \right) (\phi_l(s_k) \langle S_{X_\ell}, \phi_t \rangle) \\ &= 2 \frac{1}{n} \sum_{\ell=1}^n \sum_{k=1}^N \left(F(X_\ell)(s_k) \phi_l(s_k) \langle X_\ell, \phi_t \rangle - \sum_{i,j} c_{i,j} \phi_i(s_k) \langle S_{X_\ell}, \phi_j \rangle \phi_l(s_k) \langle S_{X_\ell}, \phi_t \rangle \right). \end{aligned}$$

Then $\frac{\partial \mathcal{F}}{\partial c_{l,t}} = 0$ implies

$$\frac{1}{n} \sum_{\ell=1}^n \sum_{k=1}^N F(X_\ell)(s_k) \phi_l(s_k) \langle S_{X_\ell}, \phi_t \rangle = \frac{1}{n} \sum_{\ell=1}^n \sum_{k=1}^N \sum_{i,j} c_{i,j} \phi_i(s_k) \langle S_{X_\ell}, \phi_j \rangle \phi_l(s_k) \langle S_{X_\ell}, \phi_t \rangle \quad (5.34)$$

for all $0 \leq l, t \leq n$. We can rewrite this as a linear system $\tilde{A} \tilde{c} = \tilde{b}$ where \tilde{c} is the vector of coefficients, \tilde{A} is an $m^2 \times m^2$ matrix with entries

$$\frac{1}{n} \sum_{\ell=1}^n \sum_{k=1}^N \phi_i(s_k) \langle S_{X_\ell}, \phi_j \rangle \phi_l(s_k) \langle S_{X_\ell}, \phi_t \rangle$$

and b is a vector of the form

$$\frac{1}{n} \sum_{\ell=1}^n \sum_{k=1}^N F(X_\ell)(s_k) \phi_l(s_k) \langle S_{X_\ell}, \phi_t \rangle.$$

To solve the linear system above we need to find the conditions for which \tilde{A} is invertible. We know that \tilde{A} is invertible if it is of full rank and the only solution to $v^T \tilde{A} v = 0$ is $v = 0$. Let v be an arbitrary vector then we have

$$\begin{aligned} v^T A v &= \frac{1}{n} \sum_{\ell=1}^n \sum_k \sum_{l,t} \sum_{i,j} v_{i,j} \left(\sum_k \phi_i(s_k) \langle S_{X_\ell}, \phi_j \rangle \phi_l(s_k) \langle S_{X_\ell}, \phi_t \rangle \right) v_{l,t} \\ &= \frac{1}{n} \sum_{\ell=1}^n \sum_k \sum_{l,m} \phi_l(s_k) \langle S_{X_\ell}, \phi_t \rangle v_{l,t} \sum_{i,j} v_{i,j} \phi_i(s_k) \langle S_{X_\ell}, \phi_j \rangle \\ &= \frac{1}{n} \sum_{\ell=1}^n \sum_k \left(\sum_{i,j} v_{i,j} \phi_i(s_k) \langle S_{X_\ell}, \phi_j \rangle \right)^2 = 0. \end{aligned}$$

To have $v^T A v = 0$ then for all $s_k \in \mathcal{D}$ we have

$$\sum_{i,j} v_{i,j} \phi_i(s_k) \langle S_{X_\ell}, \phi_j \rangle = \sum_i \left(\sum_j v_{i,j} \langle S_{X_\ell}, \phi_j \rangle \right) \phi_i(s_k) = 0. \quad (5.35)$$

The $\{\phi_i\}$ form a basis for the spline space $S_d^r(\Delta)$ hence the only solution (5.35) is for all the coefficients to be zero, that is

$$\sum_j v_{i,j} \langle S_{X_\ell}, \phi_j \rangle = 0, \quad (5.36)$$

for $\ell = 1, 2, \dots, n$. By our assumption that only the zero spline is orthogonal to X therefore

$$\langle S_{X_\ell}, \phi_j \rangle \neq 0$$

which implies that the only way $v \tilde{A} v^T = 0$ is for $v = 0$. □

CHAPTER 6

NUMERICAL EXPERIMENTS

In this chapter, we use the autoregressive and brute force methods to forecast the ground-level ozone concentrations at three locations: Atlanta, Boston and Cincinnati. We assume that the level of ozone for a given time of day in one specific city is a linear functional of the previous days' ozone concentrations measured over the geographical region containing the city of interest. For example, we would assume that today's ozone concentration in Atlanta at 9:00 a.m. is a linear functional of all the ozone values in the southeast up to 9:00 a.m. yesterday. Thus we can implement our two methods to make our forecasts. We let $f(X)$ be the hourly ozone concentration at a particular city of interest and X is the ozone concentration distribution over a geographical region containing the city of interest at the same hour of the previous day. Our domain is the continental United States and our design points are the Environment Protection Agency (EPA) stations where the ozone values are collected. For our numerical experiments, we have scaled the domain into $[0, 1] \times [0, 1]$, see Figure 6.1. We have almost 1000 EPA stations in our data set. For each station, we are given hourly ozone concentration values for three months in 2005. Some data values are missing but not very many. The missing values do not affect our computation because the missing values are filled when we approximate the surface. Below is a brief outline of the numerical experiments.

Step 1) For each hour of data, we create the approximation to X_i by using the penalized least squares method (2.63) with penalty $\lambda = 10^{-2}$ over the spline space with degree 5 and smoothness 1, $S_5^1(\Delta)$. We call this approximation S_{X_i} . We also collect Y_i the ozone concentrations at the location of interest one day ahead of X_i .

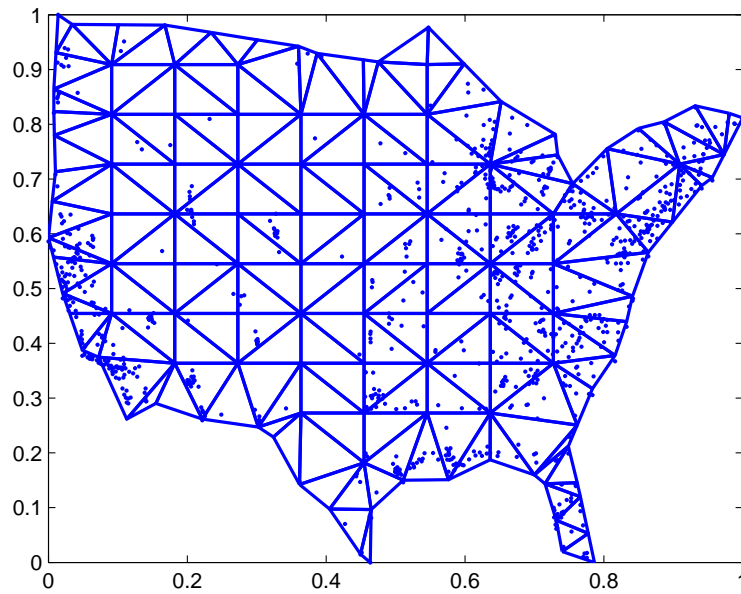


Figure 6.1: Locations of EPA stations and a Triangulation

Step 2) Then we use one of our two methods, either autoregressive or brute force, to find for the spline function $\widetilde{S}_{\alpha,24N}$ that solves the following minimization problem

$$\min_{s \in S_5^1} \frac{1}{24N} \sum_{i=1}^{24N} (Y_i - \langle s, S_{X_i} \rangle)^2$$

where N is the number of days used for learning. For example, if we want to predict Friday's ozone concentration in Atlanta by using Monday, Tuesday, Wednesday and Thursday's ozone concentrations, we would have $N = 4$.

Step 3) We make a prediction for a given day by evaluating the function $\widetilde{S}_{\alpha,24N}$ from Step 2 at on the previous days ozone concentration distribution. This gives us the prediction for that time the next day. For example, we use ozone distribution surfaces from Thursday

as the input for our function $\widetilde{S}_{\alpha,24N}$ to make a prediction for Friday.

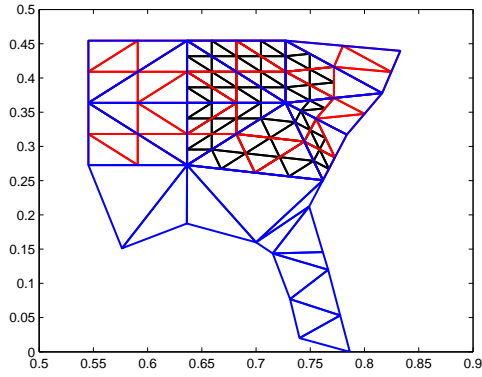
Bivariate spline theory says the smaller the triangulation size, the better the approximation of any function $\alpha \in H$, see Theorem 2.1.14. In the following numerical experiments, we use a subset of the continental United States as our domain and three different sizes of triangulations. For each day that we predict we show eight to fifteen days learning. That is, the number of days refers to the number of previous days of data used to create $\widetilde{S}_{\alpha,24N}$. So for eight days of learning, we have $N = 8$.

6.1 ATLANTA

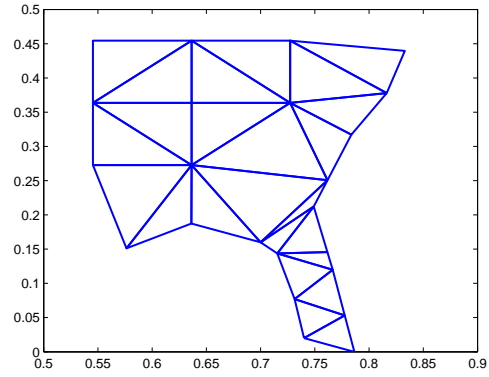
In Figure 6.2 are the triangulations used for the Atlanta ozone forecasts.

6.1.1 THE BRUTE FORCE METHOD FOR PREDICTION AT ATLANTA

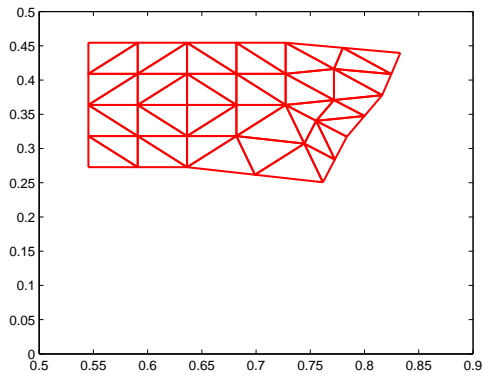
We first show our numerical experimental results using our brute force approach. In the following graphs, we show the exact measurement (green line), predictions based on triangulation 1 (the blue \cdot), based on triangulation 2 (the red $+$), and based on triangulation 3 (the black \times) as in Figs 6.3– 6.17.



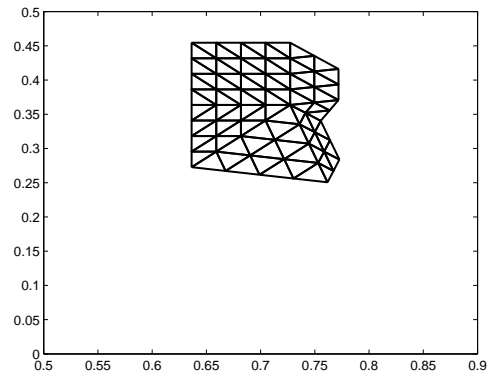
All Triangulations Superimposed



Triangulation 1



Triangulation 2



Triangulation 3

Figure 6.2: Three different sizes of triangulation of the southeast part of U.S.

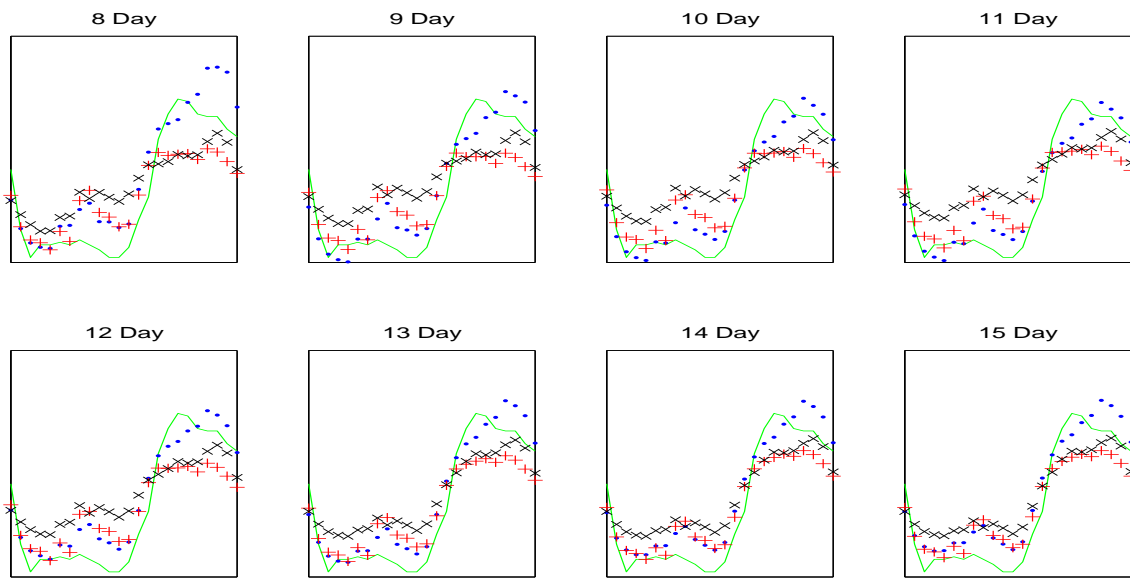


Figure 6.3: Brute force predictions (blue \cdot , red $+$, and black \times) and exact measurement (green line) on Sept. 1, 2005 in Atlanta

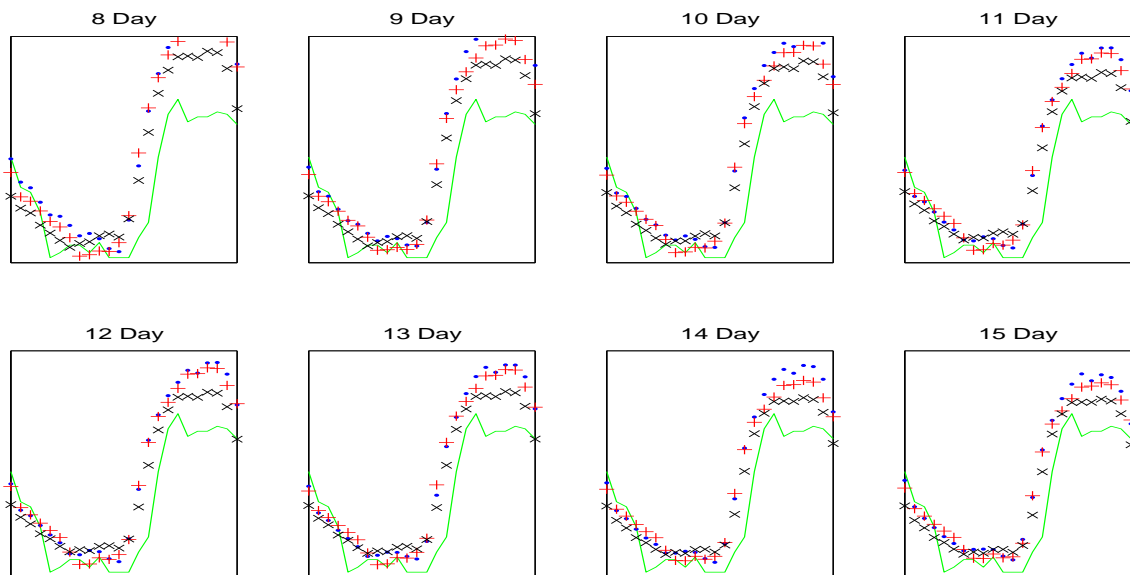


Figure 6.4: Brute force predictions (blue \cdot , red $+$, and black \times) and exact measurement (green line) on Sept. 2, 2005 in Atlanta

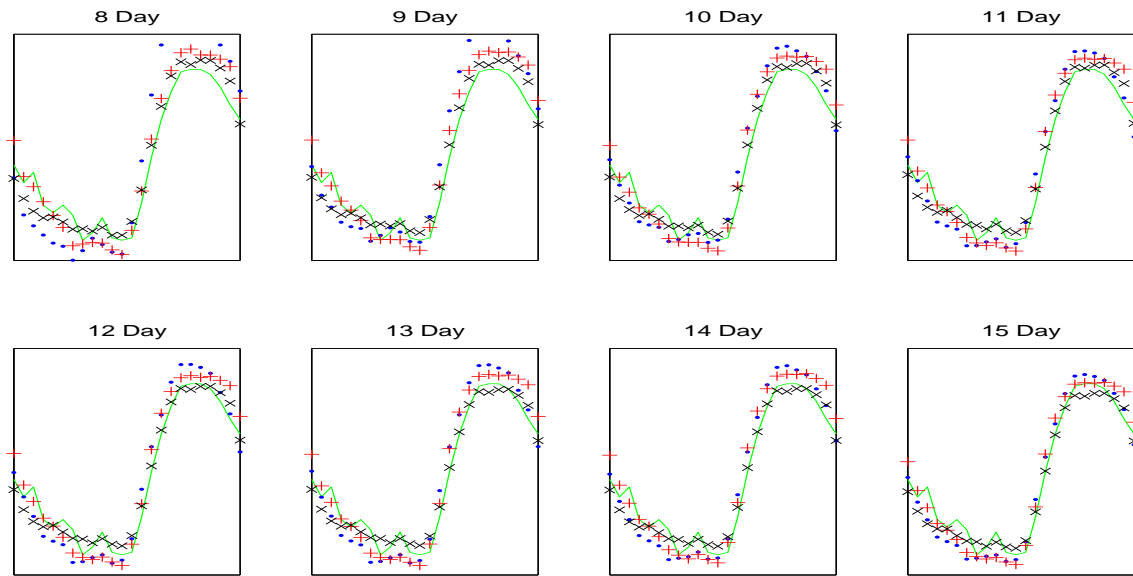


Figure 6.5: Brute force predictions (blue \cdot , red $+$, and black \times) and exact measurement (green line) on Sept. 3, 2005 in Atlanta

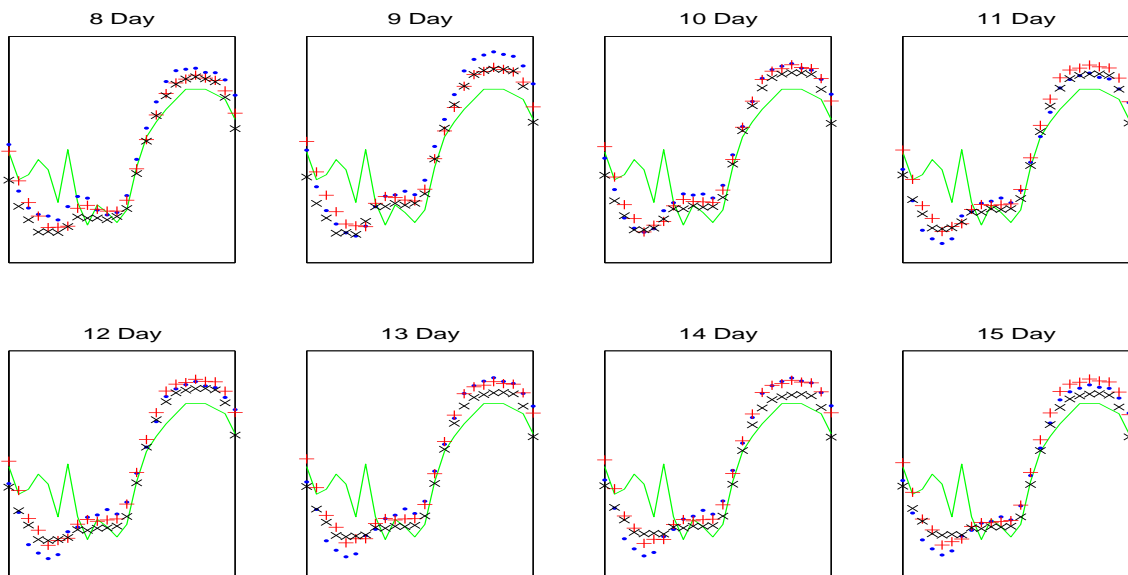


Figure 6.6: Brute force predictions (blue \cdot , red $+$, and black \times) and exact measurement (green line) on Sept. 4, 2005 in Atlanta

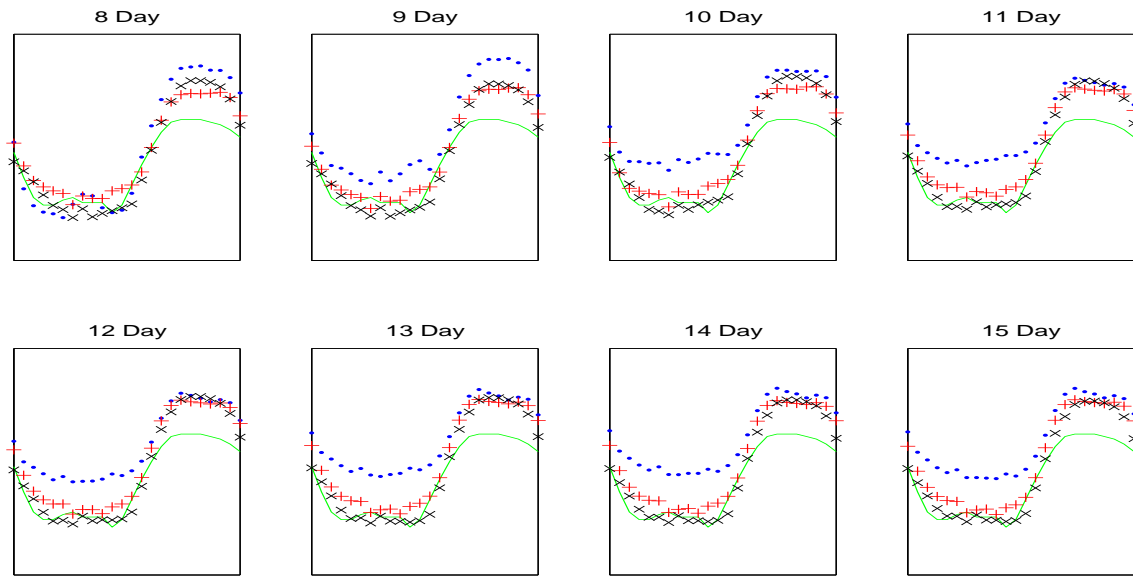


Figure 6.7: Brute force predictions (blue \cdot , red $+$, and black \times) and exact measurement (green line) on Sept. 5, 2005 in Atlanta

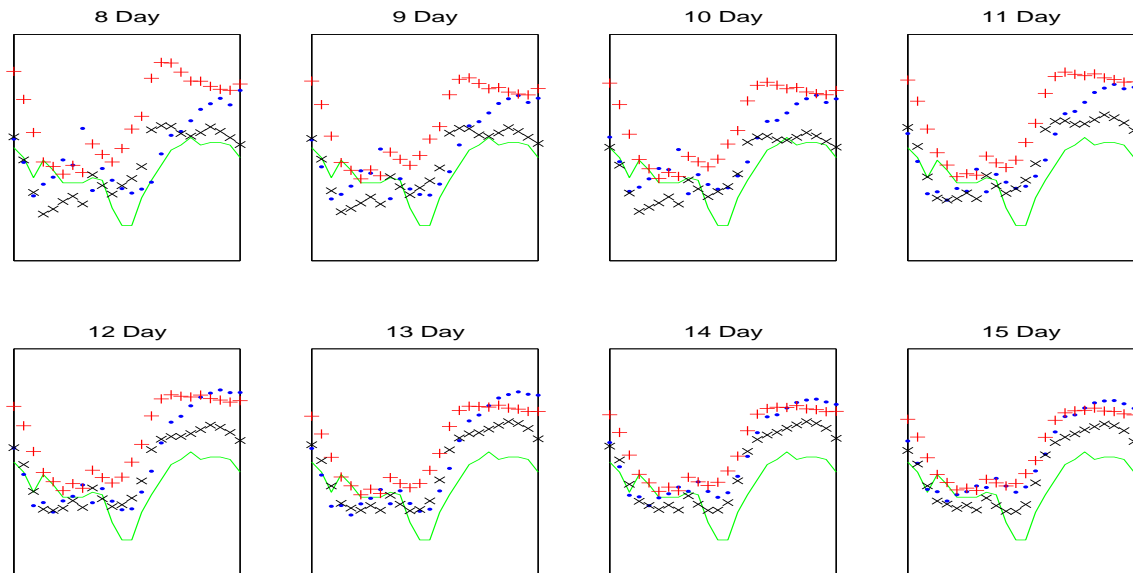


Figure 6.8: Brute force predictions (blue \cdot , red $+$, and black \times) and exact measurement (green line) on Sept. 6, 2005 in Atlanta

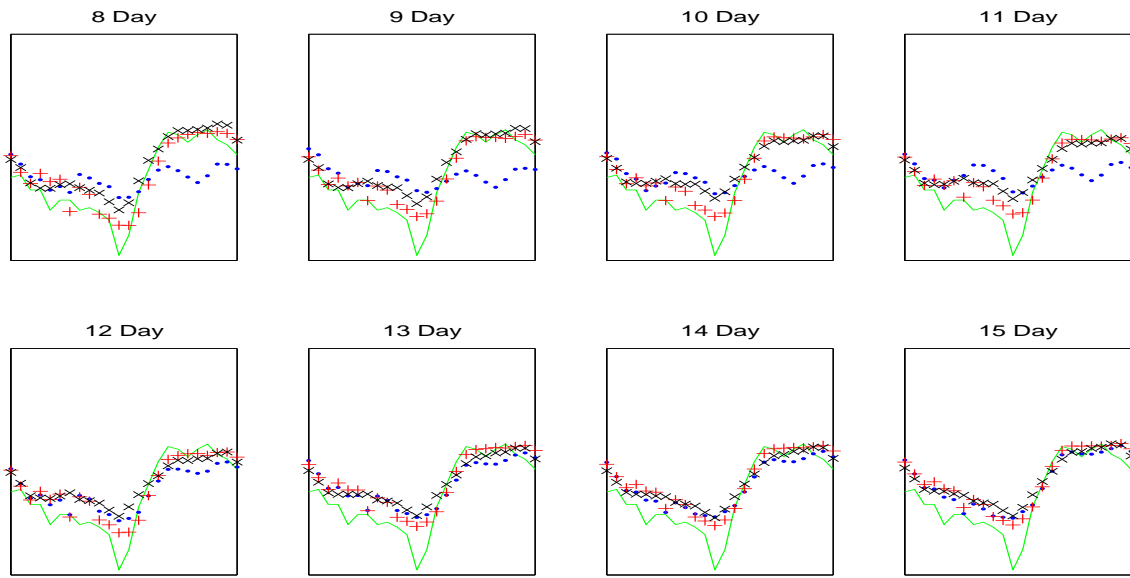


Figure 6.9: Brute force predictions (blue \cdot , red $+$, and black \times) and exact measurement (green line) on Sept. 7, 2005 in Atlanta

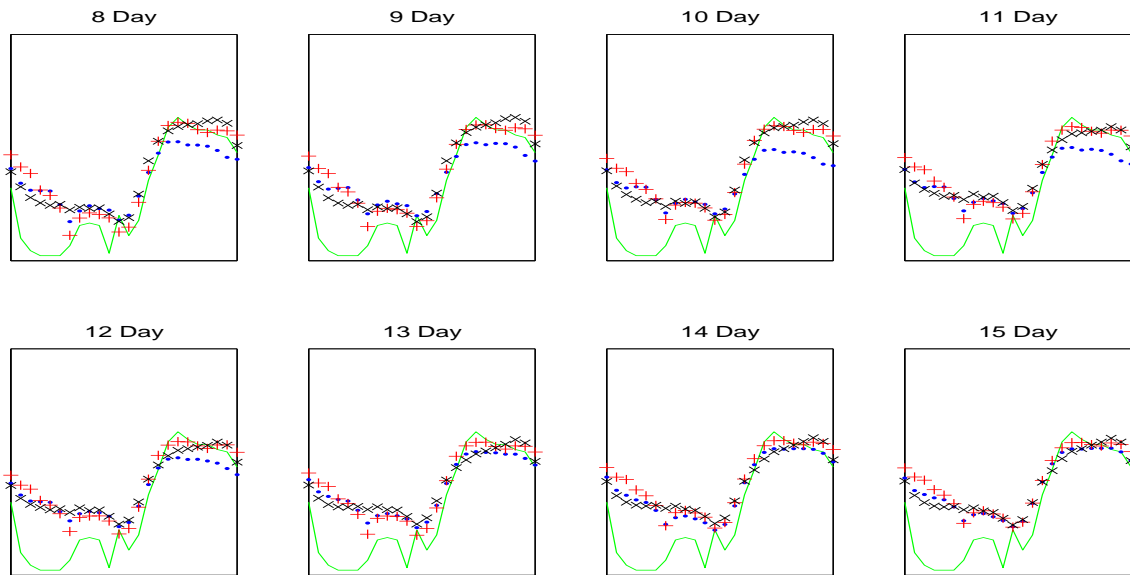


Figure 6.10: Brute force predictions (blue \cdot , red $+$, and black \times) and exact measurement (green line) on Sept. 8, 2005 in Atlanta

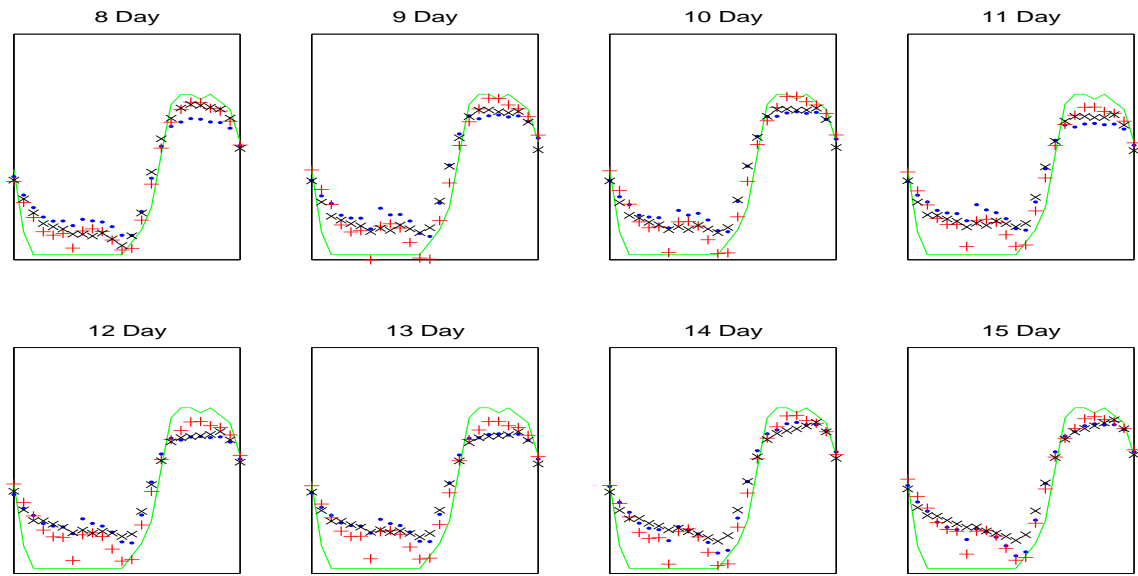


Figure 6.11: Brute force predictions (blue \cdot , red $+$, and black \times) and exact measurement (green line) on Sept. 9, 2005 in Atlanta

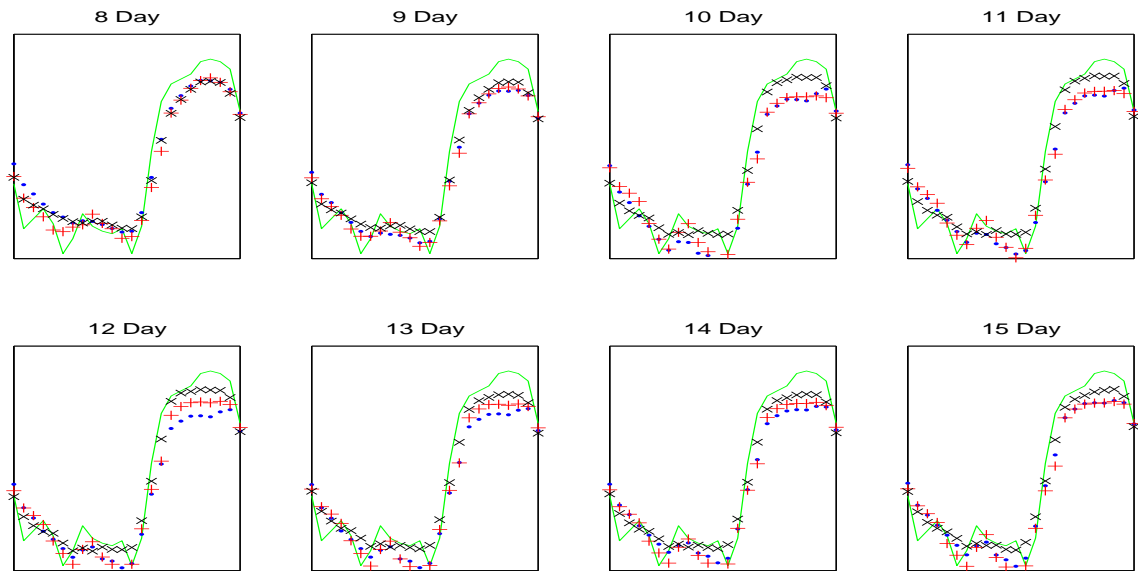


Figure 6.12: Brute force predictions (blue \cdot , red $+$, and black \times) and exact measurement (green line) on Sept. 10, 2005 in Atlanta

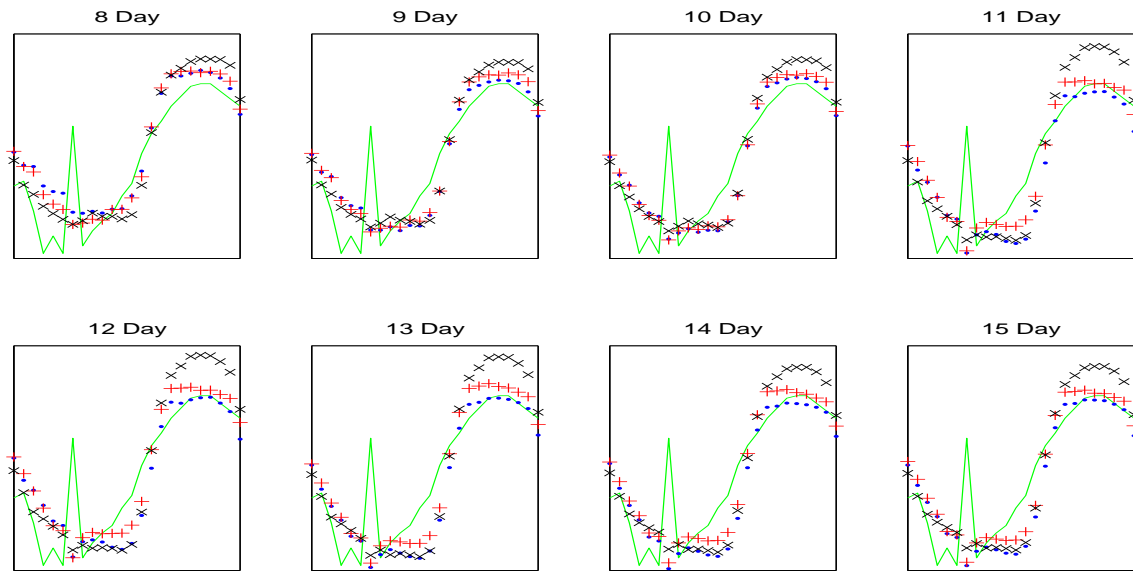


Figure 6.13: Brute force predictions (blue \cdot , red $+$, and black \times) and exact measurement (green line) on Sept. 11, 2005 in Atlanta

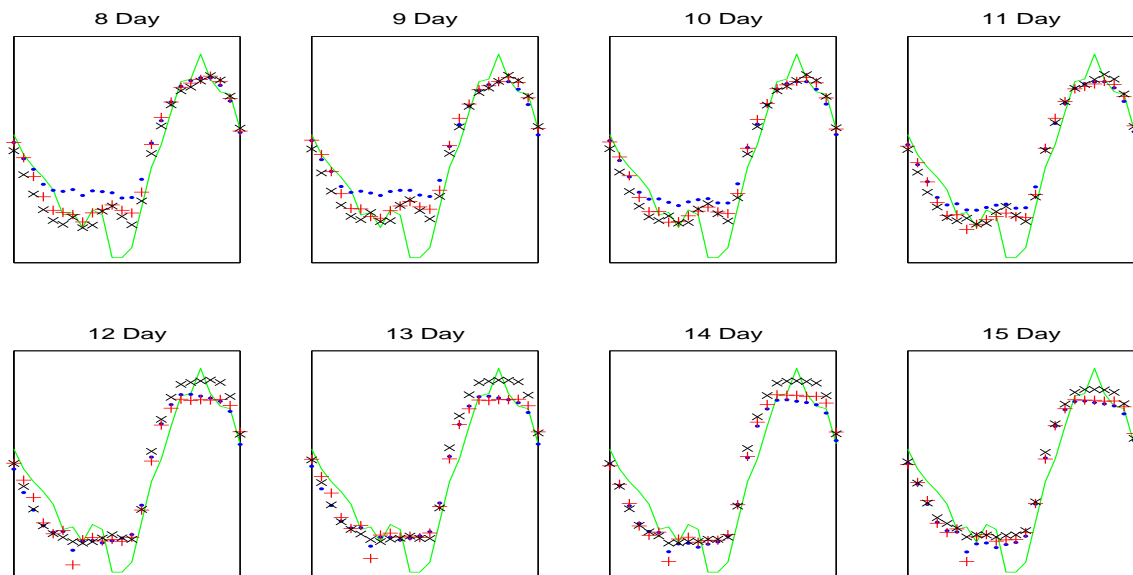


Figure 6.14: Brute force predictions (blue \cdot , red $+$, and black \times) and exact measurement (green line) on Sept. 12, 2005 in Atlanta

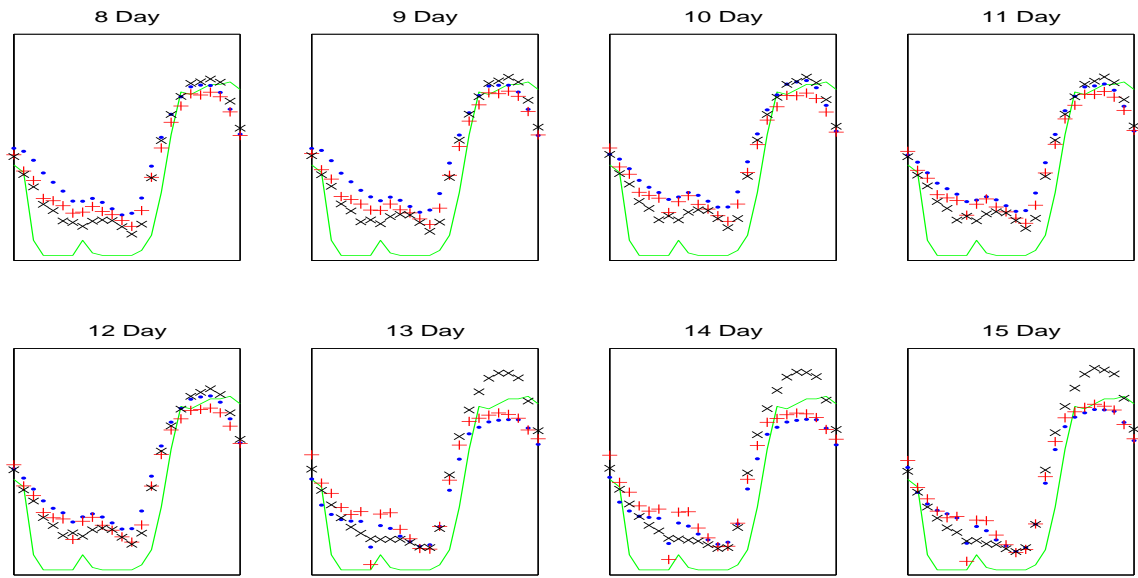


Figure 6.15: Brute force predictions (blue \cdot , red $+$, and black \times) and exact measurement (green line) on Sept. 13, 2005 in Atlanta

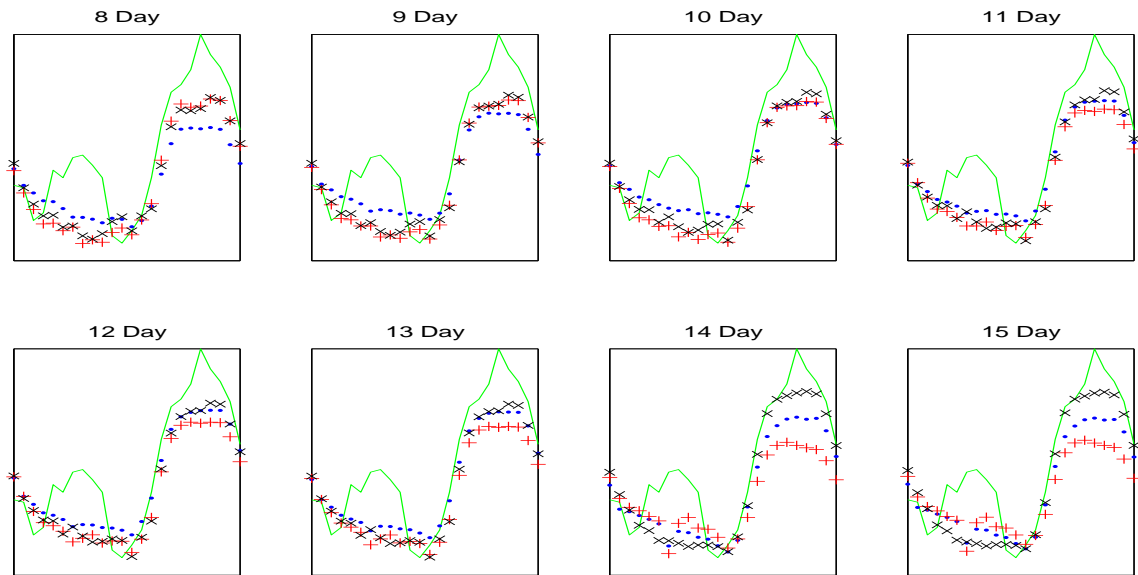


Figure 6.16: Brute force predictions (blue \cdot , red $+$, and black \times) and exact measurement (green line) on Sept. 14, 2005 in Atlanta

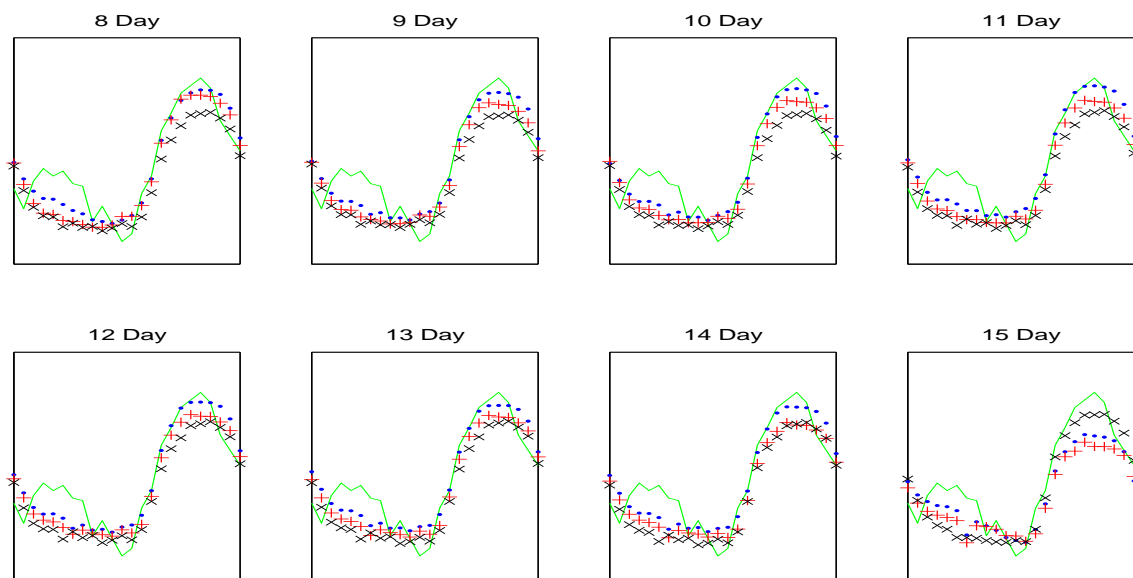


Figure 6.17: Brute force predictions (blue \cdot , red $+$, and black \times) and exact measurement (green line) on Sept. 15, 2005 in Atlanta

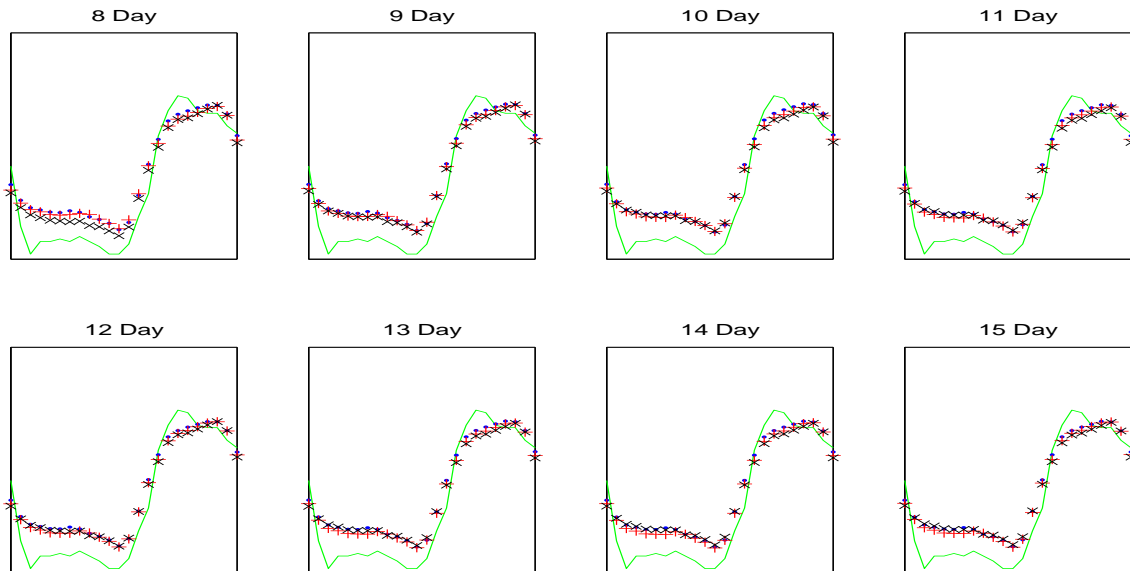


Figure 6.18: Autoregressive predictions (blue ·, red +, and black ×) and exact measurement (green line) on Sept. 1, 2005 in Atlanta

6.1.2 THE AUTOREGRESSIVE APPROACH FOR PREDICTION AT ATLANTA

We now show our numerical experimental results using our autoregressive approach. In the following graphs, we show the exact measurement (green line), predictions based on triangulation 1 (the red +), based on triangulation 2 (the black ×) and based on triangulation 3 (the blue ·) as in Figs 6.18– 6.32. We only use the first two eigenvalues to compute the predictions.

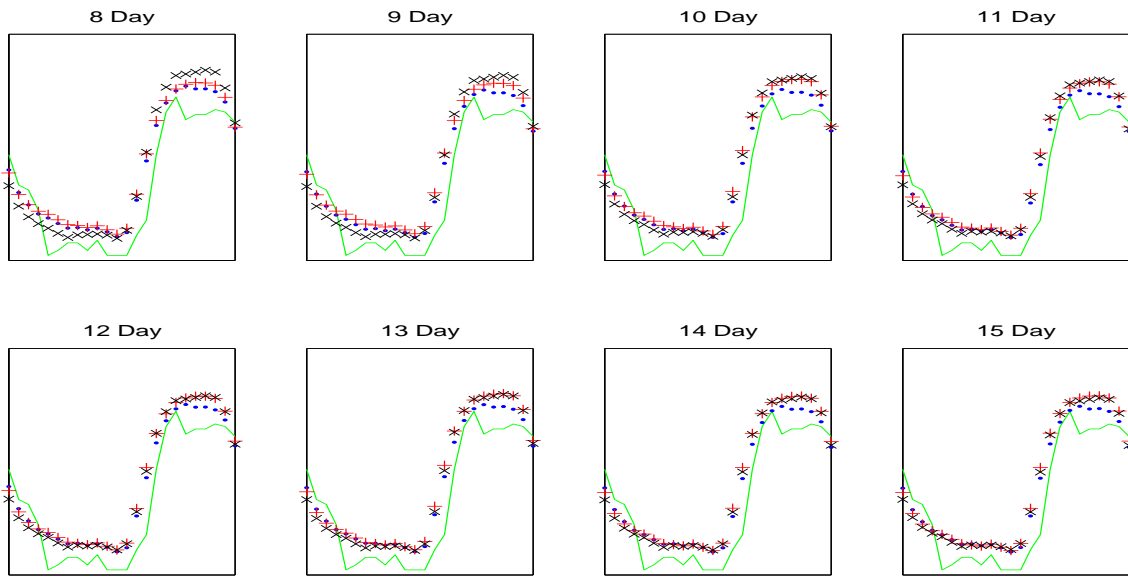


Figure 6.19: Autoregressive predictions (blue \cdot , red $+$, and black \times) and exact measurement (green line) on Sept. 2, 2005 in Atlanta

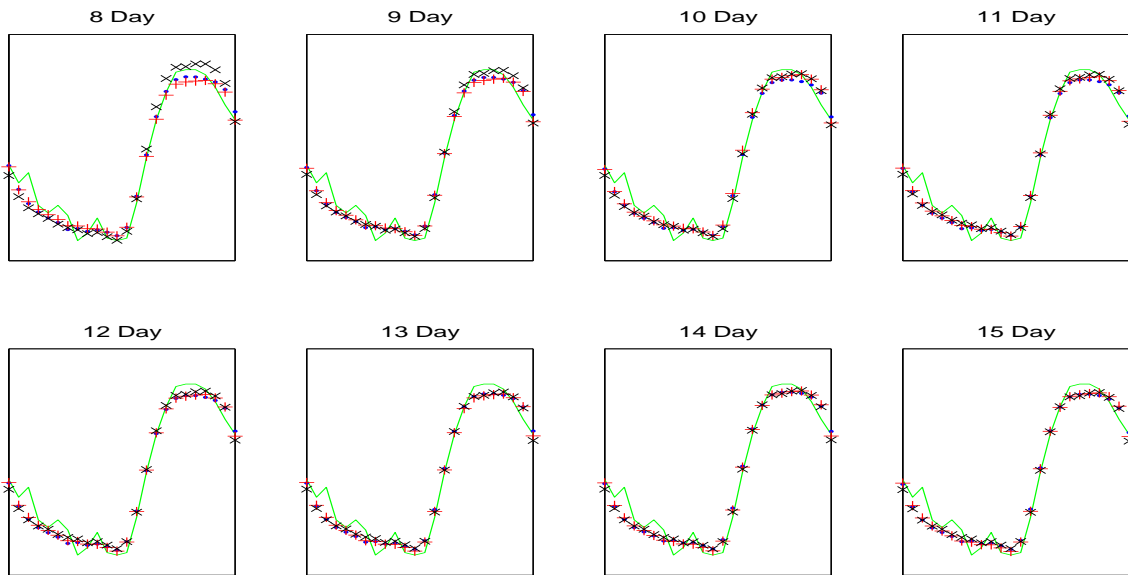


Figure 6.20: Autoregressive predictions (blue \cdot , red $+$, and black \times) and exact measurement (green line) on Sept. 3, 2005 in Atlanta

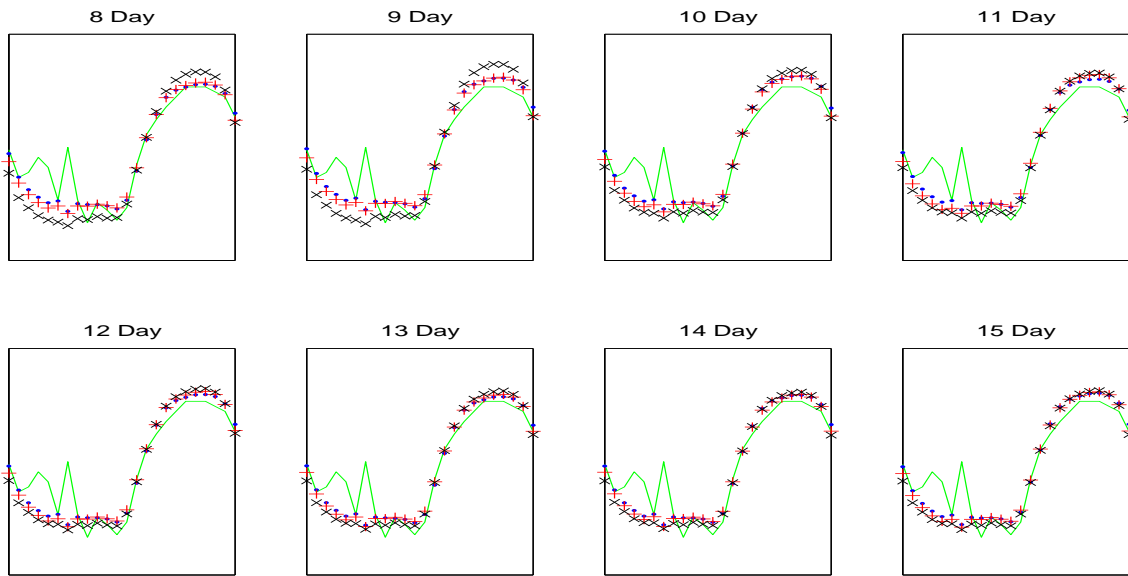


Figure 6.21: Autoregressive predictions (blue \cdot , red $+$, and black \times) and exact measurement (green line) on Sept. 4, 2005 in Atlanta

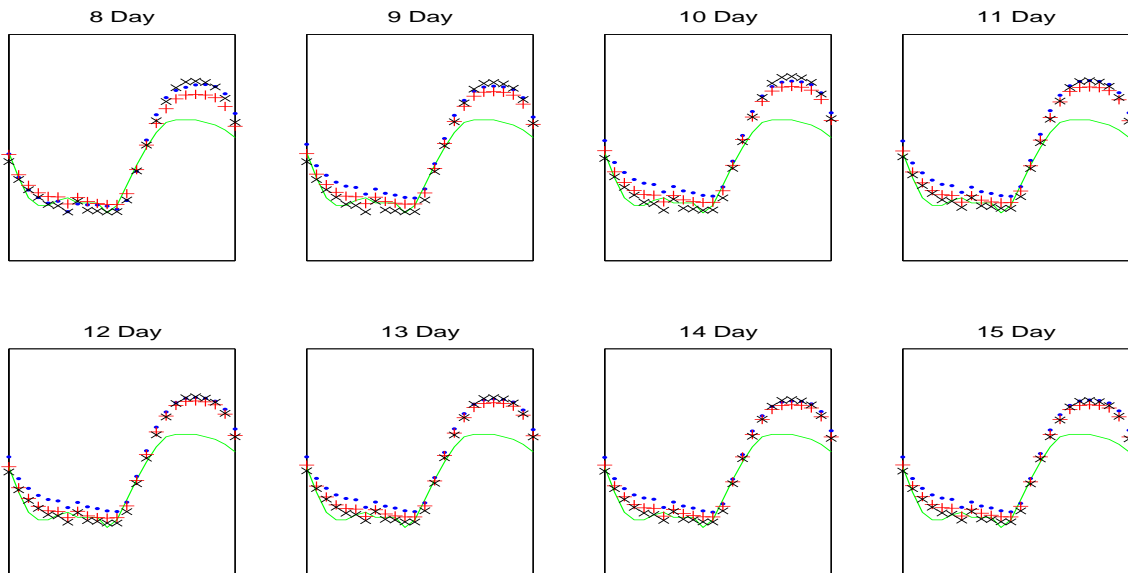


Figure 6.22: Autoregressive predictions (blue \cdot , red $+$, and black \times) and exact measurement (green line) on Sept. 5, 2005 in Atlanta

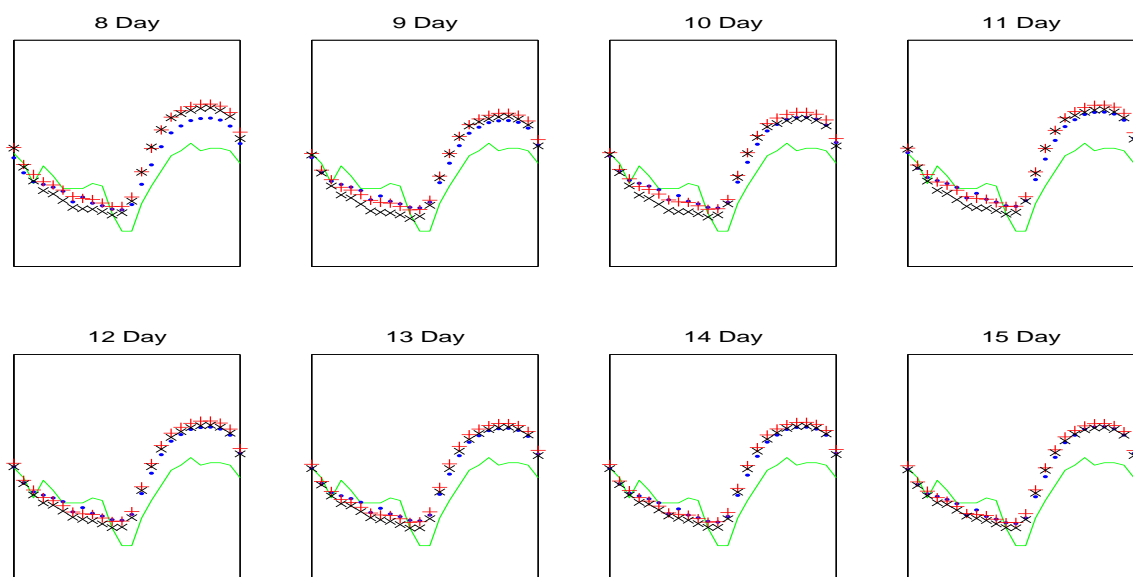


Figure 6.23: Autoregressive predictions (blue \cdot , red $+$, and black \times) and exact measurement (green line) on Sept. 6, 2005 in Atlanta

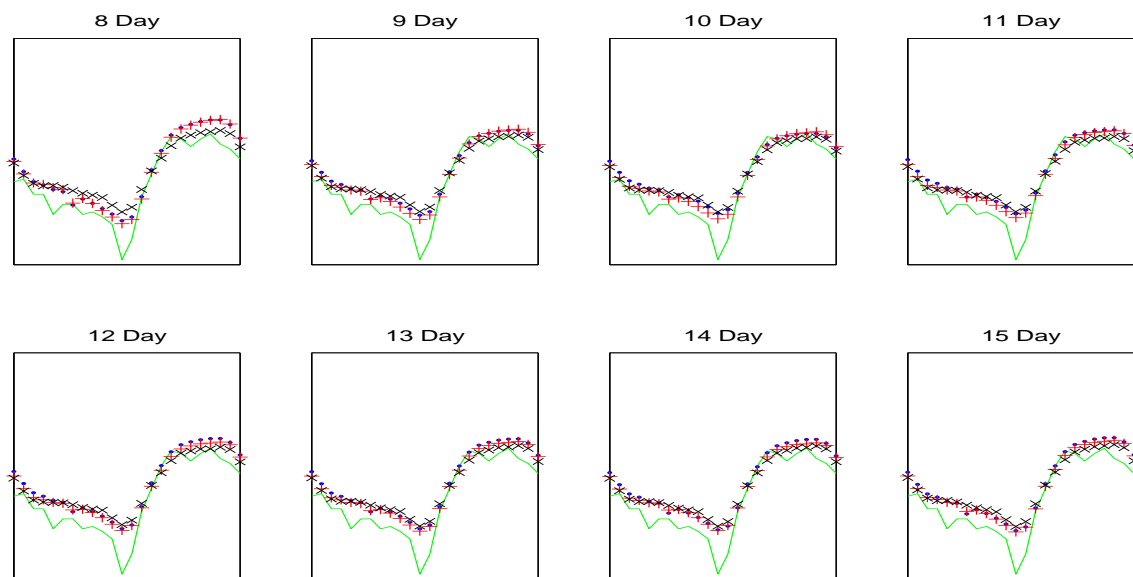


Figure 6.24: Autoregressive predictions (blue \cdot , red $+$, and black \times) and exact measurement (green line) on Sept. 7, 2005 in Atlanta

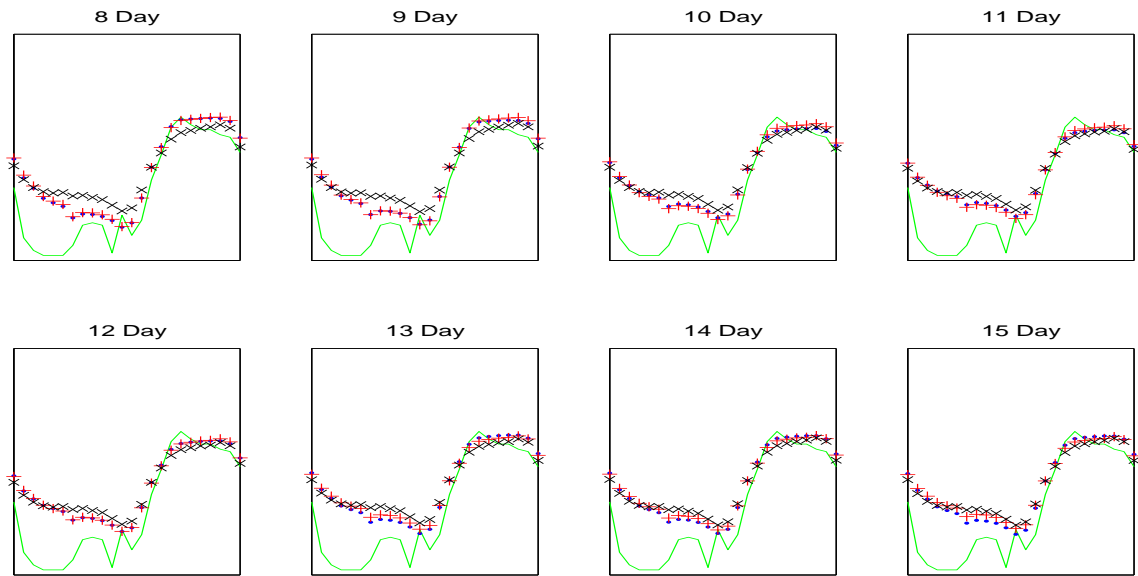


Figure 6.25: Autoregressive predictions (blue \cdot , red $+$, and black \times) and exact measurement (green line) on Sept. 8, 2005 in Atlanta

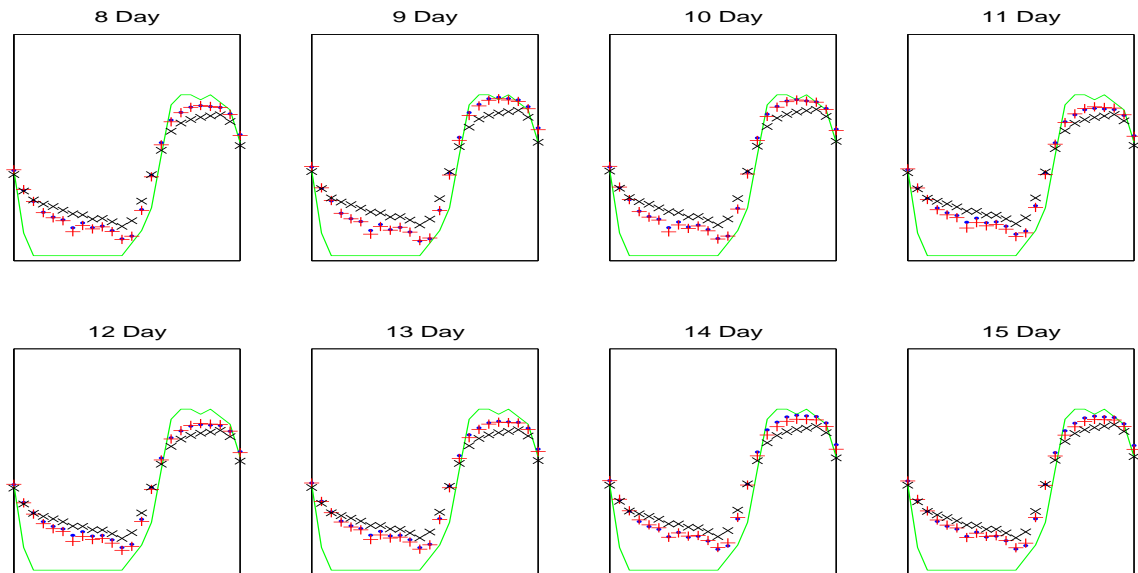


Figure 6.26: Autoregressive predictions (blue \cdot , red $+$, and black \times) and exact measurement (green line) on Sept. 9, 2005 in Atlanta

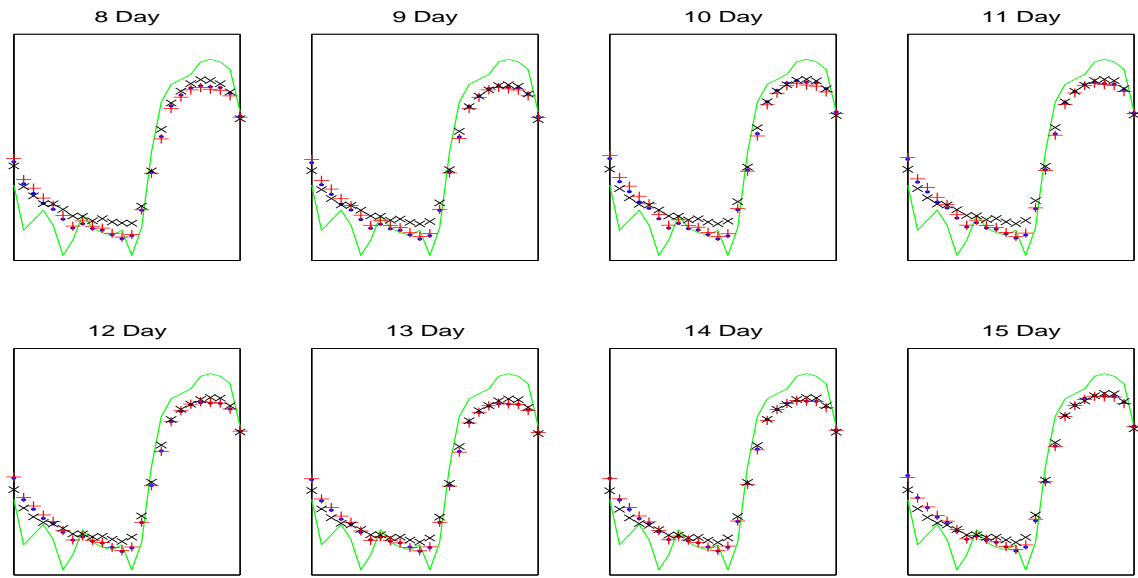


Figure 6.27: Autoregressive predictions (blue \cdot , red $+$, and black \times) and exact measurement (green line) on Sept. 10, 2005 in Atlanta

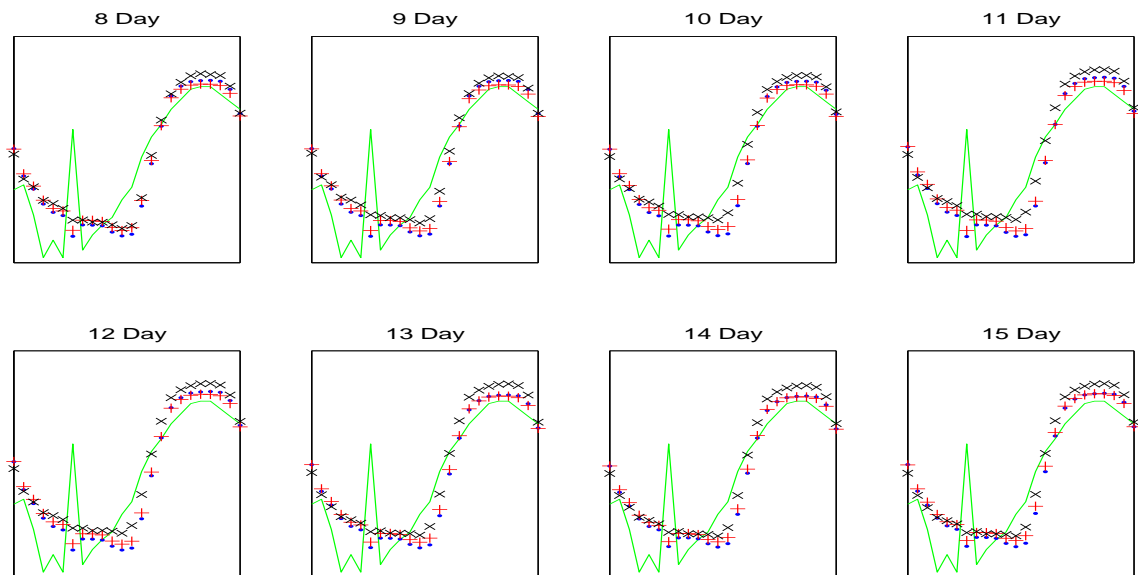


Figure 6.28: Autoregressive predictions (blue \cdot , red $+$, and black \times) and exact measurement (green line) on Sept. 11, 2005 in Atlanta

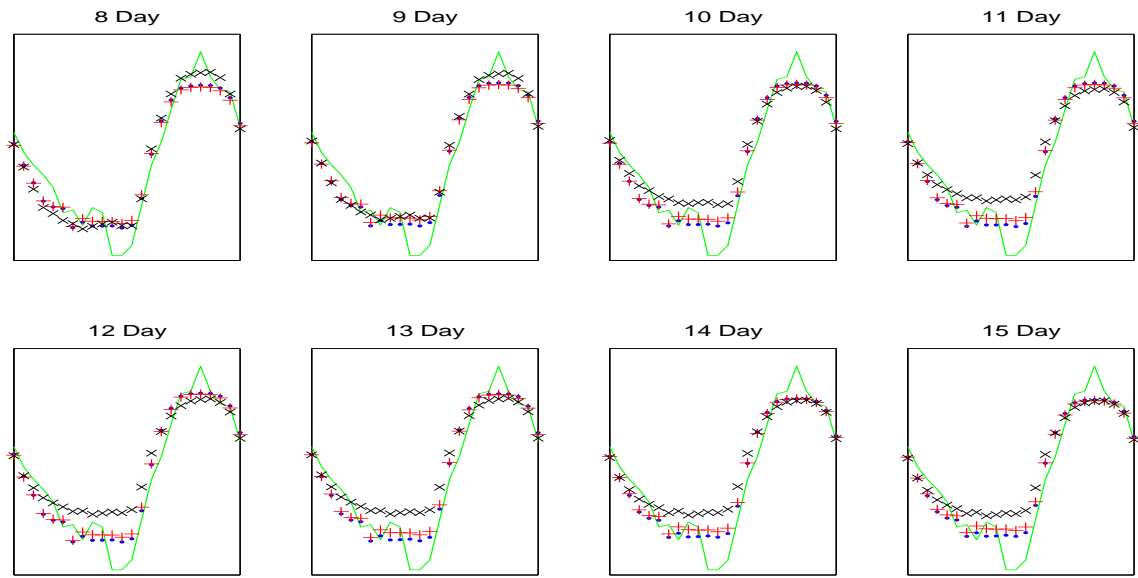


Figure 6.29: Autoregressive predictions (blue \cdot , red $+$, and black \times) and exact measurement (green line) on Sept. 12, 2005 in Atlanta

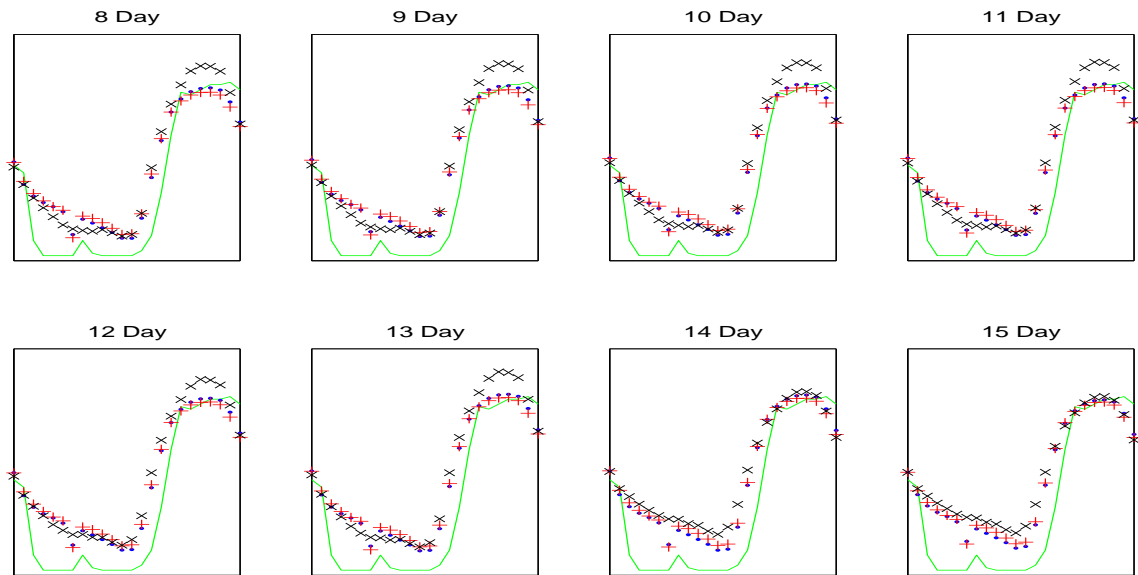


Figure 6.30: Autoregressive predictions (blue \cdot , red $+$, and black \times) and exact measurement (green line) on Sept. 13, 2005 in Atlanta

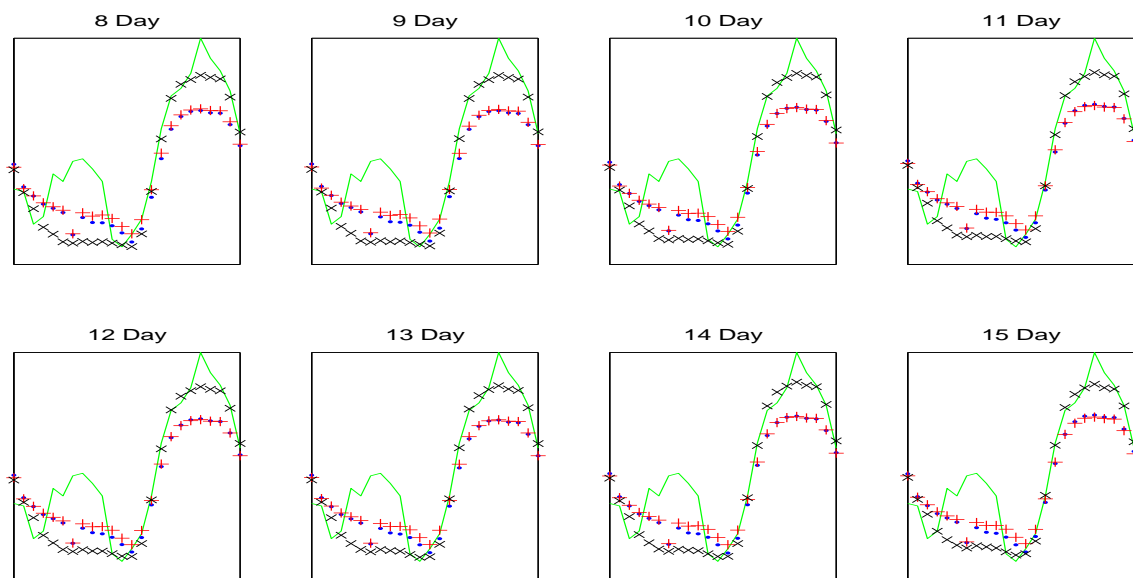


Figure 6.31: Autoregressive predictions (blue \cdot , red $+$, and black \times) and exact measurement (green line) on Sept. 14, 2005 in Atlanta

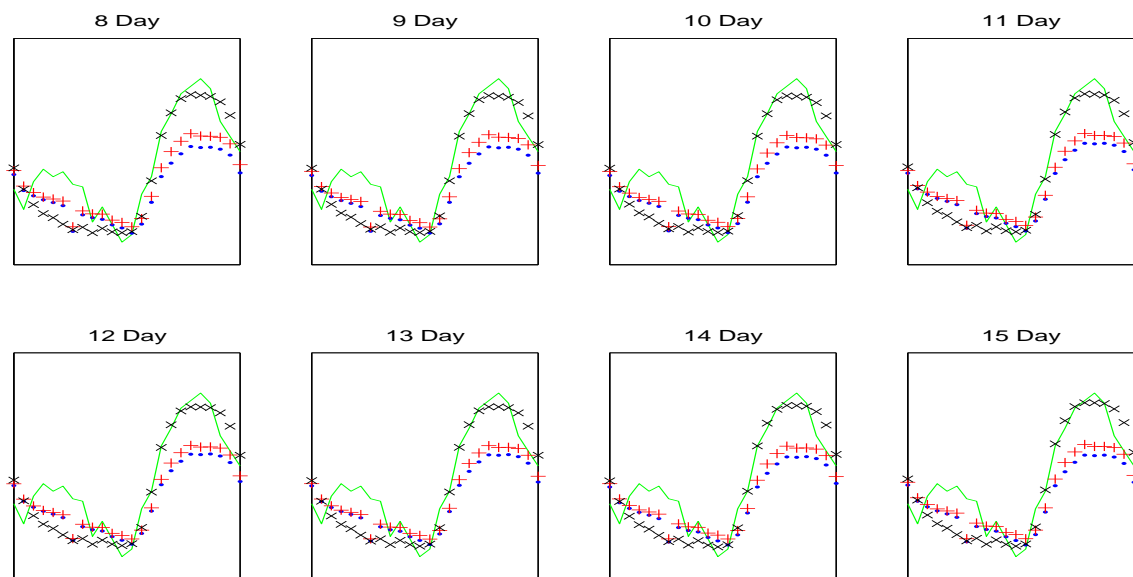
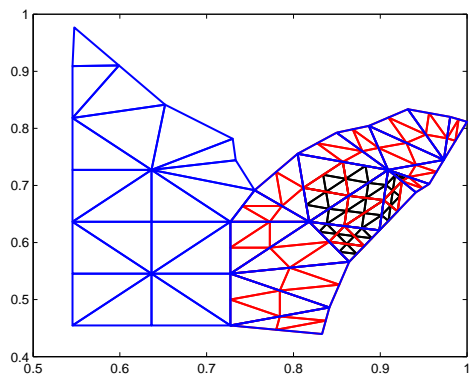


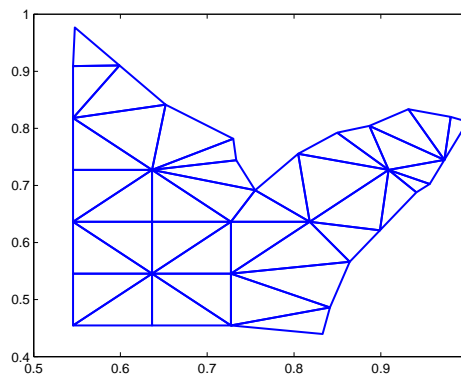
Figure 6.32: Autoregressive predictions (blue \cdot , red $+$, and black \times) and exact measurement (green line) on Sept. 15, 2005 in Atlanta

6.2 BOSTON

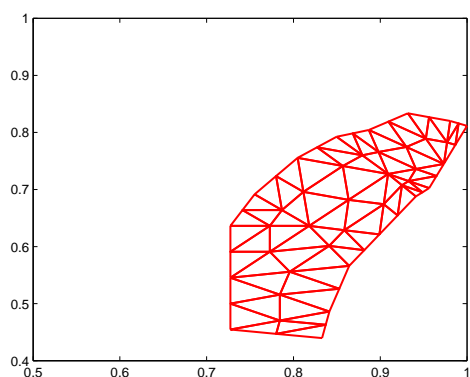
In Figure 6.33 are the triangulations used for the Boston ozone forecasts.



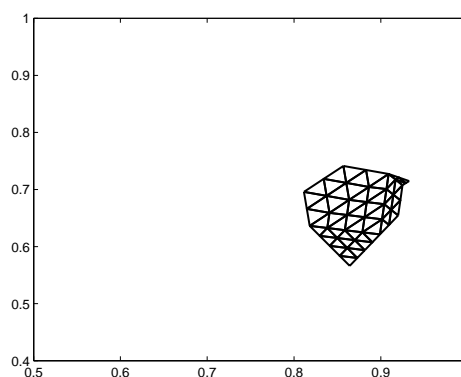
All Triangulations Superimposed



Triangulation 1



Triangulation 2



Triangulation 3

Figure 6.33: Three different sizes of triangulation of the northeast part of U.S.

6.2.1 THE BRUTE FORCE METHOD FOR PREDICTION AT BOSTON

We first show our numerical experimental results using our brute force approach. In the following graphs, we show the exact measurement (green line), predictions based on triangulation 1 (the blue \cdot), based on triangulation 2 (the red $+$), and based on triangulation 3 (the black \times) as in Figs 6.34– 6.48.

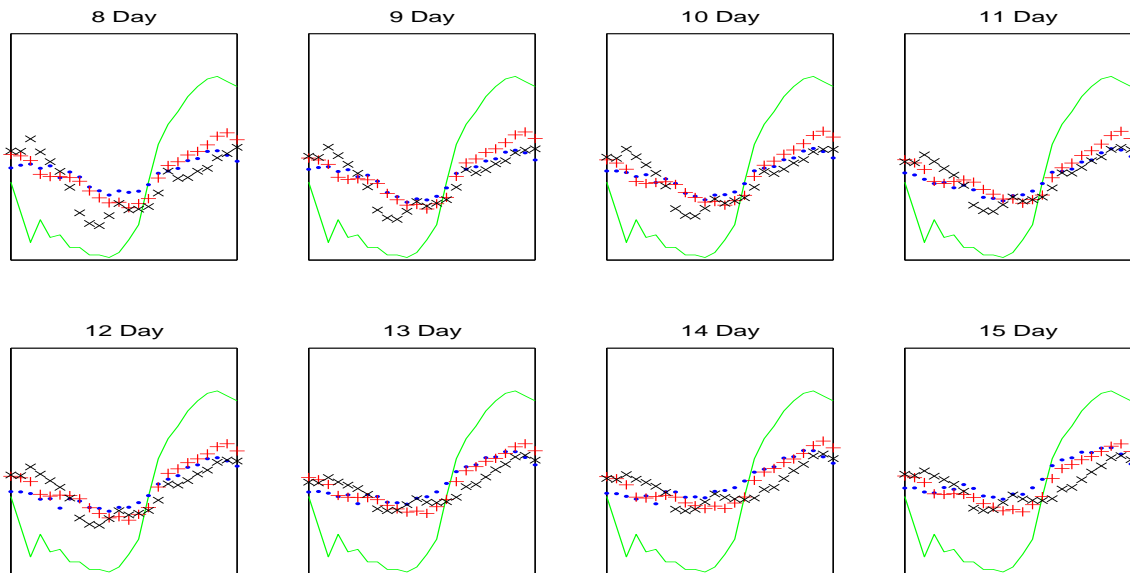


Figure 6.34: Brute force predictions (blue \cdot , red $+$, and black \times) and exact measurement (green line) on Sept. 1, 2005 in Boston

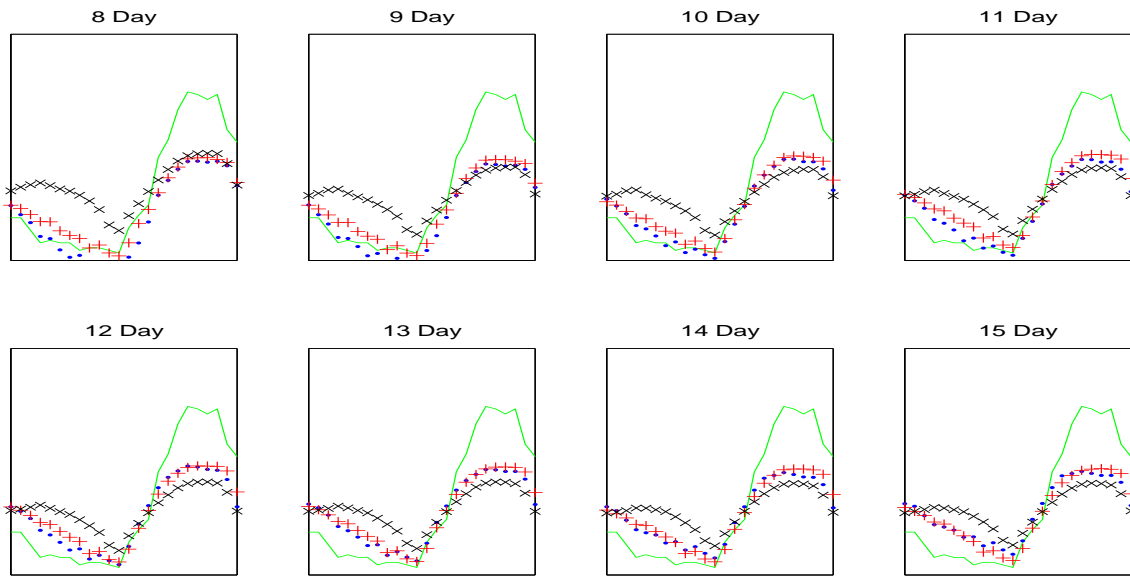


Figure 6.35: Brute force predictions (blue \cdot , red $+$, and black \times) and exact measurement (green line) on Sept. 2, 2005 in Boston

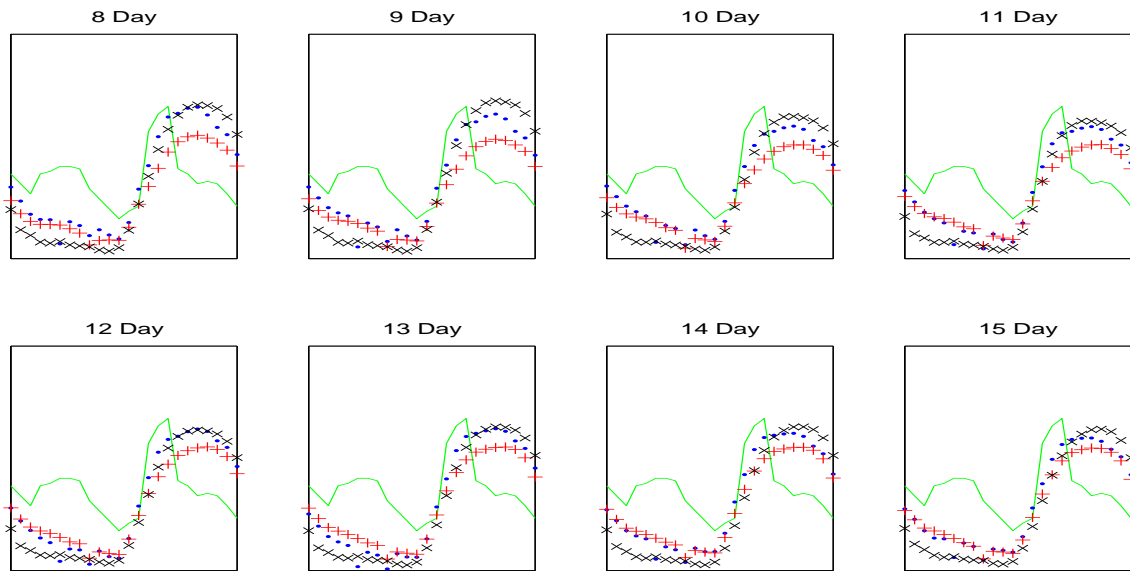


Figure 6.36: Brute force predictions (blue \cdot , red $+$, and black \times) and exact measurement (green line) on Sept. 3, 2005 in Boston

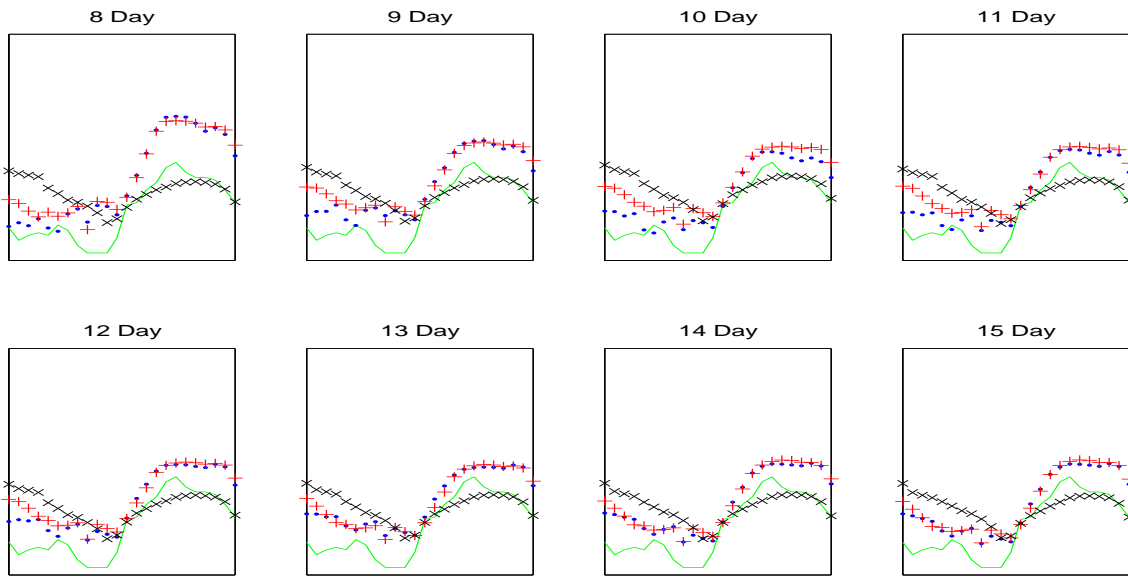


Figure 6.37: Brute force predictions (blue \cdot , red $+$, and black \times) and exact measurement (green line) on Sept. 4, 2005 in Boston

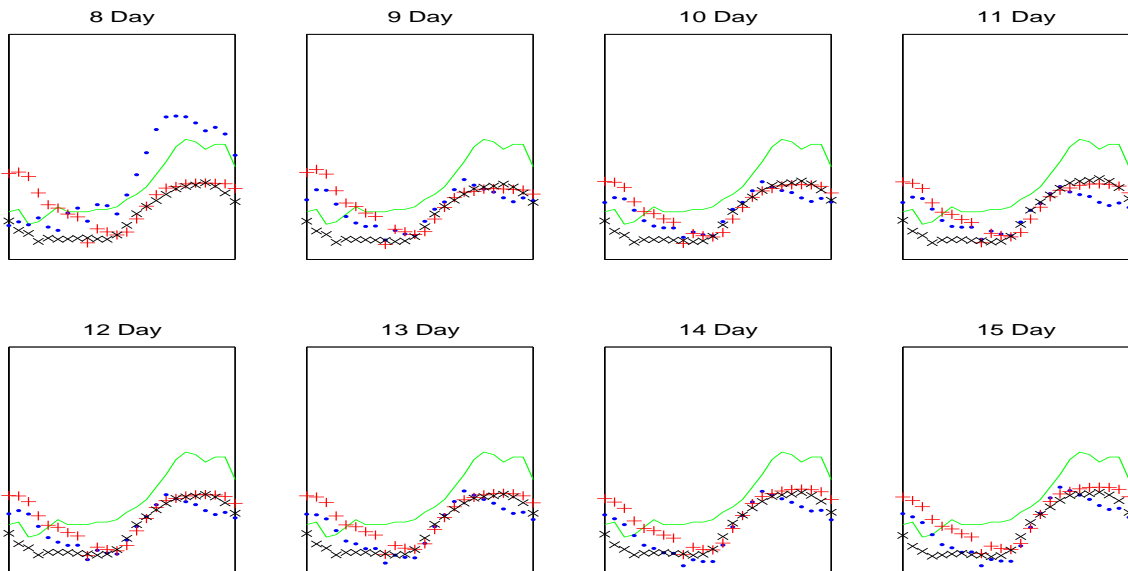


Figure 6.38: Brute force predictions (blue \cdot , red $+$, and black \times) and exact measurement (green line) on Sept. 5, 2005 in Boston

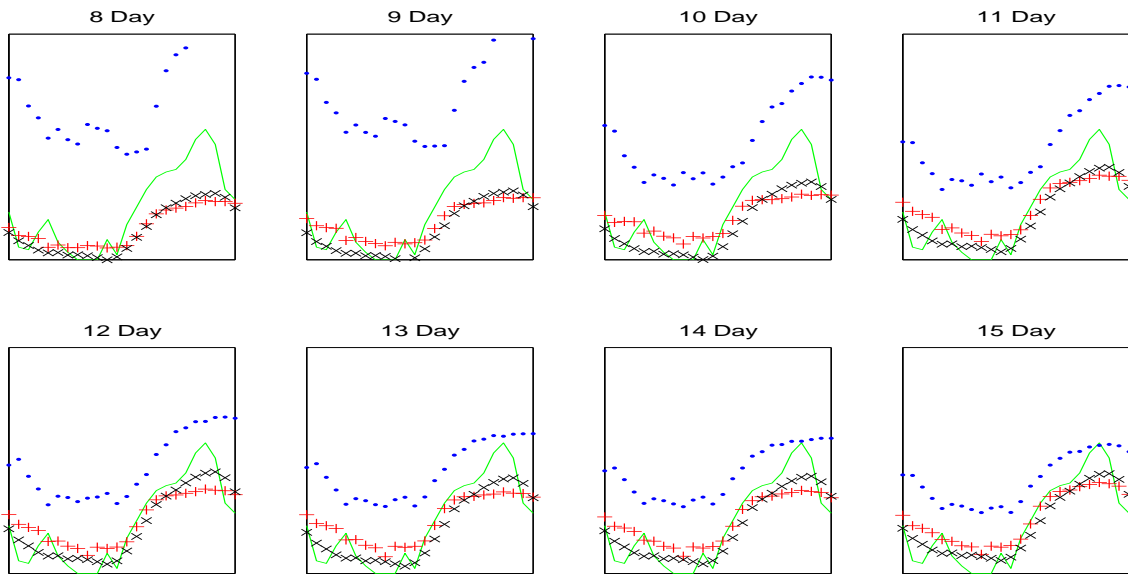


Figure 6.39: Brute force predictions (blue \cdot , red $+$, and black \times) and exact measurement (green line) on Sept. 6, 2005 in Boston

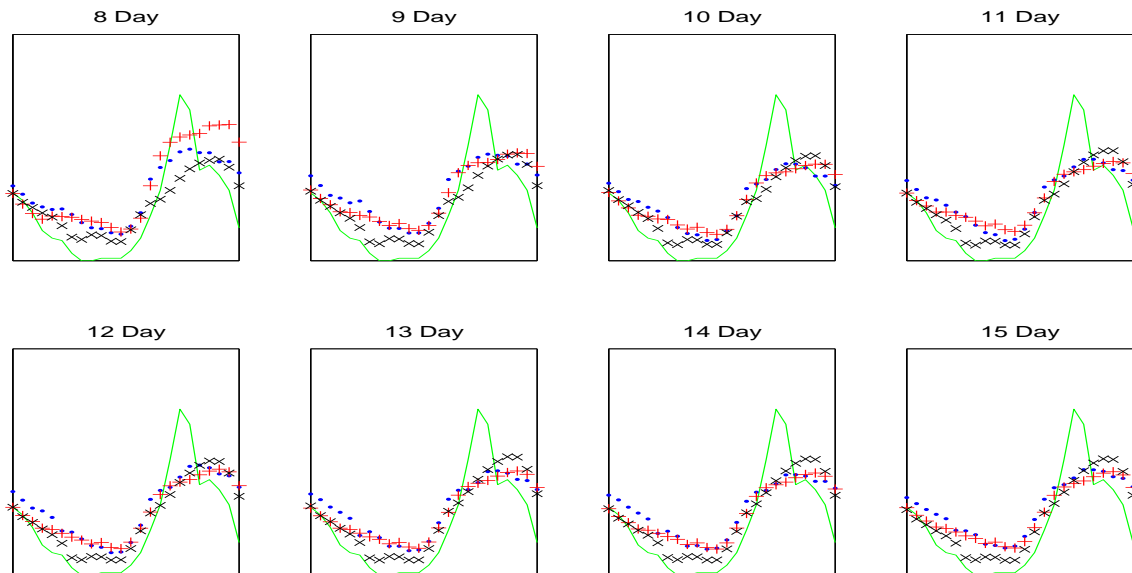


Figure 6.40: Brute force predictions (blue \cdot , red $+$, and black \times) and exact measurement (green line) on Sept. 7, 2005 in Boston

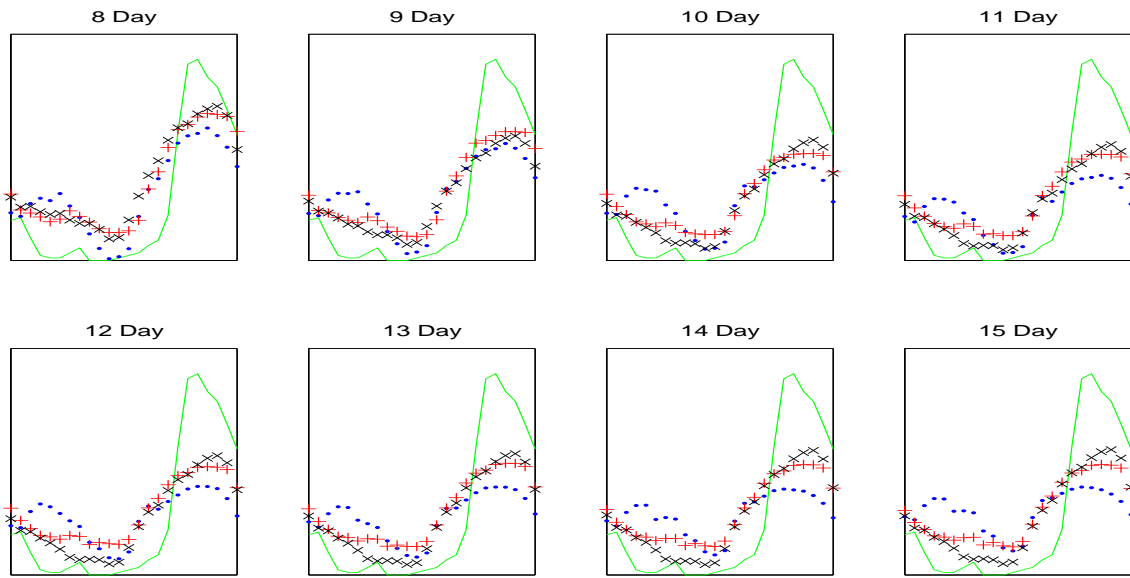


Figure 6.41: Brute force predictions (blue \cdot , red $+$, and black \times) and exact measurement (green line) on Sept. 8, 2005 in Boston

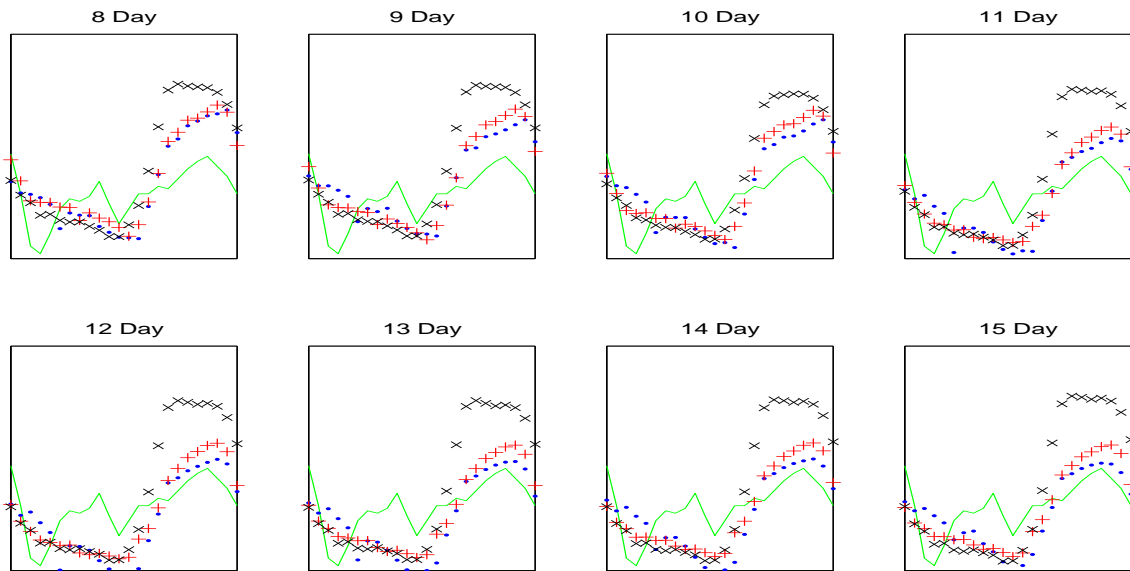


Figure 6.42: Brute force predictions (blue \cdot , red $+$, and black \times) and exact measurement (green line) on Sept. 9, 2005 in Boston

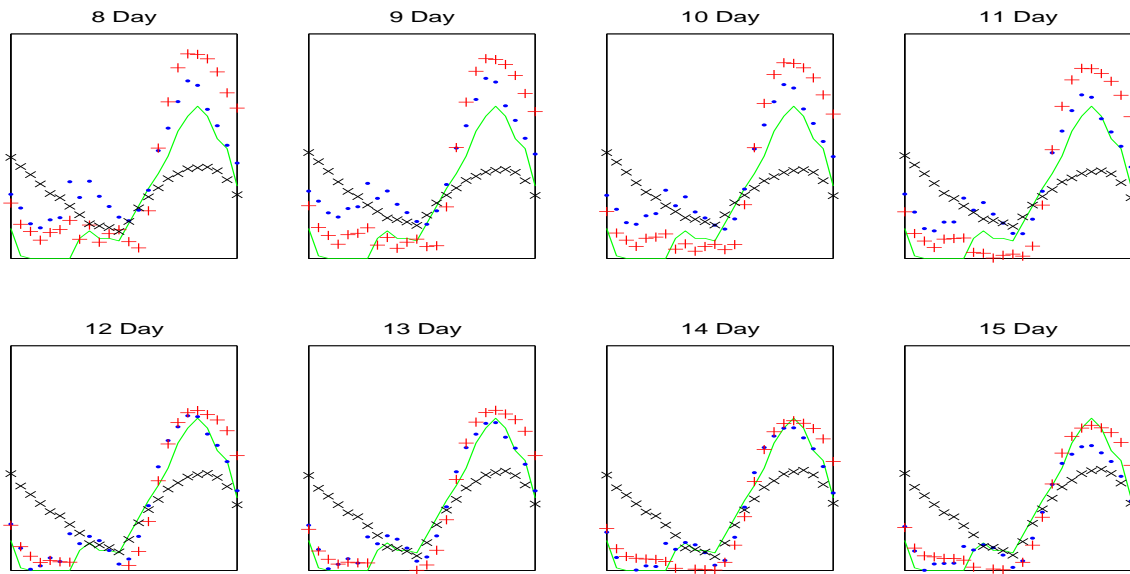


Figure 6.43: Brute force predictions (blue \cdot , red $+$, and black \times) and exact measurement (green line) on Sept. 10, 2005 in Boston

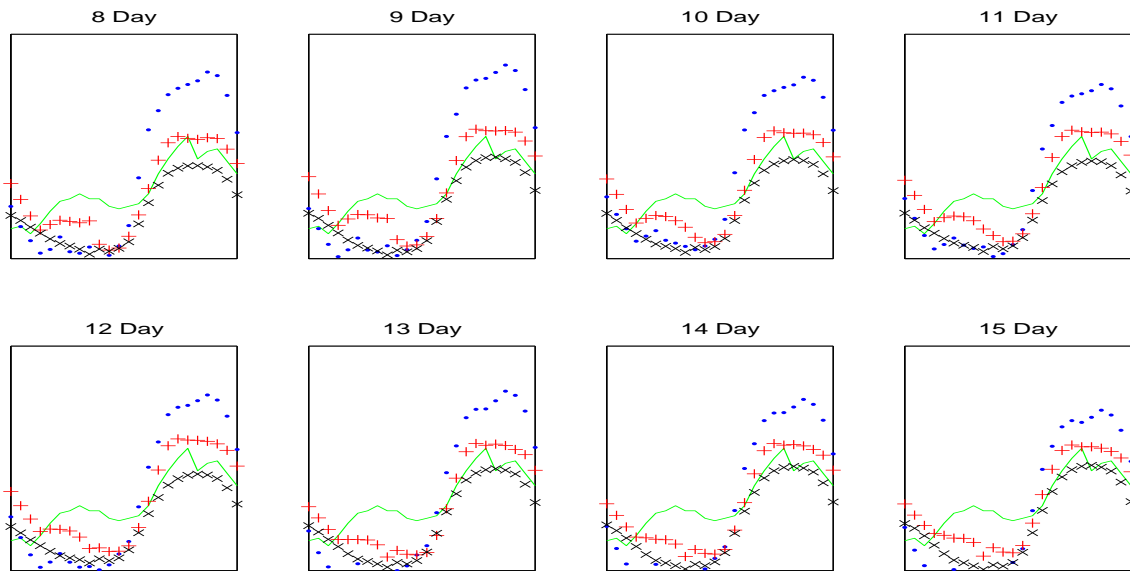


Figure 6.44: Brute force predictions (blue \cdot , red $+$, and black \times) and exact measurement (green line) on Sept. 11, 2005 in Boston

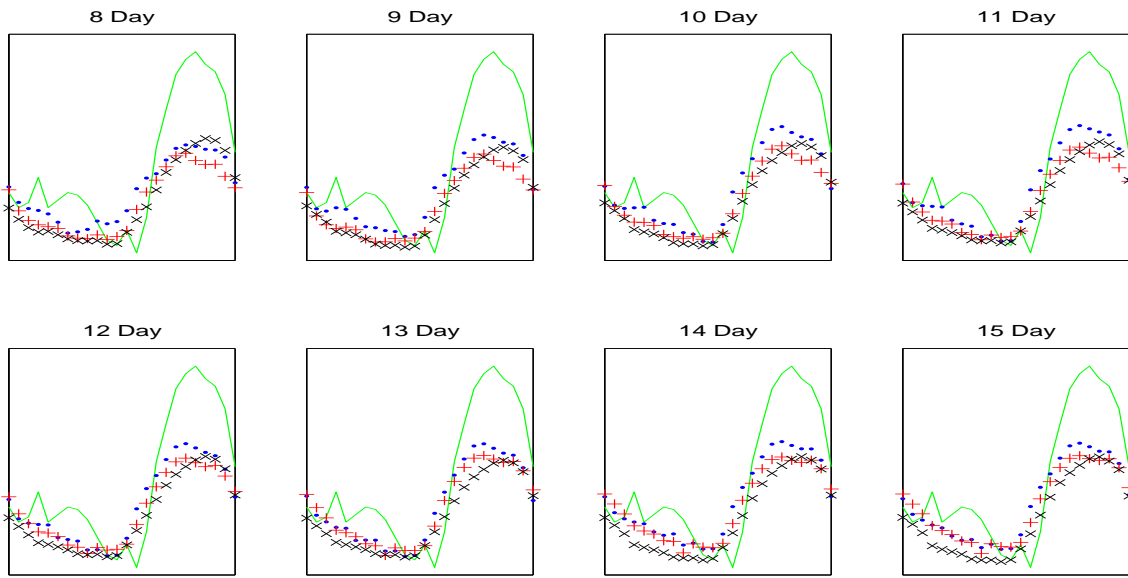


Figure 6.45: Brute force predictions (blue \cdot , red $+$, and black \times) and exact measurement (green line) on Sept. 12, 2005 in Boston

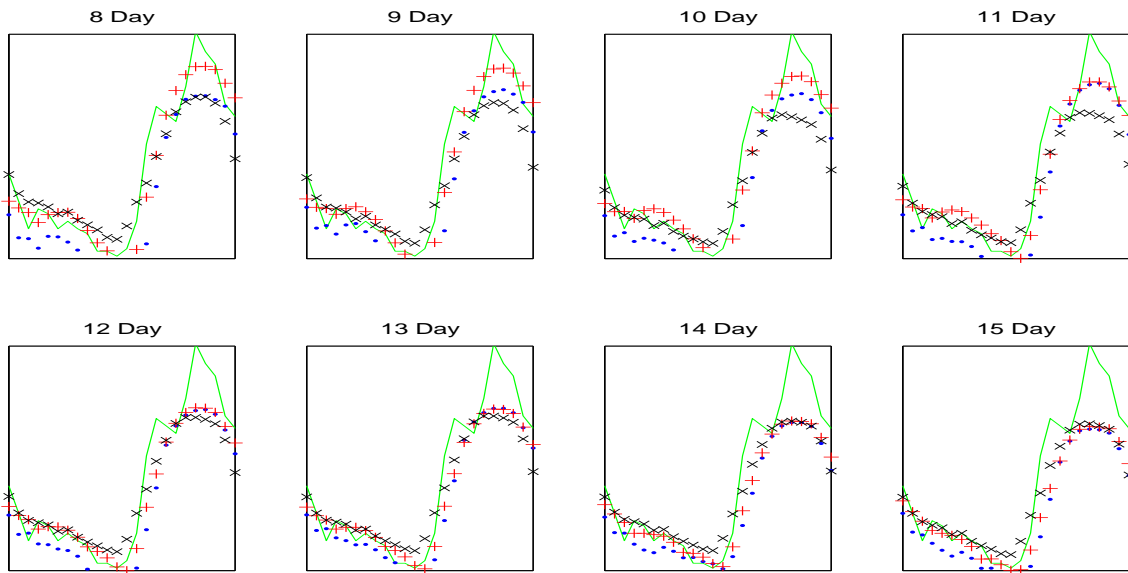


Figure 6.46: Brute force predictions (blue \cdot , red $+$, and black \times) and exact measurement (green line) on Sept. 13, 2005 in Boston

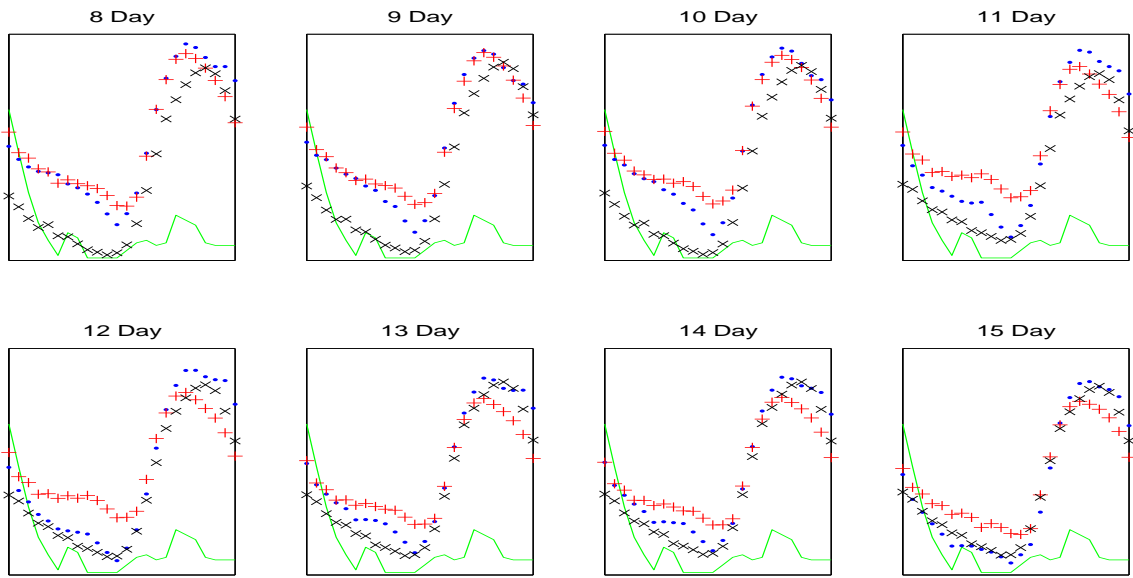


Figure 6.47: Brute force predictions (blue \cdot , red $+$, and black \times) and exact measurement (green line) on Sept. 14, 2005 in Boston

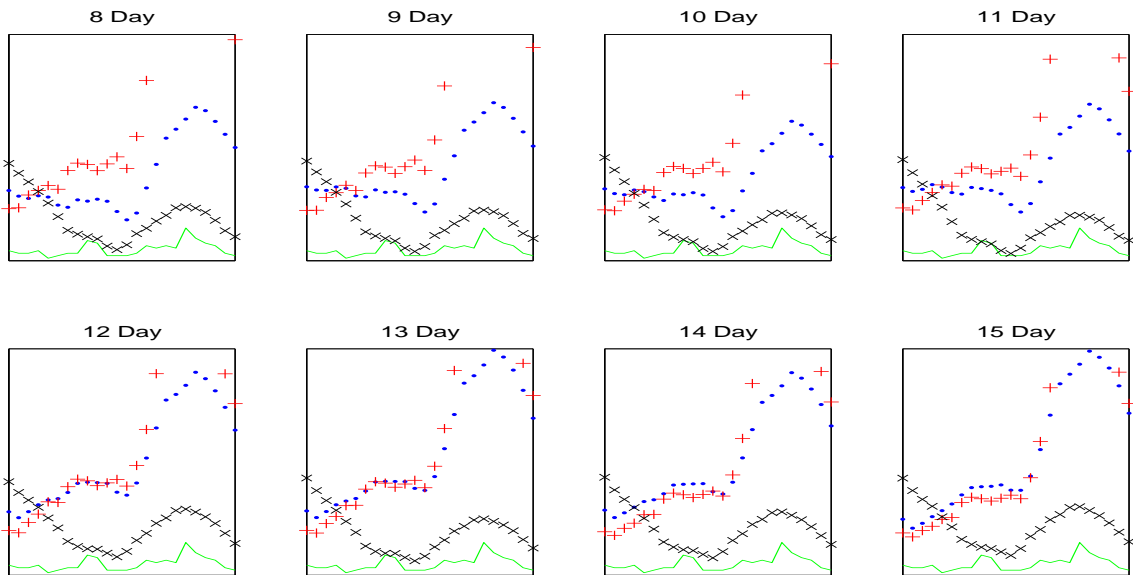


Figure 6.48: Brute force predictions (blue \cdot , red $+$, and black \times) and exact measurement (green line) on Sept. 15, 2005 in Boston

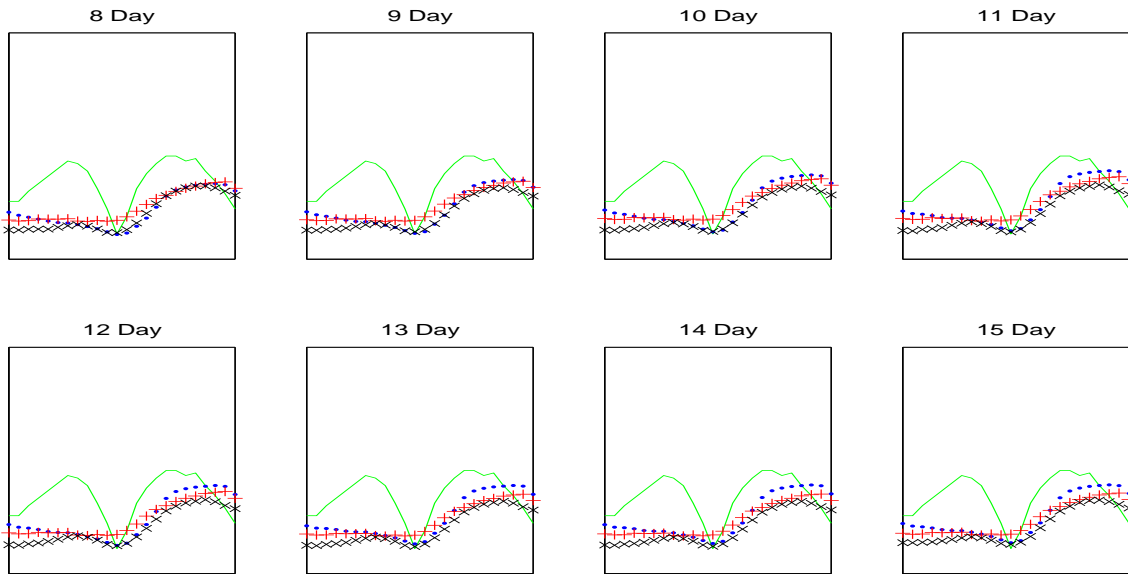


Figure 6.49: Autoregressive predictions (blue \cdot , red $+$, and black \times) and exact measurement (green line) on Sept. 1, 2005 in Boston

6.2.2 THE AUTOREGRESSIVE APPROACH FOR PREDICTION AT BOSTON

We now show our numerical experimental results using our autoregressive approach. In the following graphs, we show the exact measurement (green line), predictions based on triangulation 1 (the red $+$), based on triangulation 2 (the black \times) and based on triangulation 3 (the blue \cdot) as in Figs 6.49– 6.63. We only use the first seven eigenvalues to compute the predictions.

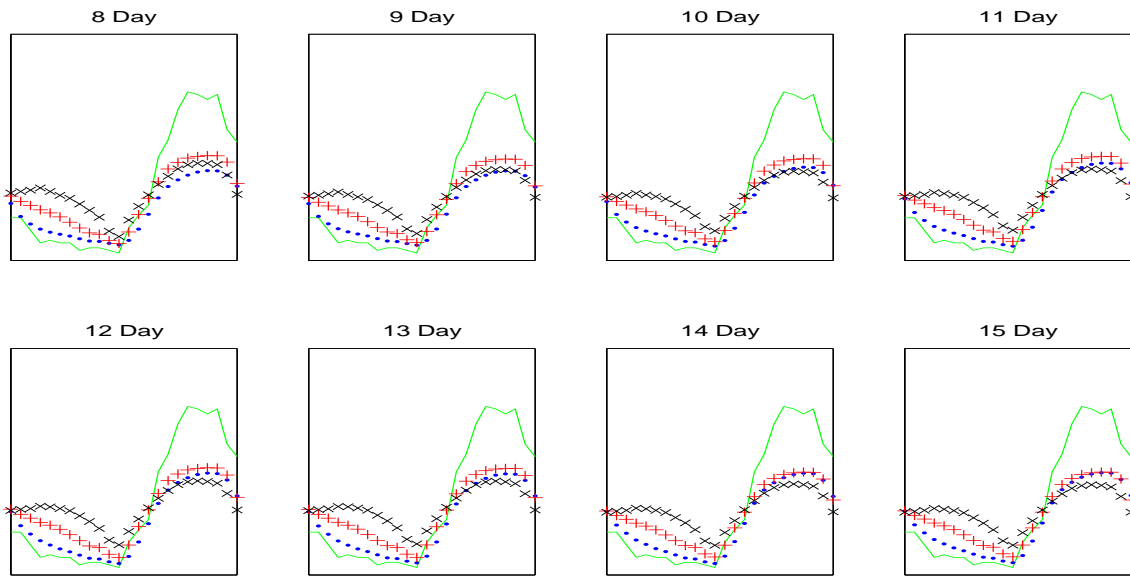


Figure 6.50: Autoregressive predictions (blue \cdot , red $+$, and black \times) and exact measurement (green line) on Sept. 2, 2005 in Boston

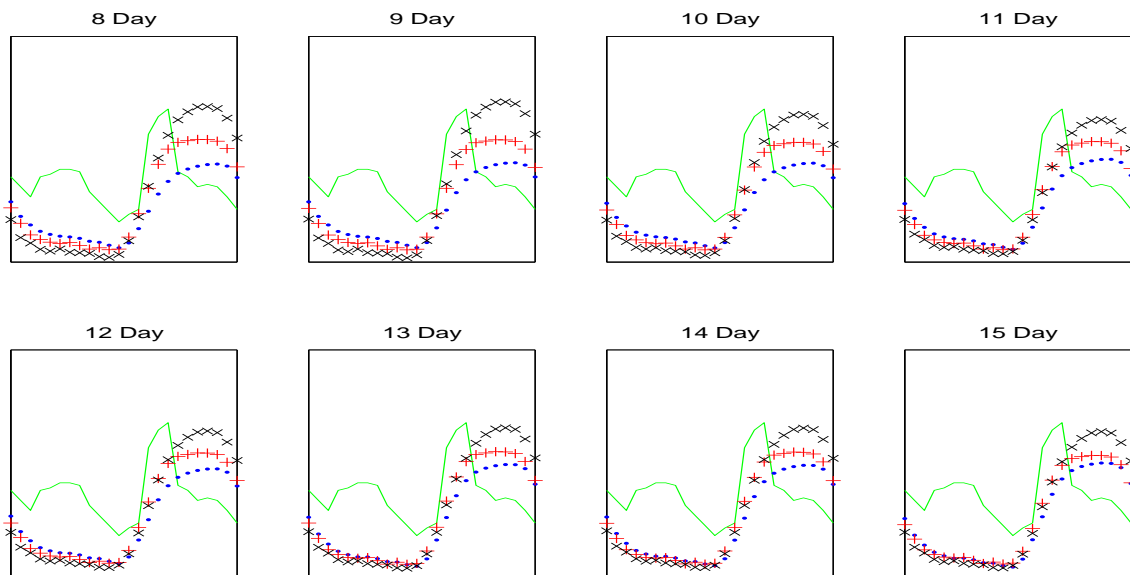


Figure 6.51: Autoregressive predictions (blue \cdot , red $+$, and black \times) and exact measurement (green line) on Sept. 3, 2005 in Boston

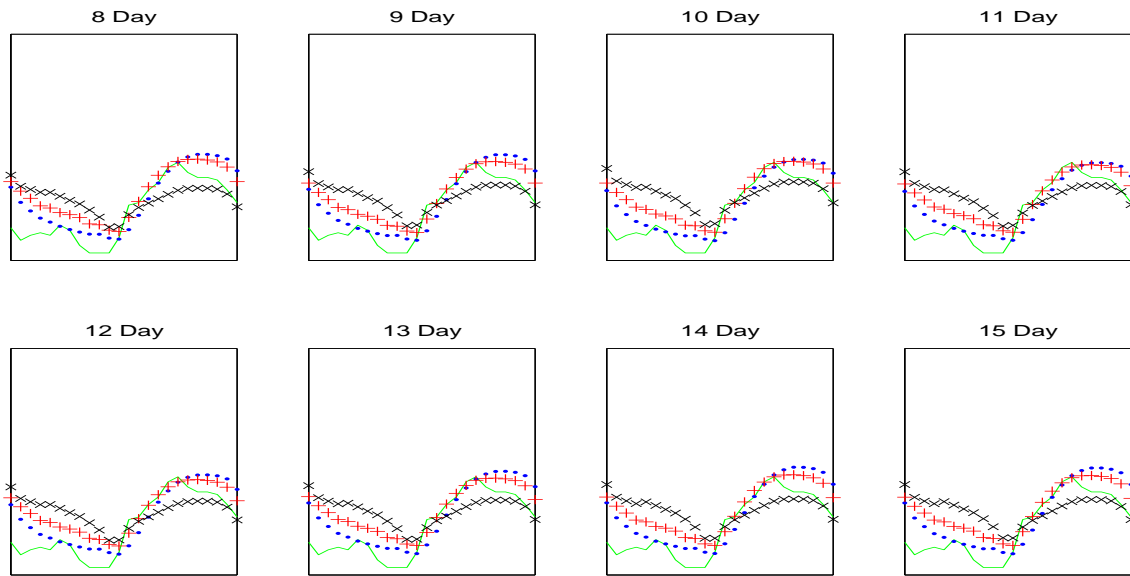


Figure 6.52: Autoregressive predictions (blue \cdot , red $+$, and black \times) and exact measurement (green line) on Sept. 4, 2005 in Boston

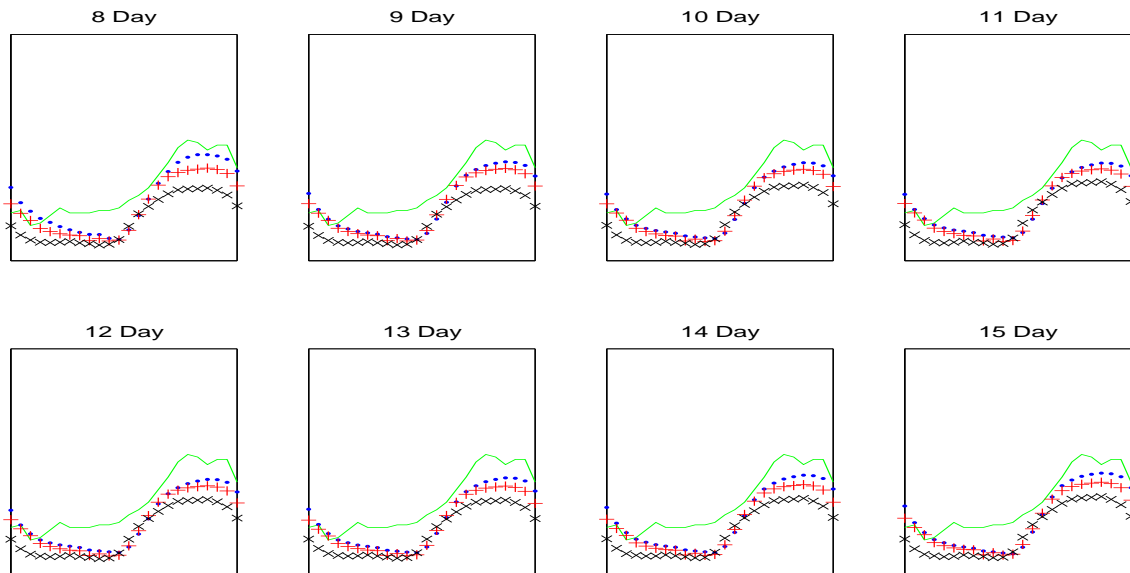


Figure 6.53: Autoregressive predictions (blue \cdot , red $+$, and black \times) and exact measurement (green line) on Sept. 5, 2005 in Boston

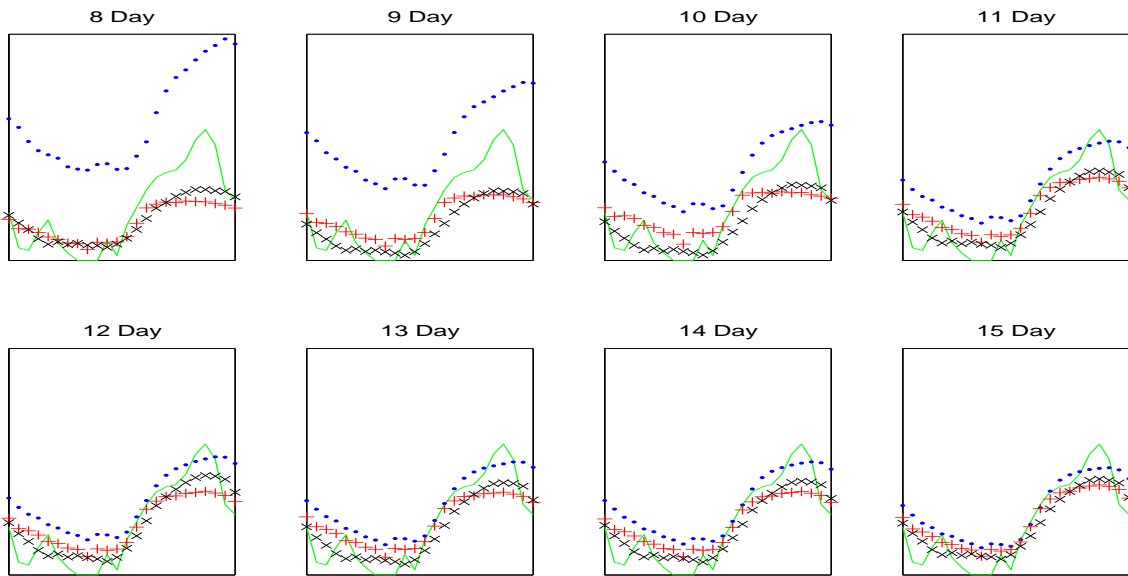


Figure 6.54: Autoregressive predictions (blue \cdot , red $+$, and black \times) and exact measurement (green line) on Sept. 6, 2005 in Boston

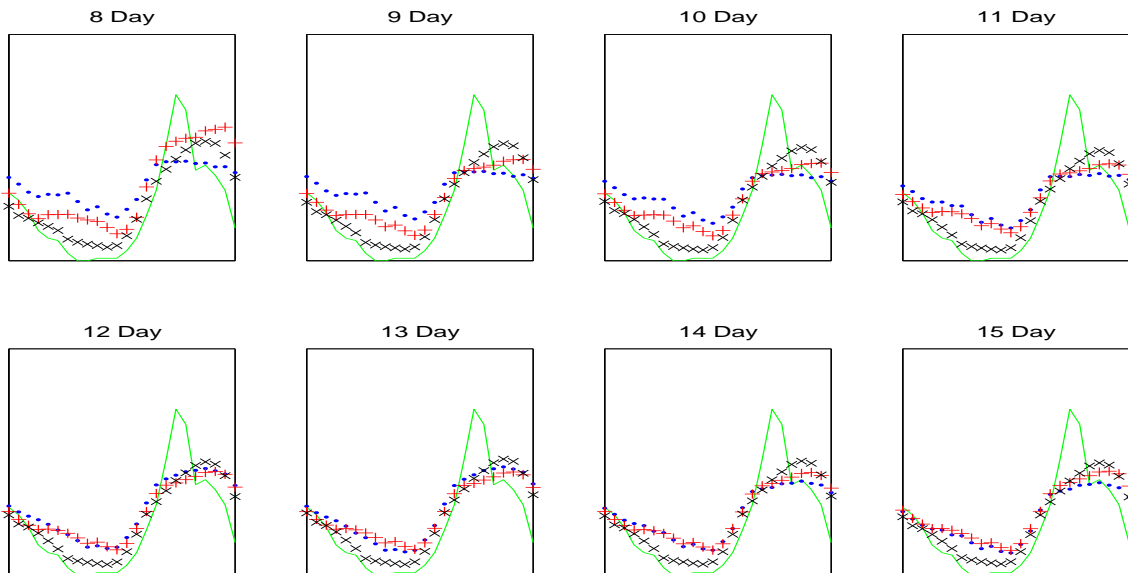


Figure 6.55: Autoregressive predictions (blue \cdot , red $+$, and black \times) and exact measurement (green line) on Sept. 7, 2005 in Boston

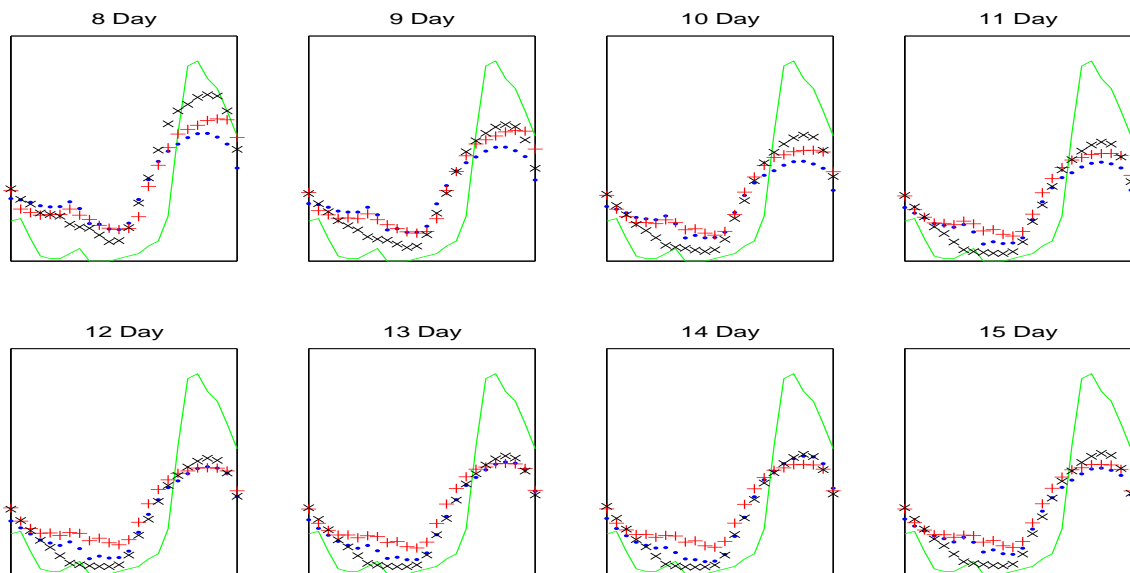


Figure 6.56: Autoregressive predictions (blue \cdot , red $+$, and black \times) and exact measurement (green line) on Sept. 8, 2005 in Boston

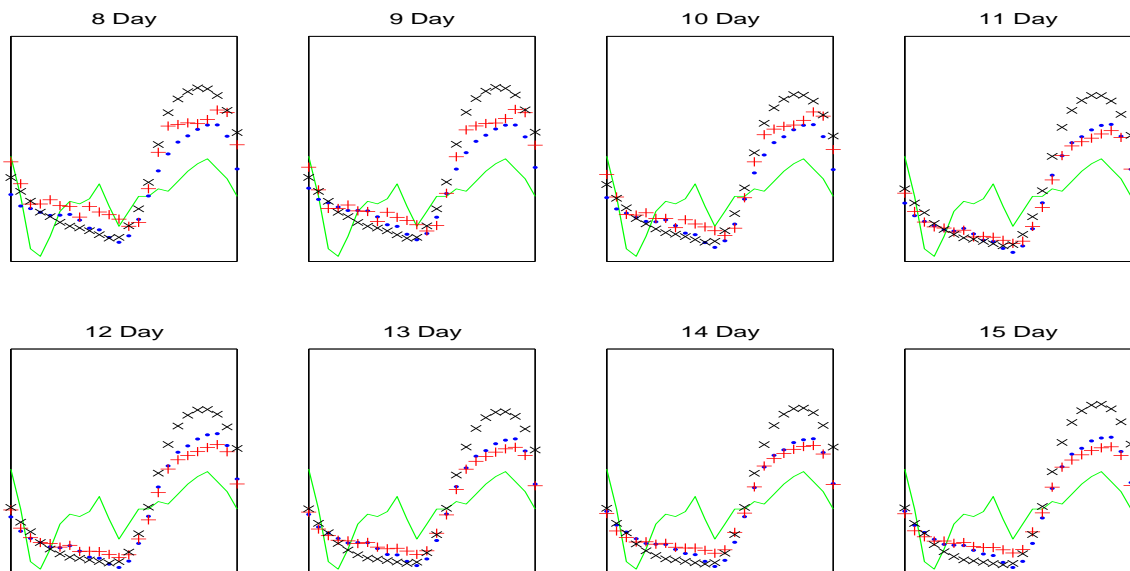


Figure 6.57: Autoregressive predictions (blue \cdot , red $+$, and black \times) and exact measurement (green line) on Sept. 9, 2005 in Boston

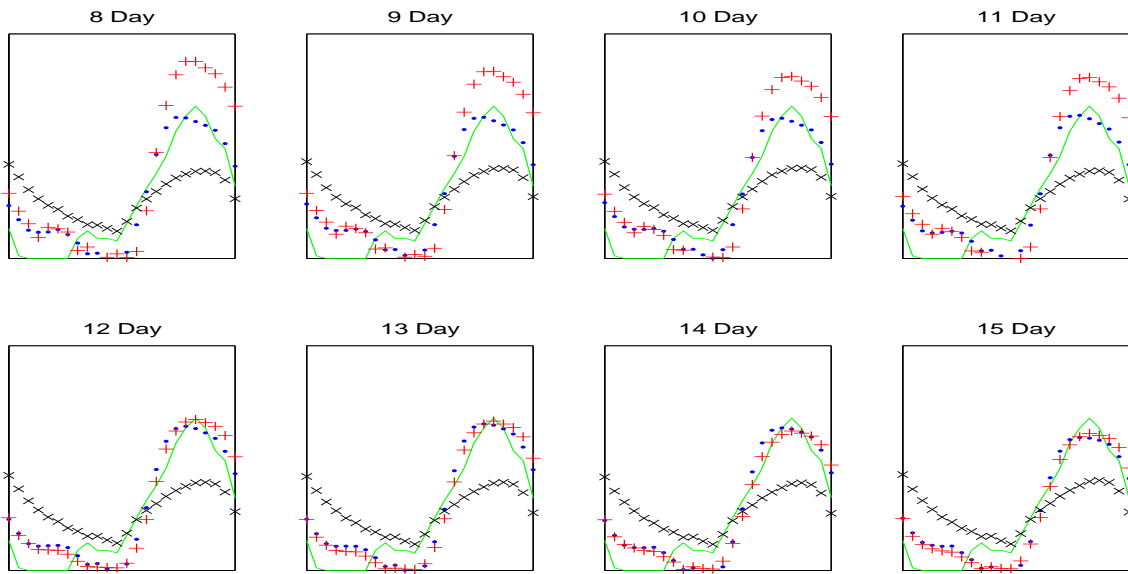


Figure 6.58: Autoregressive predictions (blue \cdot , red $+$, and black \times) and exact measurement (green line) on Sept. 10, 2005 in Boston

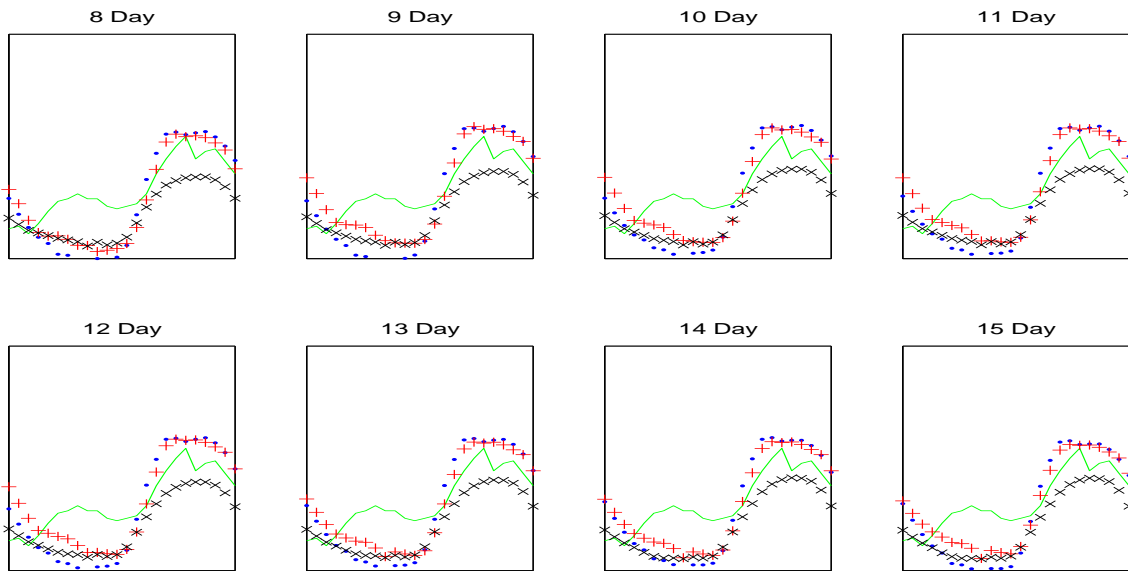


Figure 6.59: Autoregressive predictions (blue \cdot , red $+$, and black \times) and exact measurement (green line) on Sept. 11, 2005 in Boston

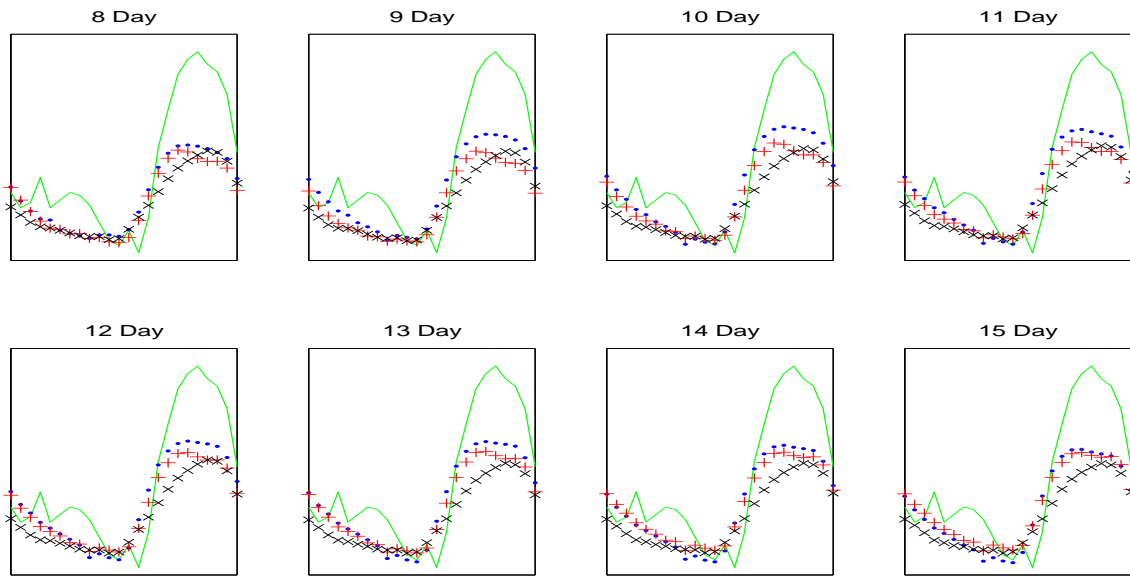


Figure 6.60: Autoregressive predictions (blue \cdot , red $+$, and black \times) and exact measurement (green line) on Sept. 12, 2005 in Boston

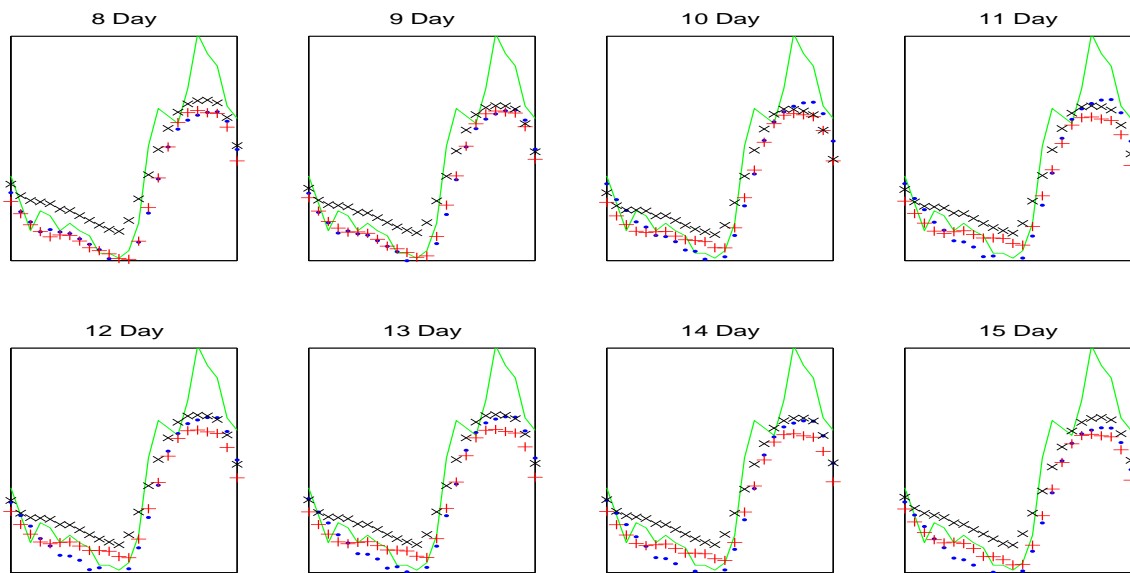


Figure 6.61: Autoregressive predictions (blue \cdot , red $+$, and black \times) and exact measurement (green line) on Sept. 13, 2005 in Boston

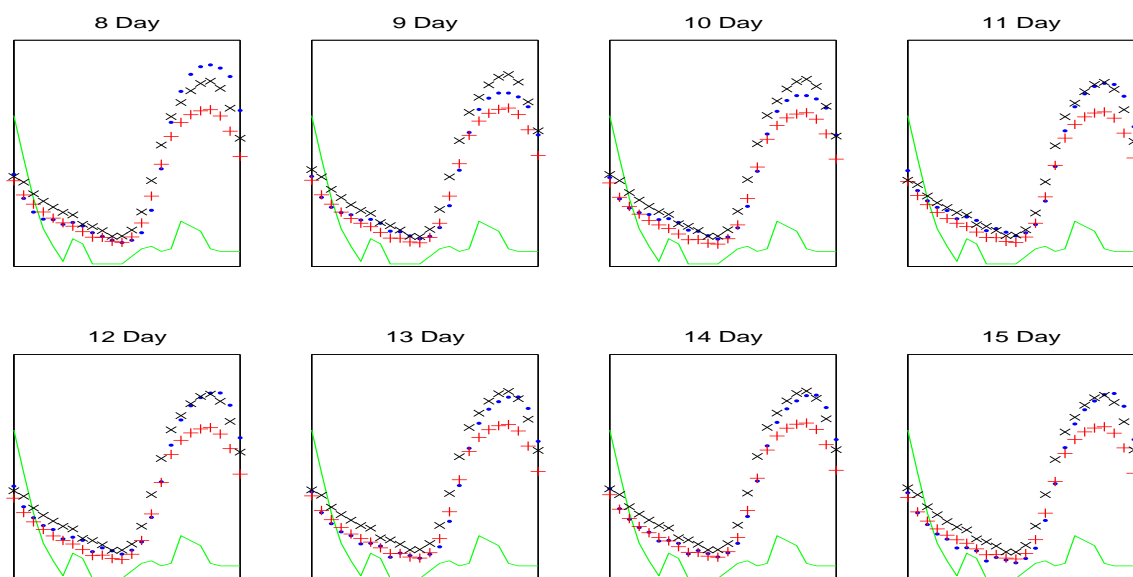


Figure 6.62: Autoregressive predictions (blue \cdot , red $+$, and black \times) and exact measurement (green line) on Sept. 14, 2005 in Boston

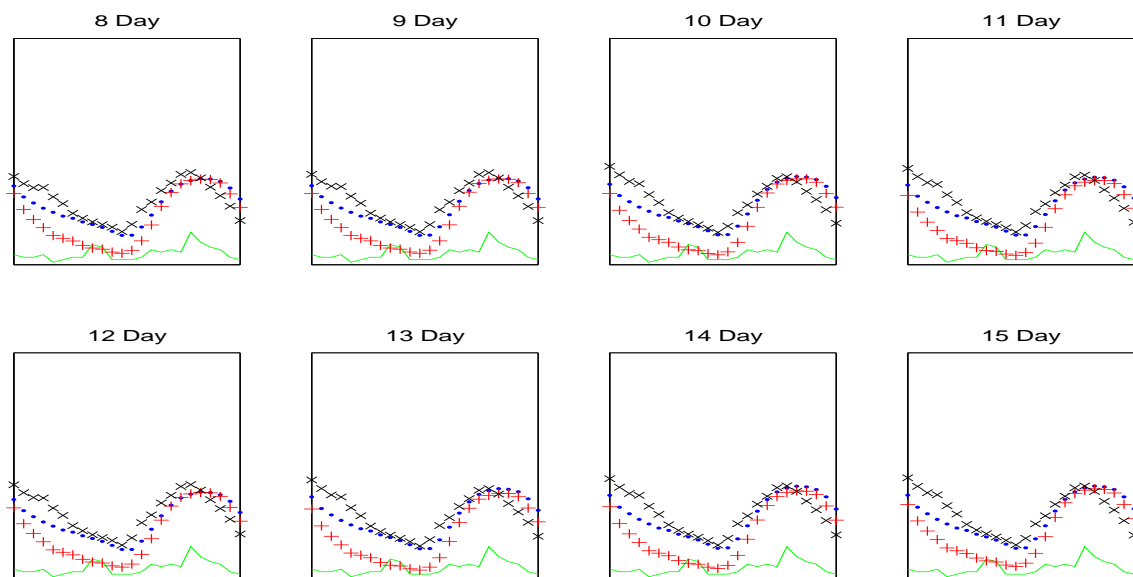
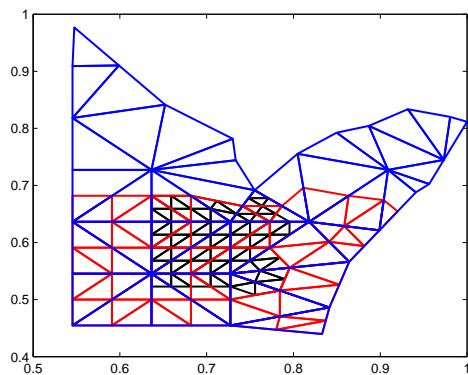


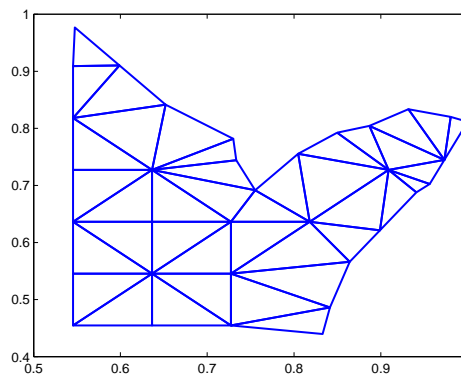
Figure 6.63: Autoregressive predictions (blue \cdot , red $+$, and black \times) and exact measurement (green line) on Sept. 15, 2005 in Boston

6.3 CINCINNATI

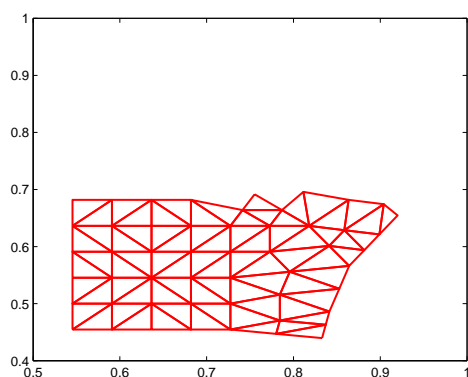
In Figure 6.64 are the triangulations used for the Cincinnati ozone forecasts.



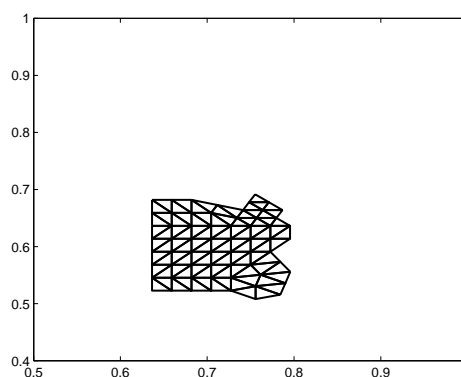
All Triangulations Superimposed



Triangulation 1



Triangulations 2



Triangulation 3

Figure 6.64: Three different sizes of triangulation of the northeast part of U.S.

6.3.1 THE BRUTE FORCE METHOD FOR PREDICTION AT CINCINNATI

We first show our numerical experimental results using our brute force approach. In the following graphs, we show the exact measurement (green line), predictions based on triangulation 1 (the blue \cdot), based on triangulation 2 (the red $+$), and based on triangulation 3 (the black \times) as in Figs 6.65– 6.79.

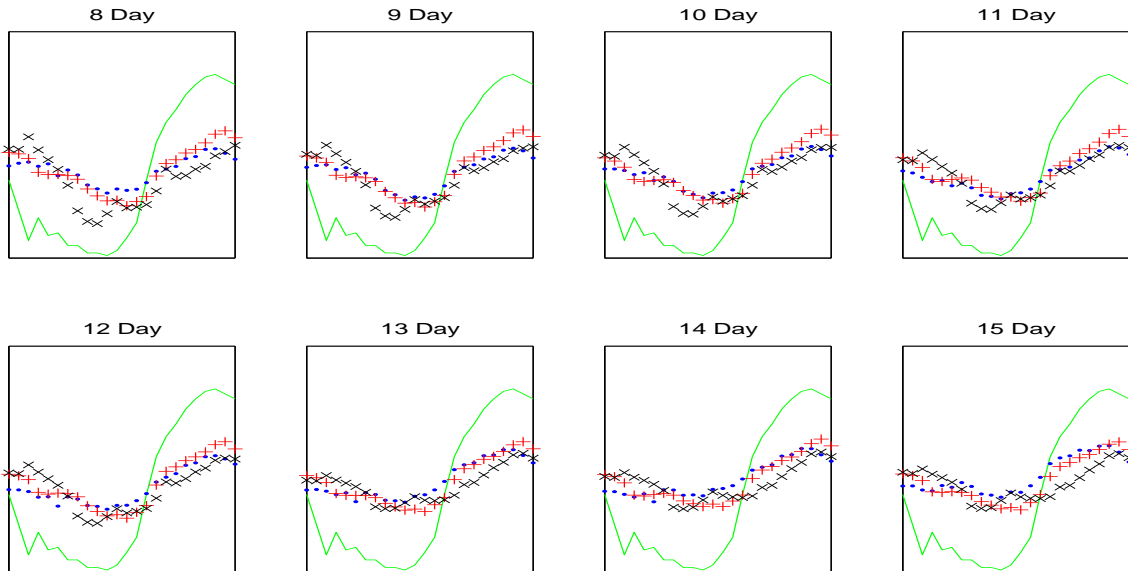


Figure 6.65: Brute force predictions (blue \cdot , red $+$, and black \times) and exact measurement (green line) on Sept. 1, 2005 in Cincinnati

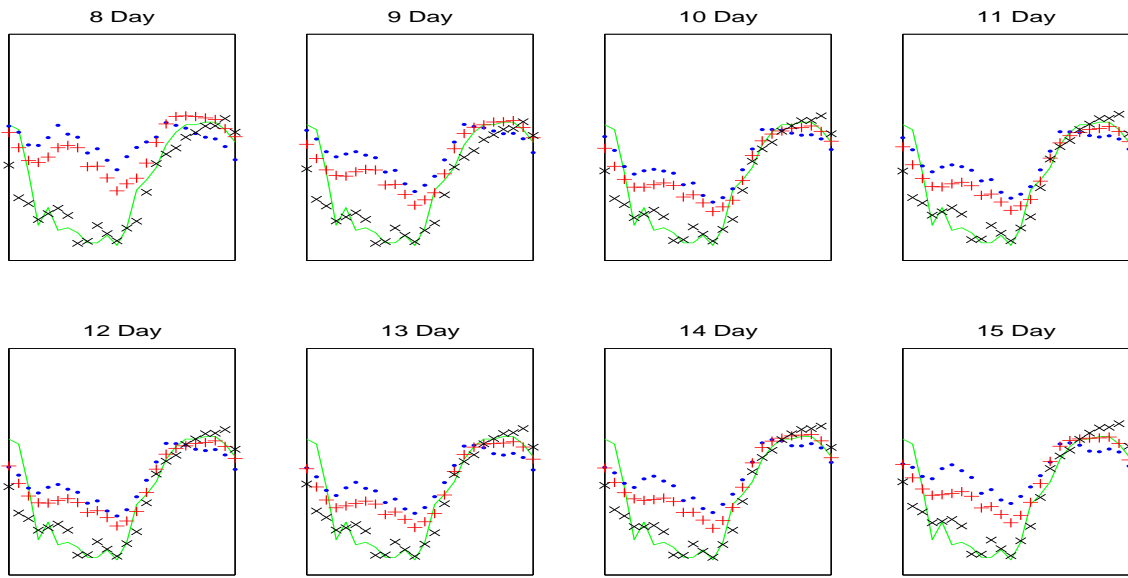


Figure 6.66: Brute force predictions (blue \cdot , red $+$, and black \times) and exact measurement (green line) on Sept. 2, 2005 in Cincinnati

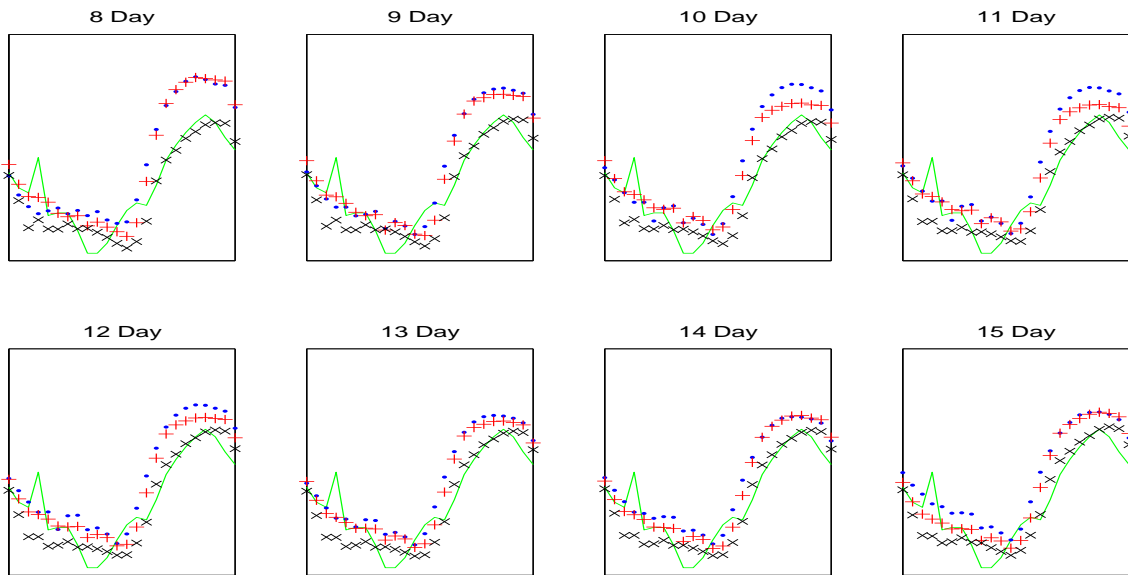


Figure 6.67: Brute force predictions (blue \cdot , red $+$, and black \times) and exact measurement (green line) on Sept. 3, 2005 in Cincinnati

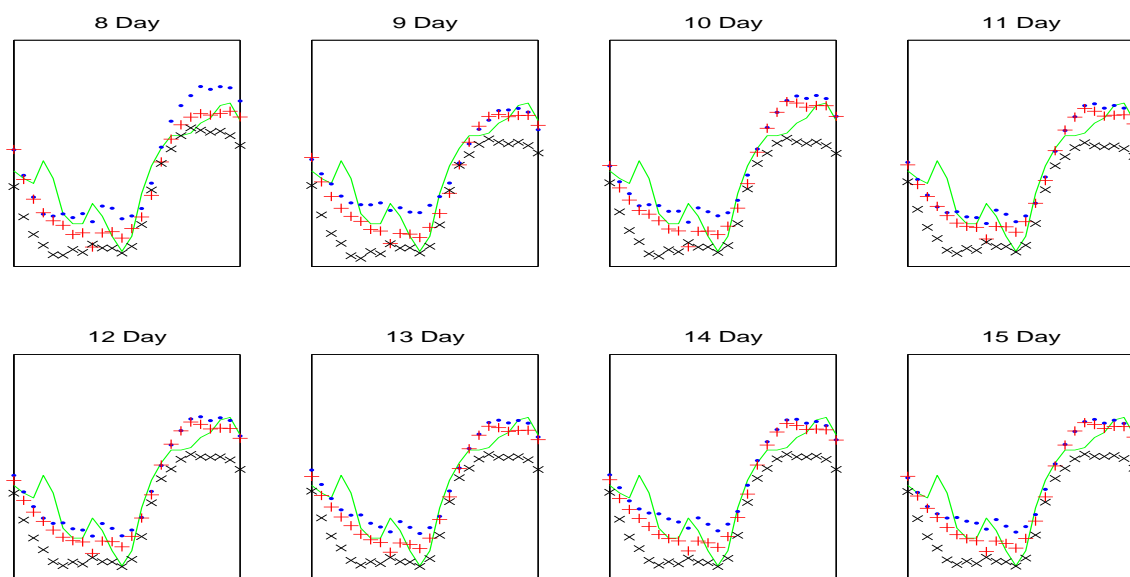


Figure 6.68: Brute force predictions (blue \cdot , red $+$, and black \times) and exact measurement (green line) on Sept. 4, 2005 in Cincinnati

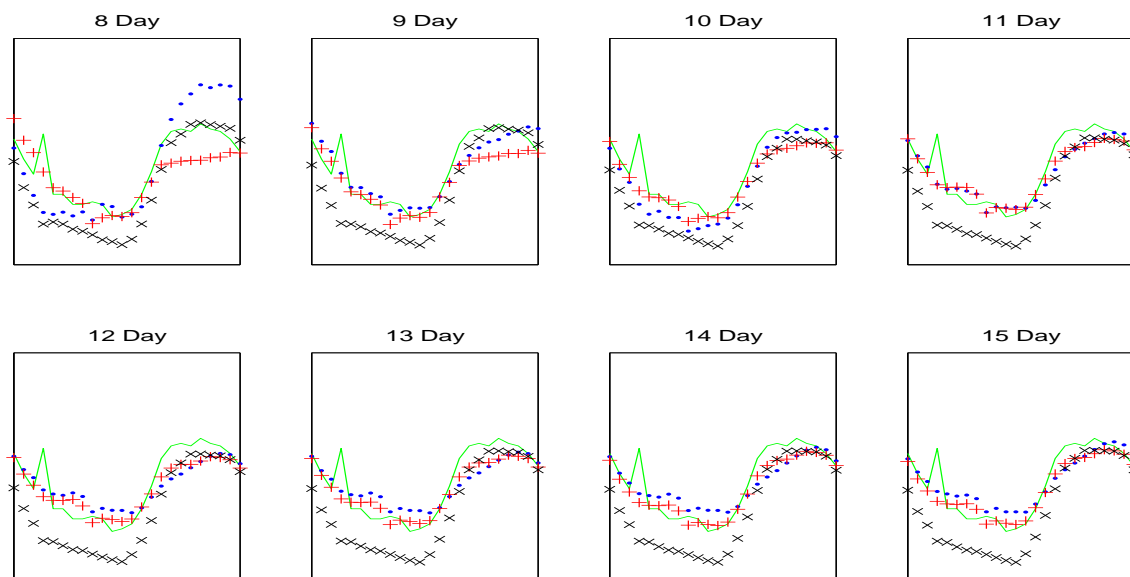


Figure 6.69: Brute force predictions (blue \cdot , red $+$, and black \times) and exact measurement (green line) on Sept. 5, 2005 in Cincinnati

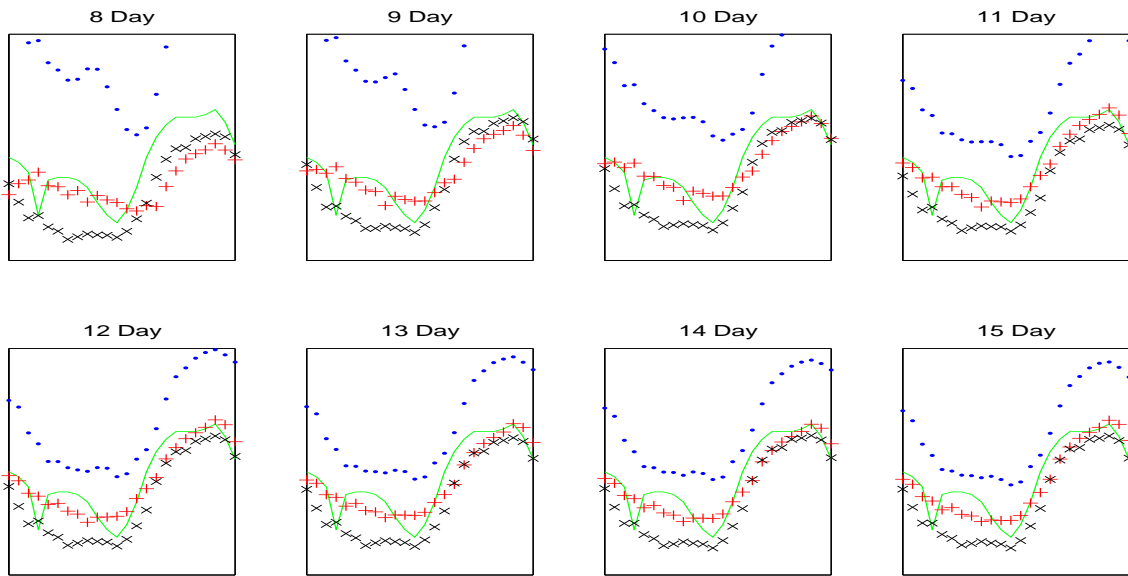


Figure 6.70: Brute force predictions (blue \cdot , red $+$, and black \times) and exact measurement (green line) on Sept. 6, 2005 in Cincinnati

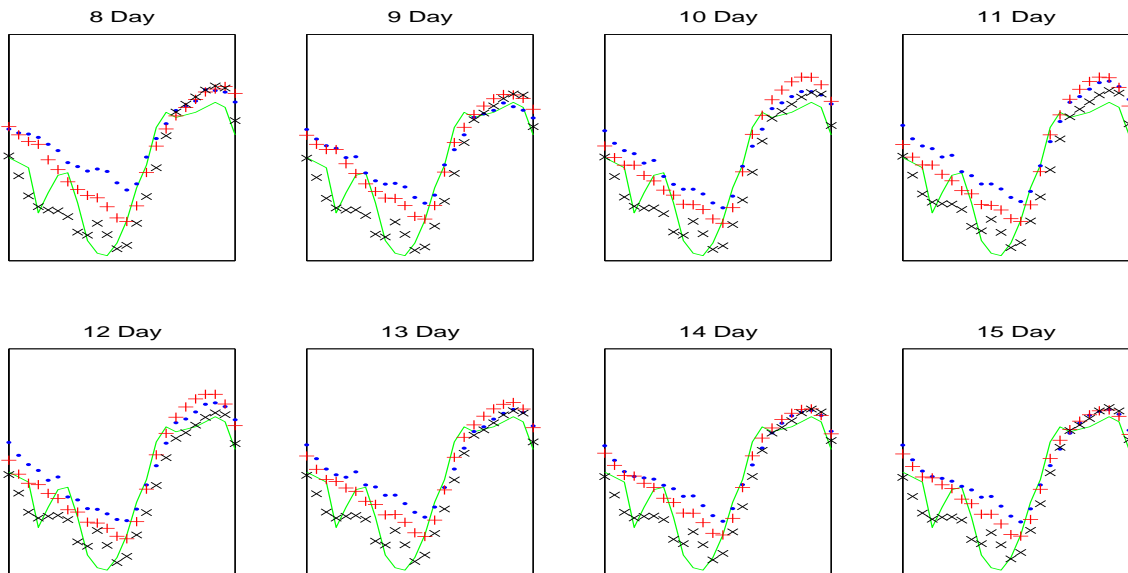


Figure 6.71: Brute force predictions (blue \cdot , red $+$, and black \times) and exact measurement (green line) on Sept. 7, 2005 in Cincinnati

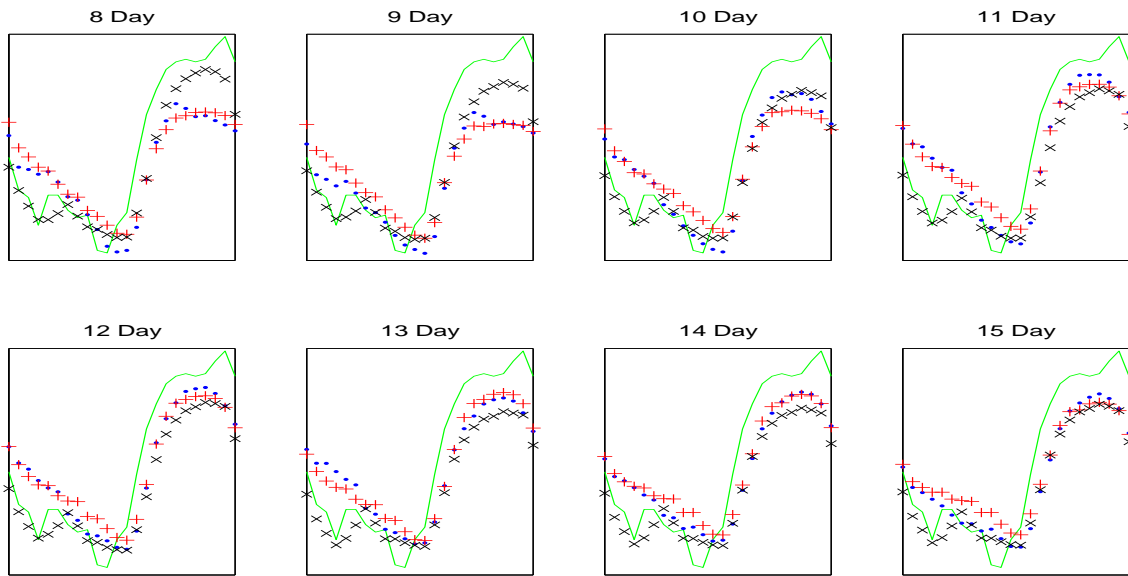


Figure 6.72: Brute force predictions (blue \cdot , red $+$, and black \times) and exact measurement (green line) on Sept. 8, 2005 in Cincinnati

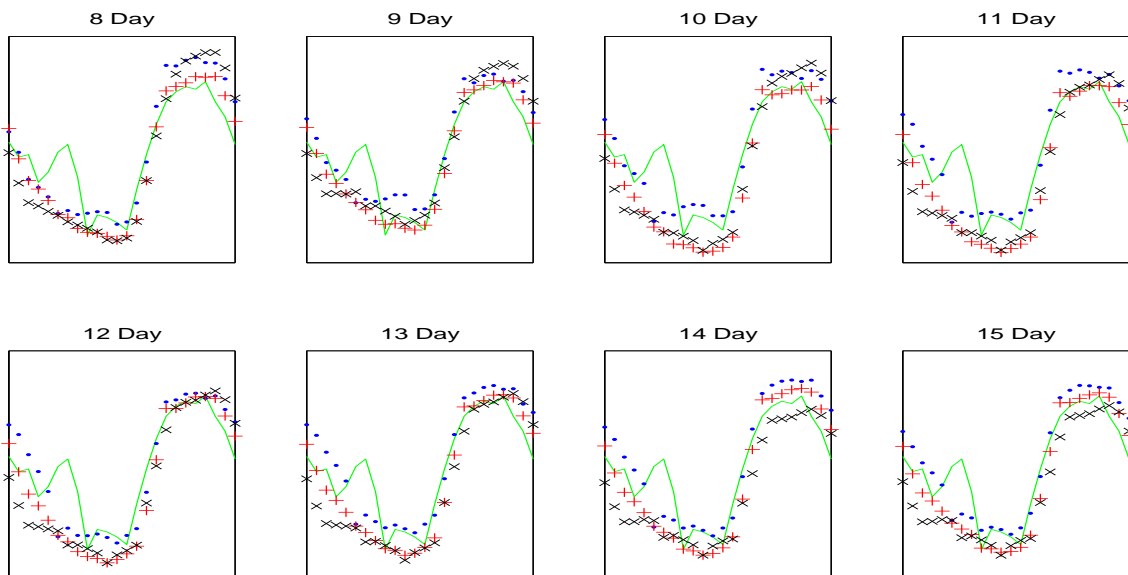


Figure 6.73: Brute force predictions (blue \cdot , red $+$, and black \times) and exact measurement (green line) on Sept. 9, 2005 in Cincinnati

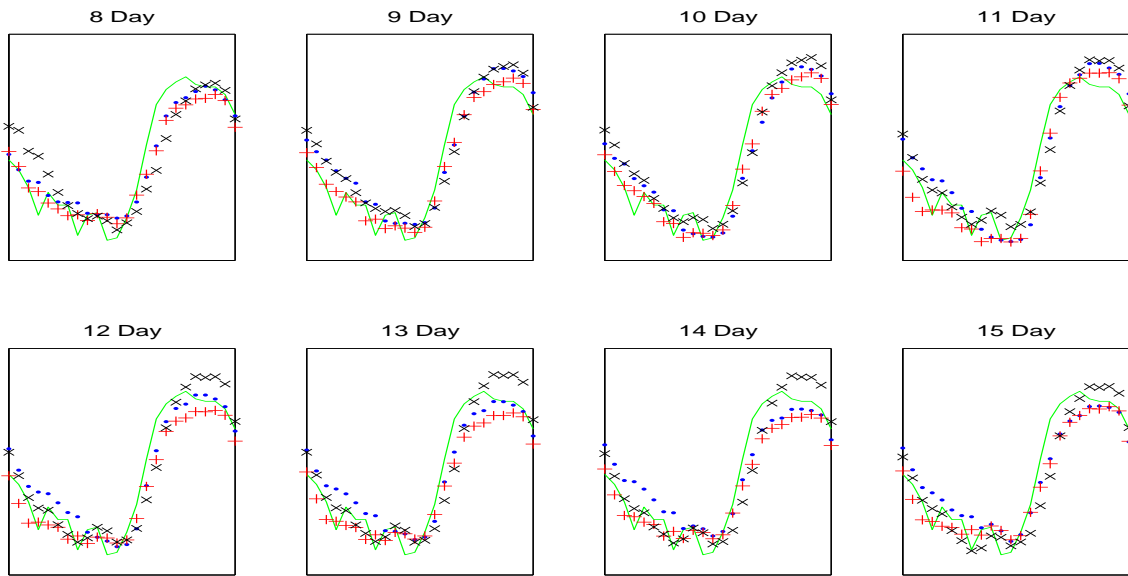


Figure 6.74: Brute force predictions (blue \cdot , red $+$, and black \times) and exact measurement (green line) on Sept. 10, 2005 in Cincinnati

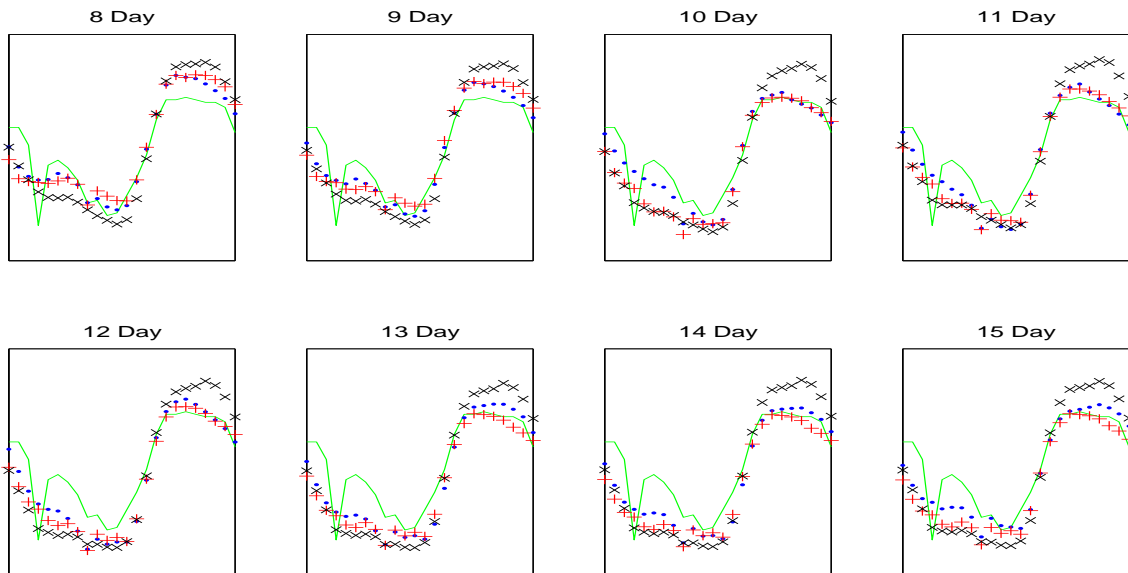


Figure 6.75: Brute force predictions (blue \cdot , red $+$, and black \times) and exact measurement (green line) on Sept. 11, 2005 in Cincinnati

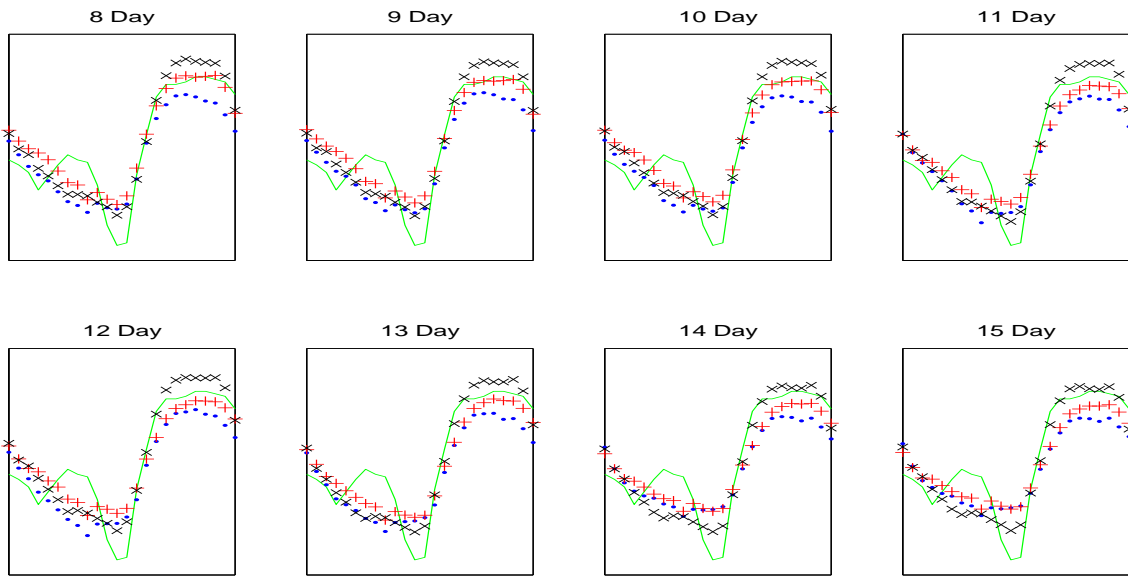


Figure 6.76: Brute force predictions (blue \cdot , red $+$, and black \times) and exact measurement (green line) on Sept. 12, 2005 in Cincinnati

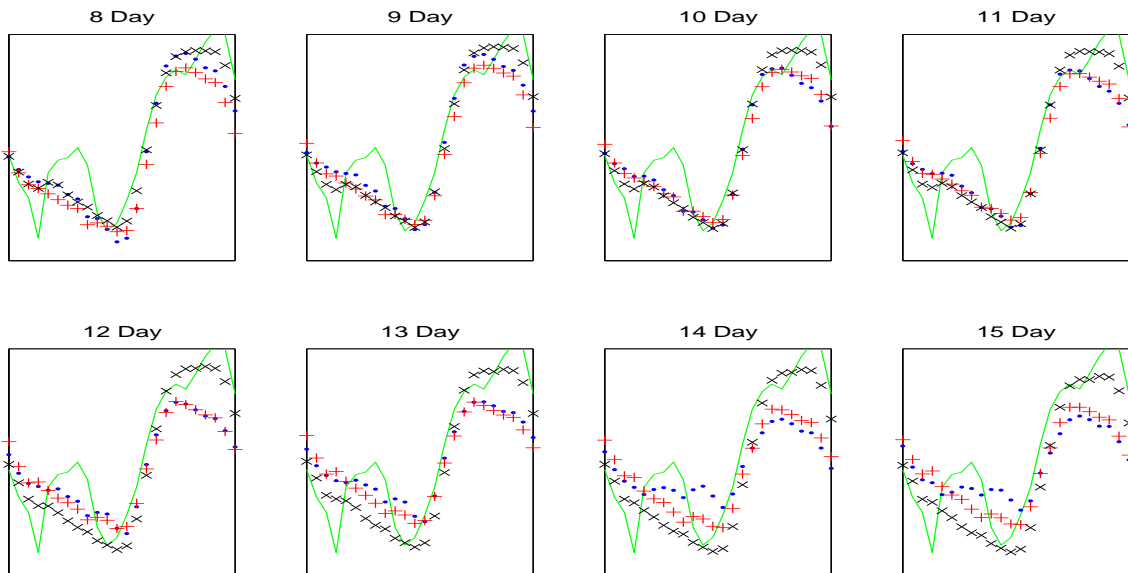


Figure 6.77: Brute force predictions (blue \cdot , red $+$, and black \times) and exact measurement (green line) on Sept. 13, 2005 in Cincinnati

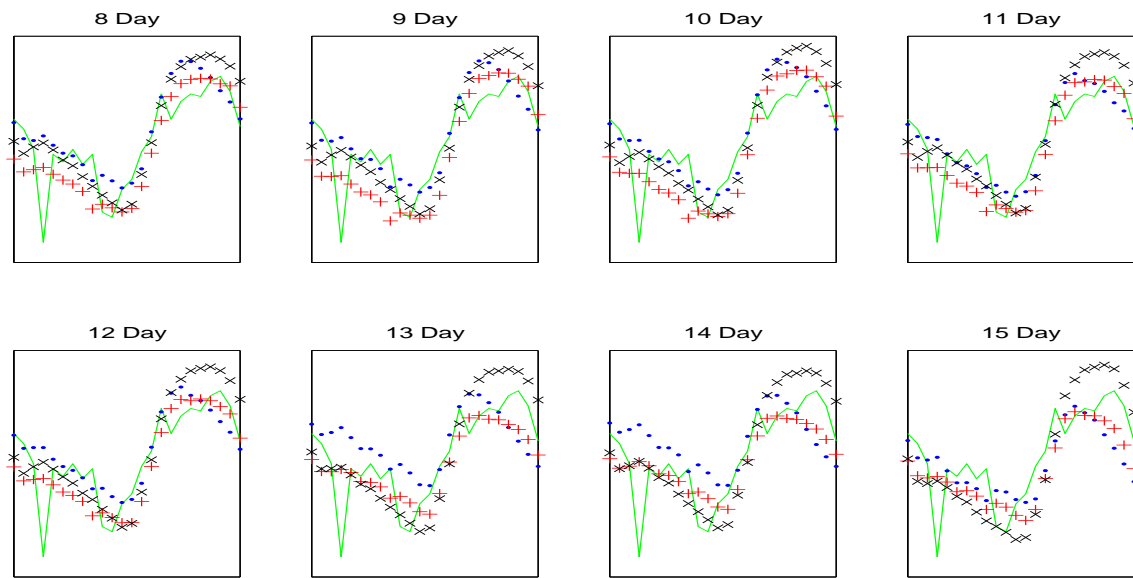


Figure 6.78: Brute force predictions (blue \cdot , red $+$, and black \times) and exact measurement (green line) on Sept. 14, 2005 in Cincinnati

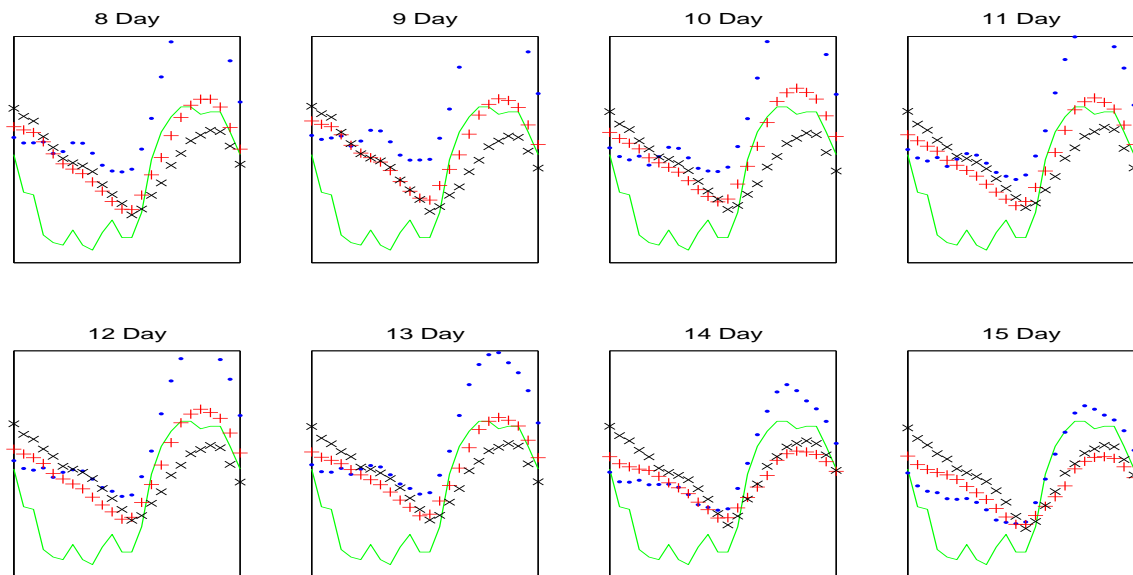


Figure 6.79: Brute force predictions (blue \cdot , red $+$, and black \times) and exact measurement (green line) on Sept. 15, 2005 in Cincinnati

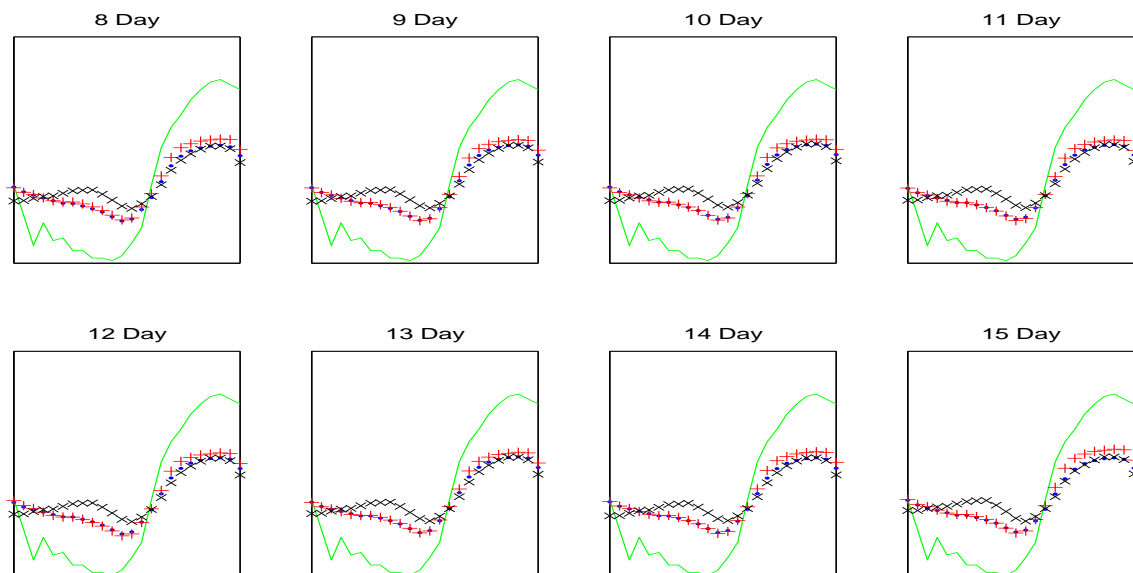


Figure 6.80: Autoregressive predictions (blue \cdot , red $+$, and black \times) and exact measurement (green line) on Sept. 1, 2005 in Cincinnati

6.3.2 THE AUTOREGRESSIVE APPROACH FOR PREDICTION AT CINCINNATI

We now show our numerical experimental results using our autoregressive approach. In the following graphs, we show the exact measurement (green line), predictions based on triangulation 1 (the red $+$), based on triangulation 2 (the black \times) and based on triangulation 3 (the blue \cdot) as in Figs 6.80– 6.94. We only use the first two eigenvalues to compute the predictions.

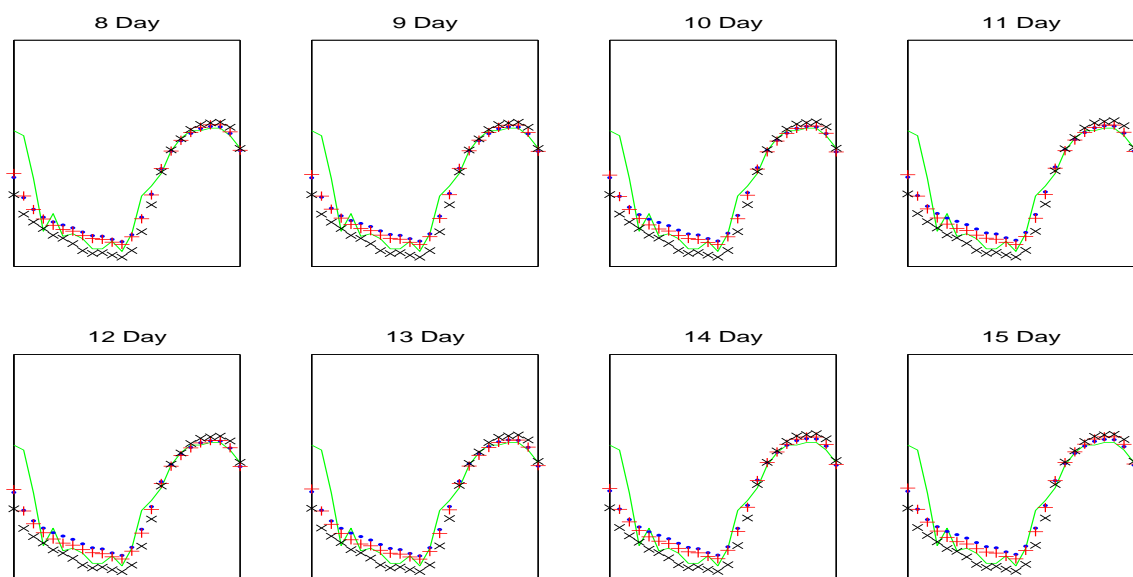


Figure 6.81: Autoregressive predictions (blue \cdot , red $+$, and black \times) and exact measurement (green line) on Sept. 2, 2005 in Cincinnati

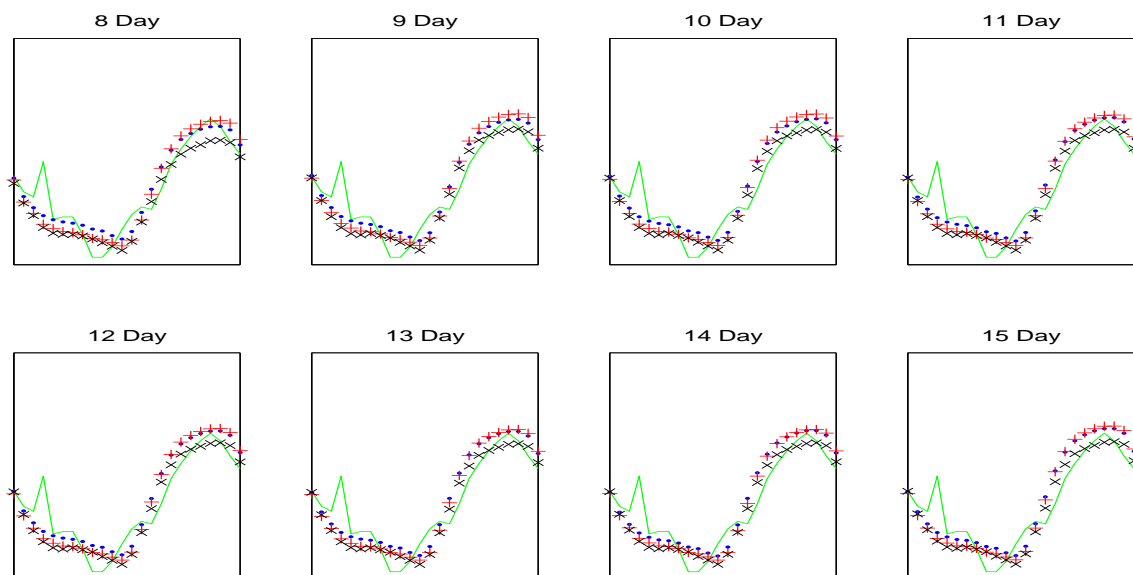


Figure 6.82: Autoregressive predictions (blue \cdot , red $+$, and black \times) and exact measurement (green line) on Sept. 3, 2005 in Cincinnati

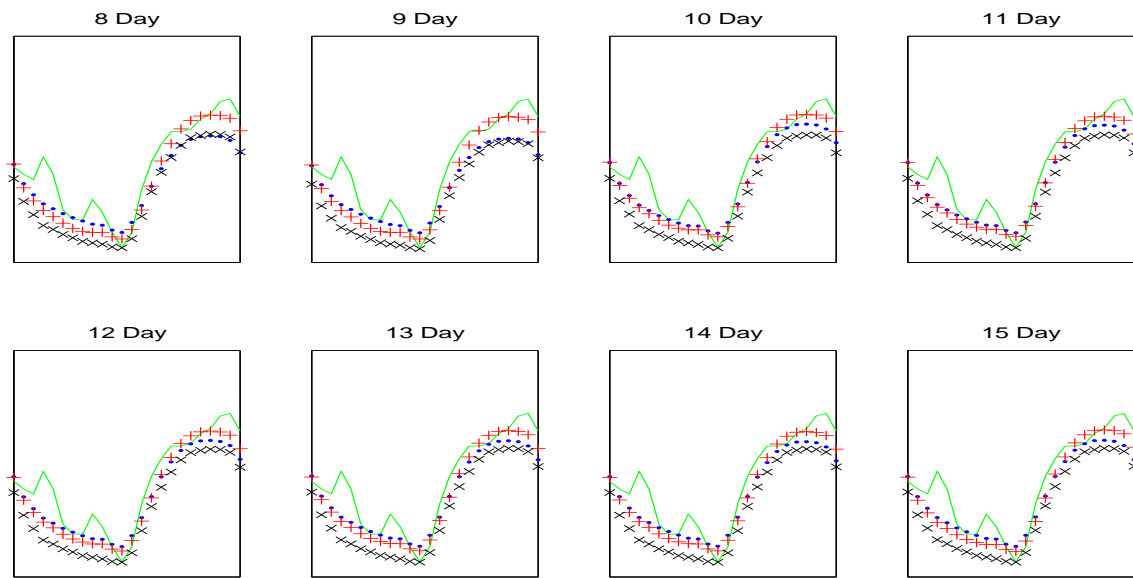


Figure 6.83: Autoregressive predictions (blue \cdot , red $+$, and black \times) and exact measurement (green line) on Sept. 4, 2005 in Cincinnati

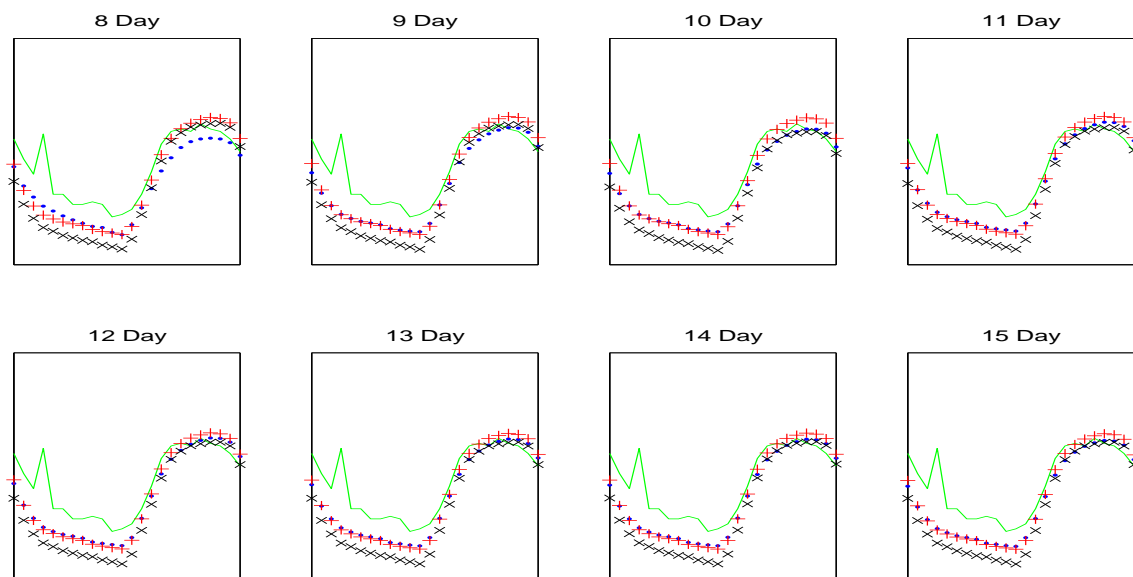


Figure 6.84: Autoregressive predictions (blue \cdot , red $+$, and black \times) and exact measurement (green line) on Sept. 5, 2005 in Cincinnati

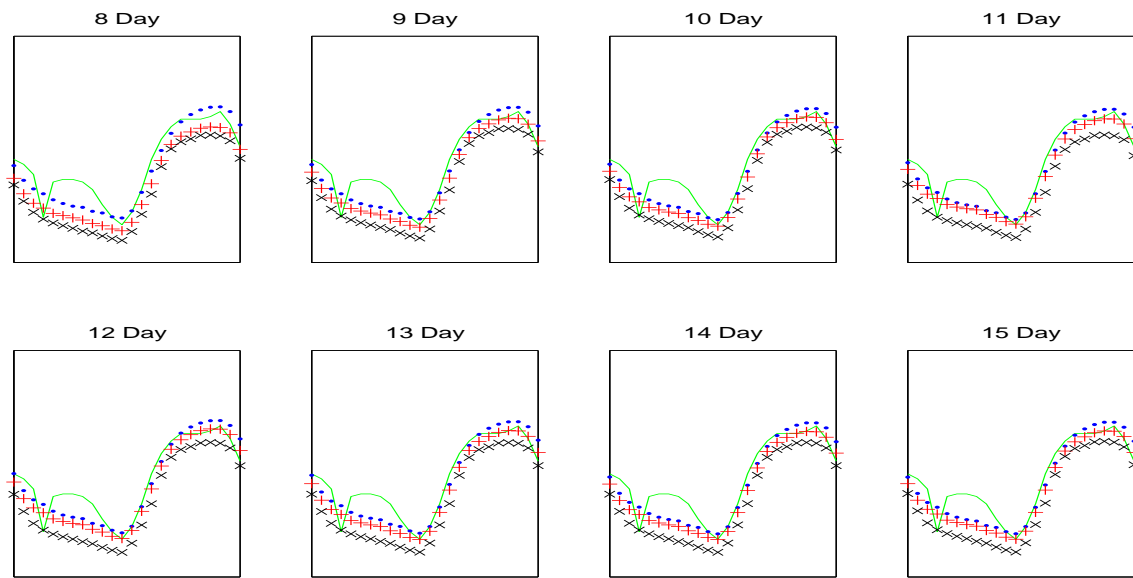


Figure 6.85: Autoregressive predictions (blue \cdot , red $+$, and black \times) and exact measurement (green line) on Sept. 6, 2005 in Cincinnati

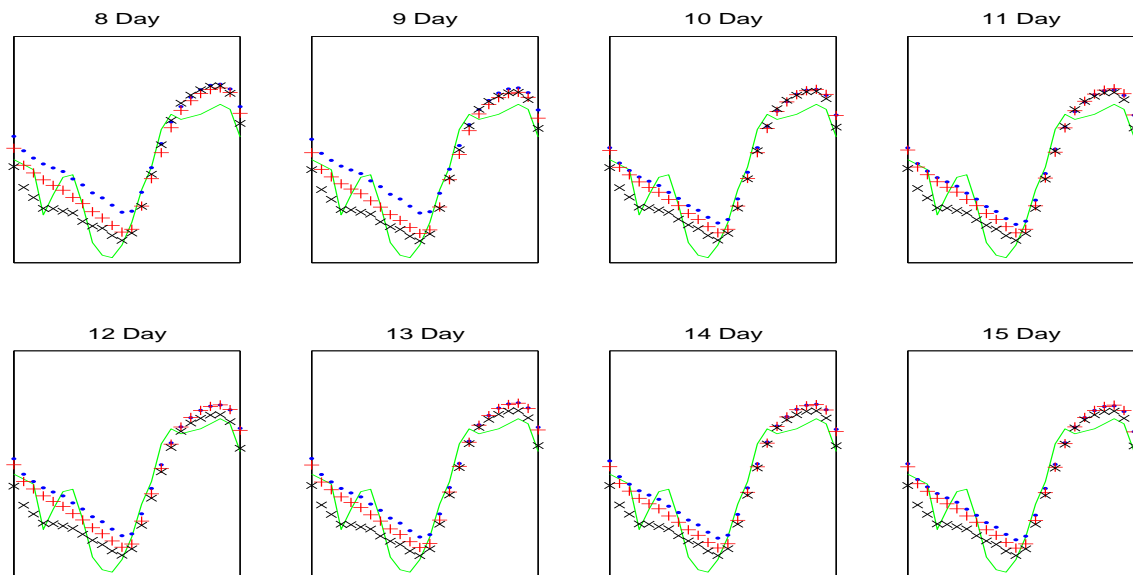


Figure 6.86: Autoregressive predictions (blue \cdot , red $+$, and black \times) and exact measurement (green line) on Sept. 7, 2005 in Cincinnati

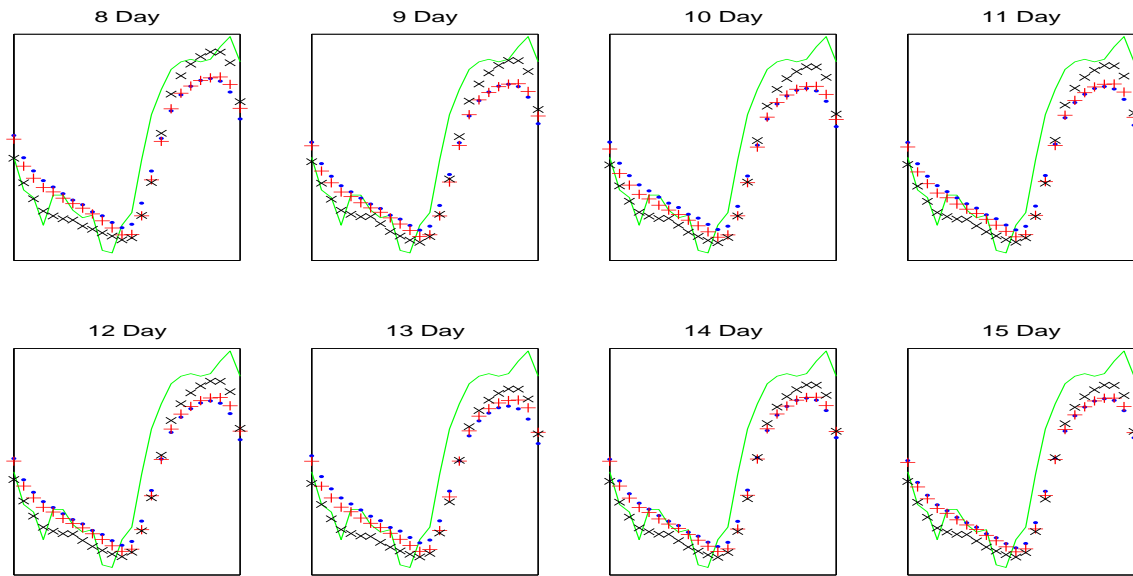


Figure 6.87: Autoregressive predictions (blue \cdot , red $+$, and black \times) and exact measurement (green line) on Sept. 8, 2005 in Cincinnati

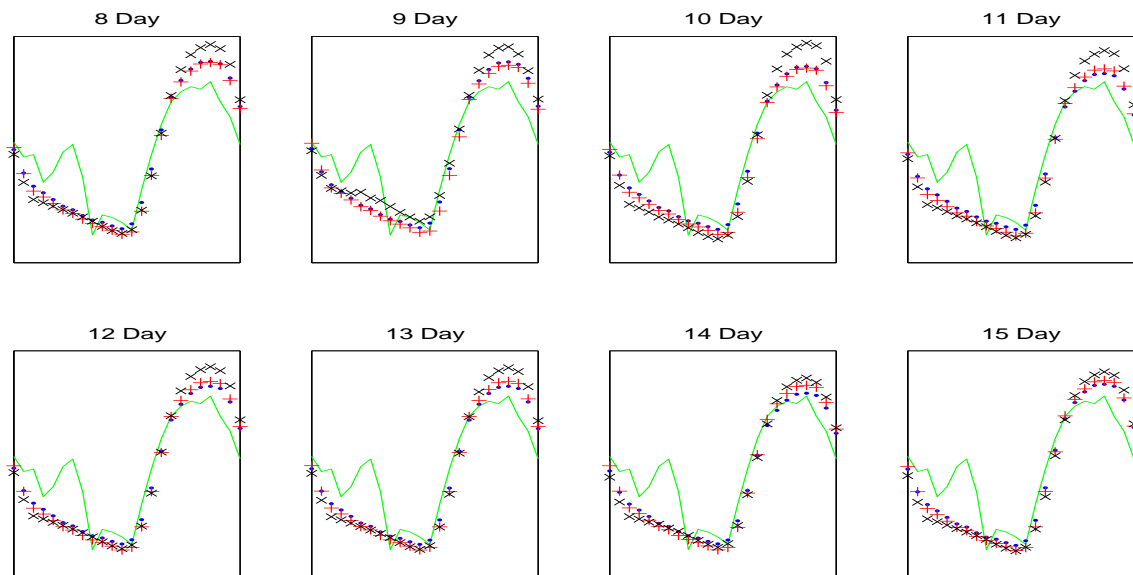


Figure 6.88: Autoregressive predictions (blue \cdot , red $+$, and black \times) and exact measurement (green line) on Sept. 9, 2005 in Cincinnati

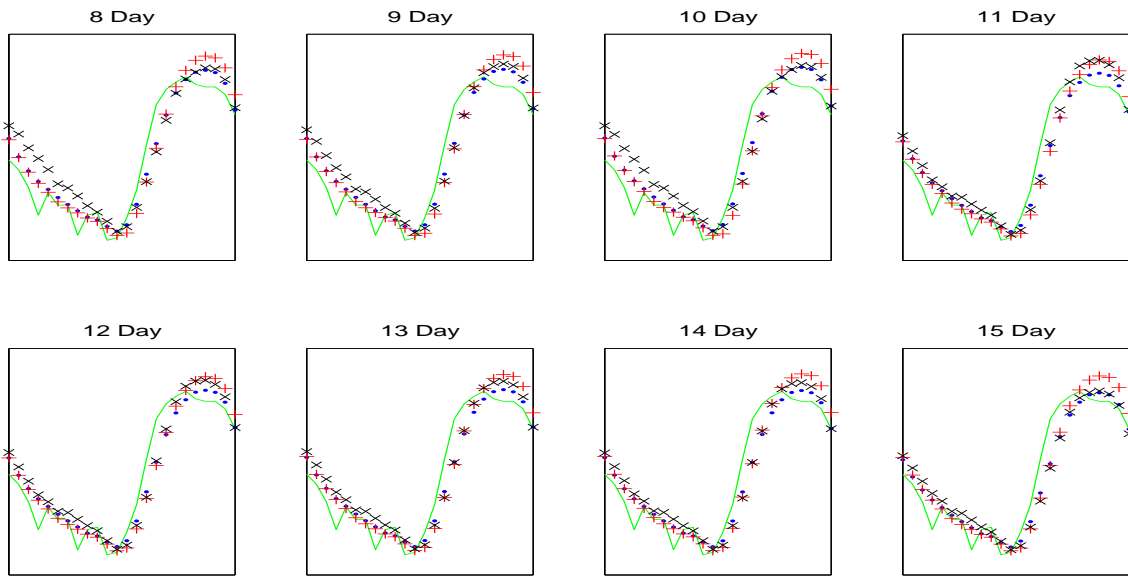


Figure 6.89: Autoregressive predictions (blue \cdot , red $+$, and black \times) and exact measurement (green line) on Sept. 10, 2005 in Cincinnati

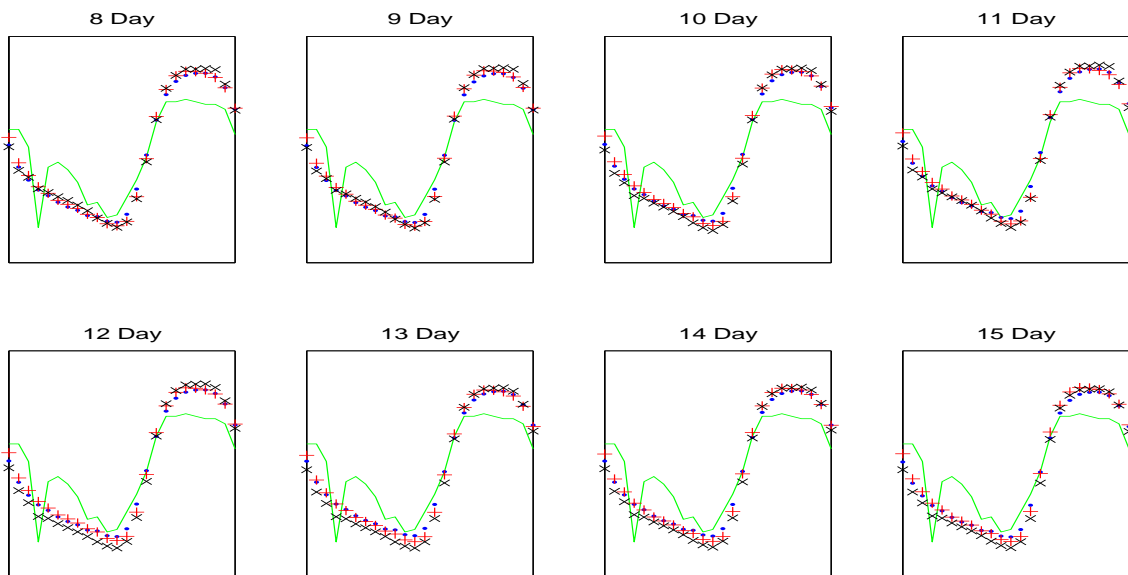


Figure 6.90: Autoregressive predictions (blue \cdot , red $+$, and black \times) and exact measurement (green line) on Sept. 11, 2005 in Cincinnati

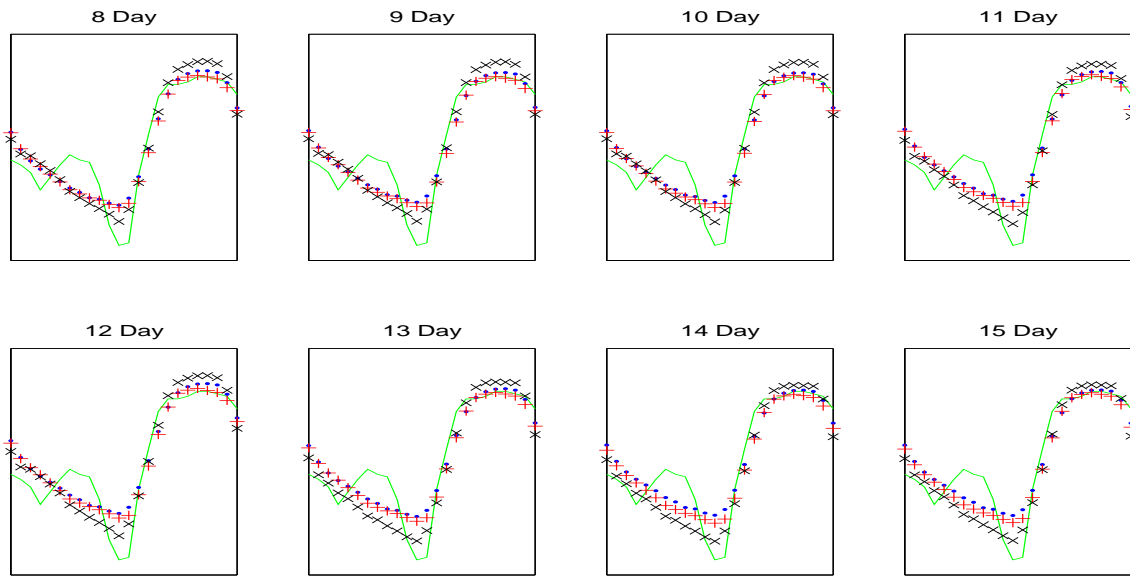


Figure 6.91: Autoregressive predictions (blue \cdot , red $+$, and black \times) and exact measurement (green line) on Sept. 12, 2005 in Cincinnati

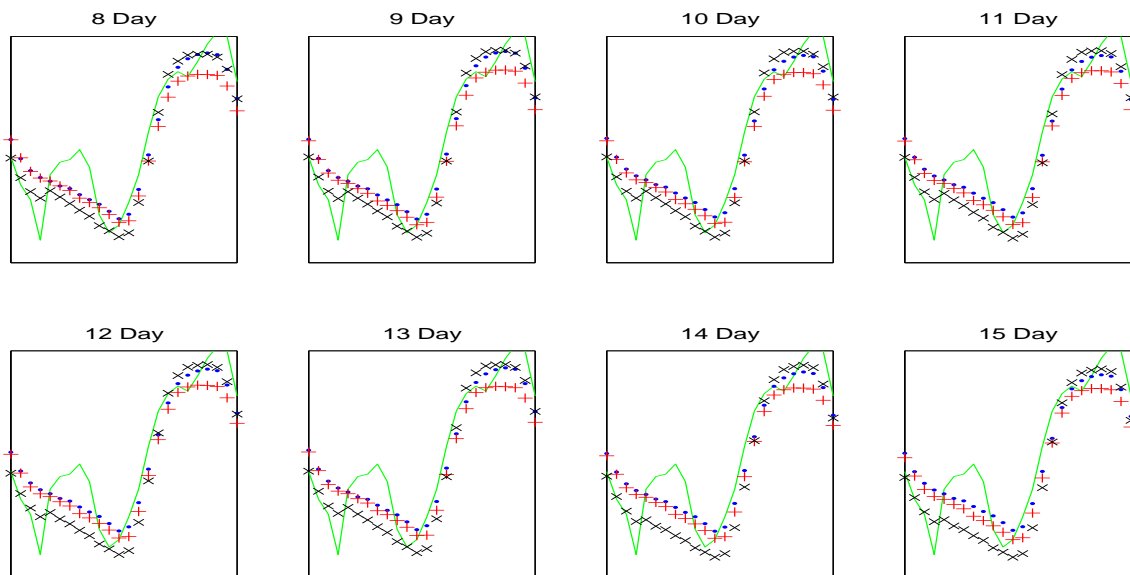


Figure 6.92: Autoregressive predictions (blue \cdot , red $+$, and black \times) and exact measurement (green line) on Sept. 13, 2005 in Cincinnati

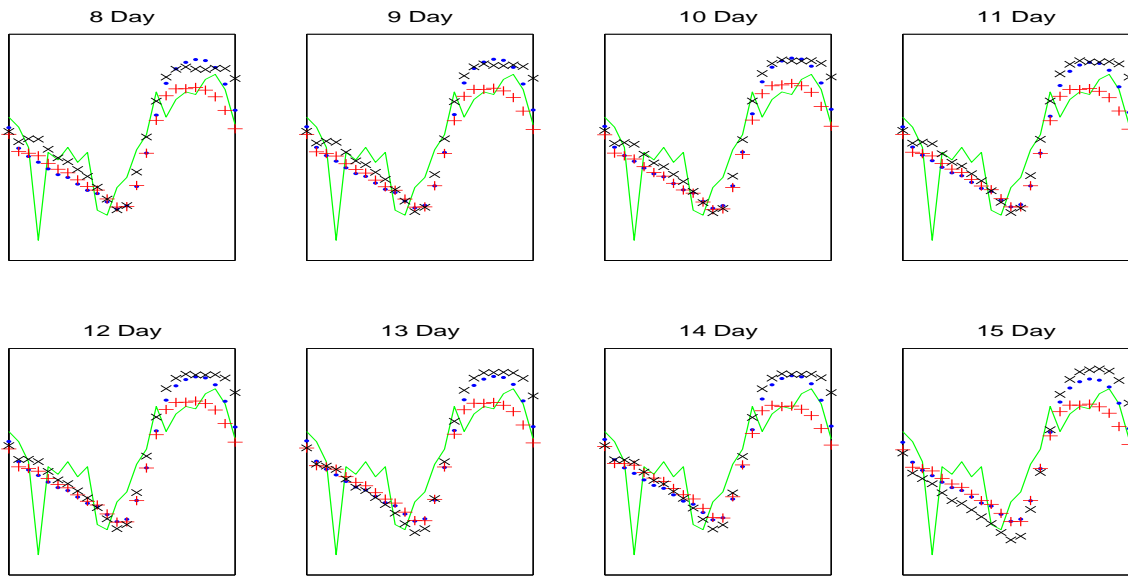


Figure 6.93: Autoregressive predictions (blue \cdot , red $+$, and black \times) and exact measurement (green line) on Sept. 14, 2005 in Cincinnati

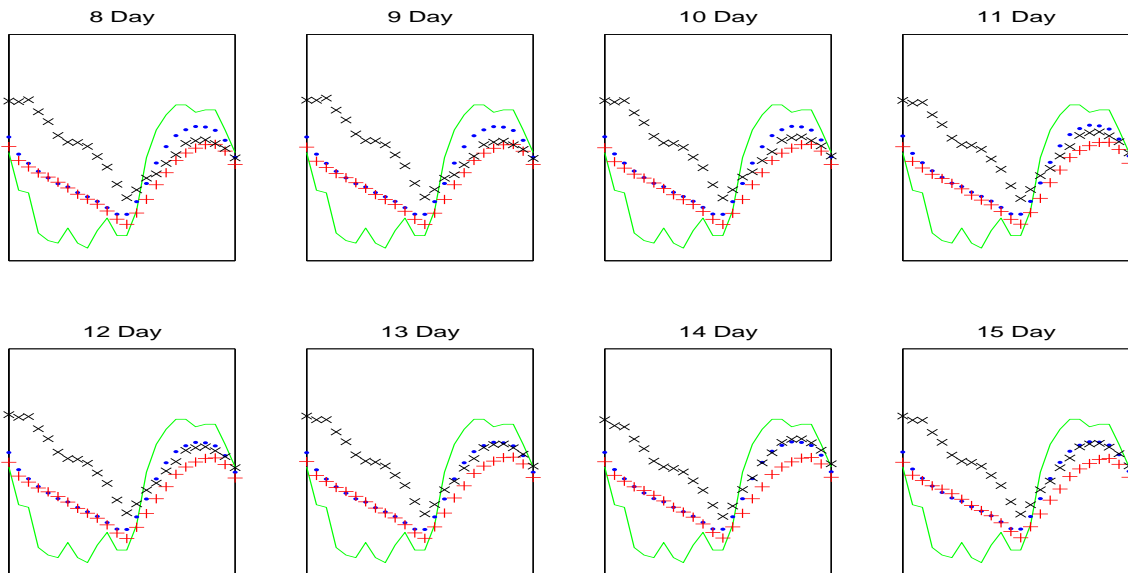


Figure 6.94: Autoregressive predictions (blue \cdot , red $+$, and black \times) and exact measurement (green line) on Sept. 15, 2005 in Cincinnati

CHAPTER 7

CONCLUSION

7.1 SIMILARITIES AND DIFFERENCES BETWEEN THE TWO APPROACHES

Theoretically, the autoregressive approach is quite different from the brute force method. The autoregressive approach uses the covariance matrix and cross covariance of the data and implements eigenvalue decompositions and orthogonal expansions to solve the problem. While the brute force method uses the fact that the spline spaces become dense in $L^2(\mathcal{D})$ and the assumption that the random surfaces, the X_i , are linearly independent. We note that this assumption on the random surfaces may not be realistic. However, the computational algorithms for both approaches are very similar.

Recall for the brute force method, we compute the empirical estimator of S_α based on discrete observations of random surfaces $X_i, i = 1, \dots, n$. The empirical estimator $\widetilde{S}_{\alpha,n} \in S_d^r(\Delta)$ with $d \geq 3r + 2$, is the solution of the following

$$\min_{\beta \in S_d^r(\Delta)} \frac{1}{n} \sum_{i=1}^n (f(X_i) + \epsilon_i - \langle \beta, S_{X_i} \rangle)^2.$$

We take $\{\phi_1, \dots, \phi_m\}$ to be a basis for $S_d^r(\Delta)$ then the solution of the above minimization is given by $\widetilde{S}_{\alpha,n} = \sum_{i=1}^m \widetilde{c}_{n,i} \phi_i$ with coefficient vector $\widetilde{\mathbf{c}}_n = (\widetilde{c}_{n,i}, i = 1, \dots, m)$ satisfying $\widetilde{A}_n \widetilde{\mathbf{c}}_n = \widetilde{\mathbf{b}}_n$, where

$$\widetilde{A}_n = \left[\frac{1}{n} \sum_{\ell=1}^n \langle \phi_i, S_{X_\ell} \rangle \langle \phi_j, S_{X_\ell} \rangle \right]_{i,j=1,\dots,m},$$

where S_{X_ℓ} is the penalized least squares fit of X_ℓ and

$$\widetilde{\mathbf{b}}_n = \left[\frac{1}{n} \sum_{\ell=1}^n f(X_\ell) \langle \phi_j, S_{X_\ell} \rangle + \frac{1}{n} \sum_{\ell=1}^n \langle \phi_j, \epsilon_\ell S_{X_\ell} \rangle \right]_{j=1,\dots,m}.$$

The second summation can be treated as zero as $n \rightarrow +\infty$ as ϵ_ℓ are sampled from a random variable with mean zero and independent of X_ℓ .

For the autoregressive approach, we take the spline approximation of the covariance operator $\widetilde{\Gamma}_n$:

$$\widetilde{\Gamma}_n(x) = \frac{1}{n} \sum_{\ell=1}^n \langle S_{X_\ell}, x \rangle S_{X_\ell} \quad (7.1)$$

from (3.12). For any $x = \sum_{i=1}^m c_i \phi_i$, the operator $\widetilde{\Gamma}_n$ maps x into $S_d^r(\Delta)$ as

$$\widetilde{\Gamma}_n(x) = \sum_{i=1}^m c_i \frac{1}{n} \sum_{\ell=1}^n \langle S_{X_\ell}, \phi_i \rangle S_{X_\ell}.$$

Therefore the matrix associated with the covariance operator in this finite dimensional space $S_d^r(\Delta)$ is

$$\left[\frac{1}{n} \sum_{\ell=1}^n \langle S_{X_\ell}, \phi_i \rangle \langle S_{X_\ell}, \phi_j \rangle \right]_{1 \leq i, j \leq m}.$$

which is the matrix \widetilde{A}_n above if the spline spaces are the same. Similarly, for spline approximation $\widetilde{\Delta}_n$ of the empirical estimator Δ_n of Δ ,

$$\widetilde{\Delta}_n(x) = \sum_{i=1}^m c_i \frac{1}{n} \sum_{\ell=1}^n \langle \widetilde{X}_\ell, \phi_i \rangle Y_\ell, \quad (7.2)$$

and the vector representation of $\widetilde{\Delta}_n$ is

$$\left[\frac{1}{n} \sum_{\ell=1}^n \langle S_{X_\ell}, \phi_i \rangle Y_i \right]_{1 \leq i \leq n}$$

which is the \widetilde{b}_n above. Hence if we use all eigenvalues and eigenvectors of the covariance matrix \widetilde{A}_n to invert the covariance operator in the autoregressive approach then the solution is the same as the brute force approach. However, our numerical results show that the autoregressive approach uses only a few principal eigenvalues and vectors to compute the \widetilde{g}_{PCA} .

In particular, if one uses a continuous $S_5^0(\Delta)$ for H_k , the covariance matrix will not be the same as \widetilde{A}_n nor is the cross covariance. In this situation, we may use the penalized least squares fit to find a smoother version \widetilde{g}_{SPCA} in $S_d^r(\Delta)$.

7.2 SUMMARY OF NUMERICAL EXPERIMENTS

As the theory suggests, the brute force method works well for Atlanta and Cincinnati, especially over triangulation 3 when the size of the triangulation, $|\Delta|$ is reduced. The brute force predictions are consistent for the various learning periods tested. The predictions are not widely different based on the number of previous days used to create the prediction. In each case the predictions are close to the exact measurements and the closeness to the exact measurements occurs in almost all fifteen days we tested from September 1 to September 15. For the autoregressive approach, we use only the first two eigenvalues in the Atlanta and Cincinnati predictions and get good results. The predictions generated by the two methods are very similar. So similar that there is not enough distinction in the numerical experiments to say which one is better.

When the size of triangulation is smaller, the predictions get better for both the brute force and the autoregressive approaches. Although, due to the limitation of the data set, we can not let the size of triangulation be too small or we would have too many triangles without data.

From a practical standpoint, the brute force method is easier to implement. While the autoregressive approach requires one to learn how many eigenvalues are needed to make a good prediction. Several days of testing would be needed to learn how to best choose the eigenvalues and even then it is debatable how many would be “best.” Indeed, there exist several methods for choosing the number of eigenvalues. For example one method suggests finding the “knee” in the plot of the eigenvalues. However, we have observed the decay of the eigenvalues and could not find a “knee” if the values of all 819 eigenvalues are plotted on a normal scale. If they are plotted in a logarithmic scale then there are several “knees.” Determining how many eigenvalues to use for the best prediction is not an easy task and requires further study. For our results we always use a set number of eigenvalues for a given location (Atlanta 2, Cincinnati 2, Boston 7). We see that the autoregressive prediction does not do a good job for September 14 and September 15 in Atlanta. However, if we use more

eigenvalues, the prediction can improve. This leaves us to question when do we need more eigenvalues and why.

In theory, the longer the learning period, the better the prediction should be. However, the numerical results varied based on our experiments. We have experimented the predictions based on twenty one to thirty six days. The predictions get better for a few days but most days the predictions get worse. This may be due to fact that the longer learning period includes the more variety of ozone concentration curve patterns.

There are several ways to extend the models in Chapters 3 and 4 in several ways. One may want to predict the ozone values a few days out. That is, we want to predict the day after tomorrow using all the ozone values up to today. To do this, we view the ozone values on the day after tomorrow in one location as a linear functional of the ozone distribution over the a region of the United States. We may also want to include another variable that influences ozone concentrations such as temperature. To do this we would want to develop a model that can consider a covariant. We may also have a reason to believe that the day of the week we are predicting is important and hence we may want to give a weight the same days of the week that are encompassed in the learning phase. To do this we could consider weighting different time lags in the current models.

For future research, we can implement the brute force models in Chapters 4 and 5 to predict the paths of hurricanes. For this application, we want to use a model where both the explanatory and response variables are random surfaces. Using such a model allows us to predict values for locations where there are no measurements. For hurricane tracking, we could use barometric pressure data to create an input surface and then implement the model in Chapter 5 acquire an output surface of barometric pressures. Or we could run the model in Chapters 4 for several locations and fit a surface through the prediction results. The path of the hurricane is tracked by identifying eye of hurricane, where the barometric pressure is lowest. As new measurements become available, the models are quickly and easily updated to consider the new information. If we can improve the prediction of hurricane movement

within fifty miles of its exact position, we could save peoples' lives, towns and money. The improved predictions give people more time to plan efficient evacuations and secure their homes and businesses for the storm surges and flooding that follow hurricane landfall.

BIBLIOGRAPHY

- [1] Awanou, G. and Lai, M. J. and Wenston, P., The multivariate spline method for numerical solution of partial differential equations and scattered data interpolation, in *Wavelets and Splines: Athens 2005*, G. Chen and M. J. Lai (eds), Nashboro Press, 2006, 24–74.
- [2] Awanou, G. and M.J. Lai, On convergence rate of the augmented Lagrangian algorithm for nonsymmetric saddle point problems, *Appl. Numer. Math.* 54 (2005), no. 2, 122134.
- [3] Besse, P., Cardot, H. and Stephenson, D., Autoregressive forecasting of some functional climatic variations, *Scandinavian Journal of Statistics*, 27(2000), 673–687.
- [4] Bosq, D. (1998). *Nonparametric Statistics for Stochastic Processes: Estimation and Prediction*, Volume 110 of *Lecture Notes in Statistics*, New York: Springer-Verlag.
- [5] Cardot, H. and Ferraty, F. and Sarda, P., Functional linear model, *Stat. Probab. Lett.*, (1999) 45, 11–22.
- [6] Cardot, H. and Ferraty, F. and Sarda, P., Spline estimators for the functional linear model, *Stat. Sin.*, 2003, 13, 571-591.
- [7] Cardot, H. and Sarda, P., Estimation in generalized linear models for functional data via penalized likelihood, *J. Multivar. Anal.*, 92 (2005), 24-41.
- [8] Chui, C. K. and Lai, M. J., Multivariate vertex splines and finite elements, *J. Approx. Theory*, 60(1990), pp245-343.
- [9] Crambes, C., A. Kneip, and P. Sarda, Smoothing splines estimators for functional linear regression, *The Annals of Statistics* (2009) 37, 3572.

- [10] Damon, J. and S. Guillas, The inclusion of exogenous variables in functional autoregressive ozone forecasting, *Environmetrics* 13 (2002), 759–774.
- [11] Ettinger, B., Guillas, S. and Lai, M. J., *Bivariate Splines for Ozone Concentration Prediction, under preparation, 2007.*
- [12] Fasshauer, G., and Schumaker, L. L., *Scattered data fitting on the sphere*, in Mathematical Methods for Curves and Surfaces II, M. Daehlen, T. Lyche, L. Schumaker, Vanderbilt University Press, 1998, pp. 117–166.
- [13] Ferraty, F. and Vieu, P., *Nonparametric Functional Data Analysis: Theory and Practice*, Springer-Verlag, London, 2006
- [14] von Golitschek, M., Lai, M. J., Schumaker, L. L., *Error bounds for minimal energy bivariate polynomial splines*, Numer. Math. 93(2002), 315–331.
- [15] von Golitschek, M., and Schumaker, L. L., *Bounds on projections onto bivariate polynomial spline spaces with stable local bases*, Const. Approx. 18(2002), 241–254.
- [16] von Golitschek, M., and Schumaker, L. L., *Penalized least squares fitting*, Serdica 18 (2002), 1001–1020.
- [17] Guillas, S. and M. J. Lai, *Bivariate Splines for Spatial Functional Regression Models*, submitted, 2008.
- [18] Golub, G. H., and Van Loan, C.F., *Matrix Computations*, John Hopkins Univeristy Press, Baltimore, MD., 1989
- [19] Lai, M.-J., *Multivariate splines for data fitting and approximation*, in *Approximation Theory XII: San Antonio 2007*, M. Neamtu and L. L. Schumaker (eds.), Nashboro Press (Brentwood), 2007, 210–228.
- [20] Lai, M. J. and Schumaker, L. L., *Approximation power of bivariate splines*, Advances in Comput. Math., 9(1998), pp. 251–279.

- [21] Lai, M. J. and Schumaker, L. L., *Spline Functions over Triangulation*, Cambridge University Press, Cambridge, U.K., 2007.
- [22] Ramsay, J. and Silverman, B.W., *Functional Data Analysis*, Springer-Verlag, 2005.